Electron Correlation by Wigner Intracules

A thesis submitted to the Australian National University for the degree of Doctor of Philosophy

Darragh P. O'Neill

May 17, 2005

This thesis contains no material which has been accepted for the award of any other degree or diploma in any university. To the best of the author's knowledge and belief, it contains no material previously published or written by another person, except where due reference is made in the text.

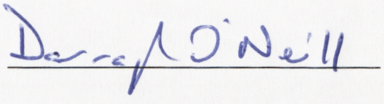

Darragh P. O'Neill

May 17, 2005

Acknowledgements

This work has taken me from Dublin to Nottingham to Canberra and in the future to new work in Germany. Along the way there have been many people who have contributed to both my professional and personal life. First and foremost I would like to thank my supervisor Peter Gill. He has provided me with a stimulating and challenging project throughout which he has always patiently provided me with the guidance I have needed. I have continually learnt from him and I hope that I will take some small amount of his scientific clarity away from this PhD.

I have been lucky enough to have many friends around me during my PhD. My friends from Ireland, although not always nearby, have always supported me and paid me visits to wherever I have travelled. Especially I'd like to thank Gill, Maria, Mary, Róisín, Orla, Thomas, Garrett, Mark and Rahim. In my time in Nottingham and Australia there have been many people who have helped to keep me sane, usually by taking me for a pint. Matt, John, Dave, Rad and Tim in Nottingham seemed particularly thirsty. Chris, Dave, Colin, Joe, Matt, Adam and Matt in Australia have never failed to provide the distractions I have needed when work both has and hasn't been going well. Leaf and Andrew travelled with me from Nottingham to Australia and have always helped me both in and out of work.

Finally I'd like to thank my parents who have supported me throughout my continuing education. They have always encouraged me in everything I do and it is they who have got me this far.

Abstract

The correlated motion of electrons is a central area of research in quantum chemistry. In the first chapter this problem is introduced and a first approximation to its solution, the Hartree-Fock model, in presented in detail. We also briefly review some more sophisticated methods for the treatment of electron correlation.

Chapter 2 introduces the concept of intracules — two-electron probability distributions. The position intracule gives the probability of finding two electrons with a given separation. The momentum intracule gives the probability of finding two electrons with a given relative momentum. The literature surrounding these quantities is reviewed and some simple examples are presented.

The third chapter presents two new types of phase-space intracules. The Wigner intracule yields the "quasi"-probability of finding two electrons with a given separation *and* relative momentum. The action intracule gives the "quasi"-probability of finding two electrons with a given product of relative position and momentum. Although neither of these intracules are true probability distributions, as they are not everywhere positive, they still possess many properties one would expect from such distributions. Some simple examples are presented.

The next chapter focuses on intracules derived from Hartree-Fock wavefunctions and we show in detail how the Wigner intracule is calculated. In particular, we have focused on the use of quadrature as a relatively simple and practical route to the evaluation of the Wigner intracule. This has been implemented in the Q-CHEM package.

Chapter 5 gives some examples of all of the different types of intracule. Firstly the Wigner intracules for the two-electron ion series from He-Ne^{8+} are examined. We then look at the four types of intracule for He, Li and Be and show how the Wigner intracule yields extra insight over the position or momentum intracules alone. The Wigner and action intracules for Ne are also presented. A detailed derivation of the intracules for He and the Hooke's Law atom follows and a comparison between the exact and Hartree-Fock intracules is made. Some molecular results are given at the end, specifically for dissociating H_2 and for H_2O and F_2.

The calibration and assessment of any new method requires accurate benchmark data. Unfortunately in the case of electron correlation these data are incredibly computationally expensive to calculate. In chapter 6 we present a set of accurate energies for some small molecules based on experimental and theoretical results which we believe will be very useful to research in the field of electron correlation.

Motivated by the information one can extract from the Wigner intracule and by physical arguments which show that the relative position and the relative momentum are important in the description of electron correlation, in chapter 7 we propose a new method for calculating the electron correlation energy based on the Wigner intracule. By recognising that certain combinations of relative position and momentum contribute more or less to the correlated motion of the electrons we believe that the electron correlation energy can be estimated by weighting and then integrating the Wigner intracule. Some results are presented which show its performance is comparable to the LYP functional in density-functional theory.

Chapter 8 describes how this new Hartree-Fock-Wigner theory may be integrated into the Hartree-Fock self-consistent-field procedure. The practical implementation of this is laid out and the calculation of the new integrals associated with this new method is discussed in some detail. We present methods based on quadrature and on an infinite series formulation for the calculation of these integrals.

In the final two chapters we present results for our benchmark data set and for all of the reactions in the G2 set. We look at the effect of basis set and the choice of parameterisation.

Results are compared to Hartree-Fock and LYP and our new method is shown to be comparable to LYP. We go on to look at some of the problems encountered in the self-consistent approach. We finish by looking at some of the aspects of this method which need to be improved and also suggest possible future directions this research should take.

Contents

List of Figures

List of Tables

Refereed publications arising from this thesis

- *Two-electron distribution functions and intracules*, P. M. W. Gill, D. P. O'Neill and N. A. Besley, *Theor. Chem. Acc.*, **109**, 241, (2003)
- *Wavefunctions and two-electron probability distributions of the Hooke's-law atom and helium*, D. P. O'Neill and P. M. W. Gill, *Phys. Rev. A.*, **68**, 022505, (2003)
- *Intracules for the Kellner Helium-Like Ions*, P. M. W. Gill, N. A. Besley and D. P. O'Neill, *Int. J. Quant. Chem.*, **100**, 166, (2004)
- *Electron Correlation in Hooke's Law atom in the high-density limit*, P. M. W. Gill and D. P. O'Neill, *J. Chem. Phys.*, **122**, 094110, (2005)
- *Benchmark correlation energies for small molecules*, D. P. O'Neill and P. M. W. Gill, *Mol. Phys.*, **103**, 763, (2005)
- *Self-Consistent Hartree-Fock-Wigner Calculations*, D. P. O'Neill and P. M. W. Gill, *ACS Symposium Series: Recent Advances in Electron Correlation Methodology*, in press
- *A new way of understanding electron correlation*, D. P. O'Neill, N. A. Besley and P. M. W. Gill, submitted
- *Hartree-Fock-Wigner Theory*, D. P. O'Neill and P. M. W. Gill, in preparation

Chapter 1

Introduction

1.1 Background

The turn of the twentieth century marks an incredibly fertile and revolutionary period in physics. Newtonian mechanics and Maxwell's theory of electromagnetism were well established and seemed to explain most observed phenomena and some even felt the subject was nearly a closed book with only minor details remaining. However, one of the outstanding problems was to lead to a whole new area of physics. Classical physics predicts that an ideal blackbody should radiate at continually increasing energy with increasing frequency — this prediction can easily be demonstrated to be false. This breakdown is known as the ultraviolet catastrophe. In 1900 Max Planck postulated a solution to this by suggesting that matter could only radiate energy at discrete, or quantized, values proportional to the frequency [1]. Although not immediately realized, Planck had opened the door to the notion of wave-particle duality. Einstein went on to extend Planck's law, proposing that quantisation was not a property of the emitting or absorbing matter, but the radiation itself. He was able to use this to explain the photo-electric effect. De Broglie put the concept of wave-particle duality on a firm footing by showing how to calculate the wavelength of so-called "matter waves" [2]. This was confirmed experimentally by Davisson and Germer [3] by applying Bragg's Law, which had previously only been used to describe diffraction in electromagnetic waves, to electrons.

Following these discoveries, a rigorous framework for this new quantum theory was sought. Two such formulations were produced nearly in parallel. The first was matrix mechanics which Heisenberg developed as a matrix based approach to quantum mechanical problems [4]. The second was that of Schrödinger, known as wave mechanics, which is centred around his eponymous equation [5]. These two approaches can be shown to be equivalent but Schrödinger's is often the more useful and will be the one which will be discussed further. Quantum mechanics, as well as other major developments, such as general relativity, made at the beginning of the last century have revolutionized research in the physical sciences and marked the birth of modern physics.

1.2 Quantum Chemistry

Quantum chemistry was conceived in 1926 when Schrödinger published his famous equation [5]

$$\hat{H}\Psi = E\Psi \tag{1.1}$$

where $\hat{H}$ is the Hamiltonian operator, Ψ is the wavefunction and E is the energy. It is the efficient calculation of this energy E and how it changes with respect to external parameters which is the goal of quantum chemistry. This would allow the determination of almost all physical properties of a system and would likely revolutionize chemistry. Unfortunately things are not so straightforward. This is an N-body problem, like the motion of the planets around the sun, and N gets large very quickly (already 35 electrons and nuclei for a small system like ethanol). Given the linear scaling of modern computers exact solutions to this type of problem are intractable for all but the smallest systems. However, this does not dissuade us from trying, and quantum chemists now strive to make better and more efficient estimates to the energy and to molecular properties and in the eight decades since this field began remarkable progress has been made.

The non-relativistic* Hamiltonian operator for a molecular system is a complicated entity

*Throughout this work we will assume that the effects of relativity are negligible. The inclusion of such effects would be important when looking at heavy atoms or systems in which spin-orbit coupling is important.

comprising all the motion of the electrons and nuclei

$$\hat{H} = -\sum_a \frac{\nabla_a^2}{2m_a} + \sum_{a<b} \frac{q_a q_b}{|\mathbf{r}_a - \mathbf{r}_b|} \tag{1.2}$$

where a and b label all of the particles, nuclei and electrons, in the system, q_a is the charge on particle a, r_a is the position of particle a and ∇_a^2 is the Laplacian operator. In general, the Ψ which would satisfy such an eigensystem is too complicated to ascertain so we must immediately seek a simplification of the problem.

An almost universal approximation used in quantum chemistry is that of Born and Oppenheimer. They proposed that since the nuclei are so massive and move so slowly in comparison to the electrons, one can consider the the electrons moving in the field of fixed nuclei. This lets us set the nuclear kinetic energy to zero and the nuclear repulsion energy is simply a constant. Born and Oppenheimer showed this in a more quantitative manner by writing an expansion in terms of the total molecular mass and were able to show which terms could be safely discarded. The Born-Oppenheimer approximation allows us to write the electronic wavefunction as a function of the electronic coordinates with a parametric dependence on the nuclear geometry

$$\Psi(\mathbf{r}_1, \ldots, \mathbf{r}_n, \mathbf{R}_1, \ldots, \mathbf{R}_N) \approx \Psi(\mathbf{r}_1, \ldots, \mathbf{r}_n; \mathbf{R}_1, \ldots, \mathbf{R}_N) \tag{1.3}$$

and the total wavefunction as a product of the nuclear and electronic components

$$\Psi \approx \Psi_{\text{nuc}} \Psi_{\text{elec}} \tag{1.4}$$

where $\mathbf{r}_i$ are the electronic coordinates and $\mathbf{R}_j$ are the nuclear coordinates and we note the semicolon on the right-hand side of eqn. (1.3). The differential equation can now be separated and we are now left with just the electronic Schrödinger equation

$$\hat{H}_{\text{elec}} \Psi_{\text{elec}} = E_{\text{elec}} \Psi_{\text{elec}} \tag{1.5}$$

Although for the most part the Born-Oppenheimer approximation is a good one, we note that the coupling of electronic and nuclear motion can be very important and must be con-

sidered when spectroscopic accuracy is required and in areas such as quantum dynamics. The electronic Hamiltonian is given by

$$\hat{H}_{\text{elec}} = -\frac{1}{2}\sum_{i}^{n}\nabla_i^2 - \sum_{i}^{n}\sum_{A}^{N}\frac{Z_A}{|\mathbf{r}_i - \mathbf{r}_A|} + \sum_{i}^{n}\sum_{j>i}^{n}\frac{1}{|\mathbf{r}_i - \mathbf{r}_j|} \tag{1.6}$$

where i and A label the electrons and nuclei respectively and n and N are the total number of electrons and nuclei respectively. The above has been written in atomic units, as will be used throughout this work. The first term corresponds to the kinetic energy of the electrons, the second to the attraction between the electrons and the nuclei and the final term is that of the repulsion between the electrons. It is the final two-electron term which is the major obstacle in the solution of this equation as it makes the differential equation inseparable (although we shall look at a counterexample to this in section 5.2) and for anything beyond systems with one electron we cannot solve the electronic Schrödinger equation exactly. In the following section a first approximation to the solution will be introduced in detail as this will form the foundation for much of the rest of the work in this thesis. A briefer review of more sophisticated methods for solving the equation will also be given.

1.3 Hartree-Fock Theory[†]

1.3.1 The Variation Method

The variation method is a powerful tool for obtaining approximate solutions to eigenvalue equations based on the variation principle. The variation principle states that given a normalized wavefunction Φ which satisfies the appropriate boundary conditions, then the expectation value of the Hamiltonian will be an upper bound on the exact energy

$$E[\Phi] = \langle\Phi|\hat{H}|\Phi\rangle \geq \mathcal{E} \qquad \langle\Phi|\Phi\rangle = 1 \tag{1.7}$$

[†]Ref. [6] provides a complete introduction to HF theory.

where $\mathcal{E}$ is the exact energy. Thus by minimizing $E[\Phi]$ the best approximate wavefunction, within the ansatz chosen for Φ, can be found. We must of course be able to evaluate the required integrals in (1.7) to use this method. Hence the approximate wavefunction Φ should be such that it is physically reasonable but also allows the efficient calculation of the various integrals.

1.3.2 The molecular orbital approximation and Slater determinants

Earlier in this chapter the Born-Oppenheimer approximation was described in which the total wavefunction is considered a product of the nuclear and electronic wavefunctions based on the assumption that the variables of nuclear and electronic motion are not strongly interdependent. An analogous approximation would be to consider each electron independently and to write the electronic wavefunction as a product of one-electron wavefunctions, termed molecular orbitals (MOs). This approximate wavefunction is known as a Hartree product [7] and is given by

$$\Psi_{\text{Hartree}}(\mathbf{x}_1, \mathbf{x}_2, \ldots, \mathbf{x}_n) = \chi_1(\mathbf{x}_1)\chi_2(\mathbf{x}_2)\ldots\chi_n(\mathbf{x}_n) \tag{1.8}$$

where χ_i are one-electron spin orbitals and $\mathbf{x}_i$ are the four-dimensional coordinates consisting of 3 spatial and one spin coordinates. Each spin orbital is the product of a spatial molecular orbital $\psi_i(\mathbf{r})$ and a spin function $\alpha(\omega)$ or $\beta(\omega)$. However, as Fock pointed out [8], this particular approximation is not a good starting point as it fails to include the Pauli Exclusion Principle which states that a fermionic wavefunction should be antisymmetric to the interchange of identical particles.

$$\hat{P}_{ij}\Phi = -\Phi \tag{1.9}$$

where $\hat{P}_{ij}$ permutes electrons i and j. The Hartree product clearly does not satisfy this principle. To antisymmetrize the wavefunction a normalized linear combination of Hartree products is used, such that all permutations $\hat{P}_{ij}\Psi_{\text{Hartree}}$ are included. This is equivalent

to the following determinant

$$\Psi = \frac{1}{\sqrt{n!}} \begin{vmatrix} \chi_1(\mathbf{x}_1) & \chi_2(\mathbf{x}_1) & \cdots & \chi_n(\mathbf{x}_1) \\ \chi_1(\mathbf{x}_2) & \chi_2(\mathbf{x}_2) & \cdots & \chi_n(\mathbf{x}_2) \\ \vdots & \vdots & \ddots & \vdots \\ \chi_1(\mathbf{x}_n) & \chi_2(\mathbf{x}_n) & \cdots & \chi_n(\mathbf{x}_n) \end{vmatrix} = |\chi_1\chi_2\cdots\chi_n\rangle \tag{1.10}$$

which is termed a Slater determinant. We will assume that the orbitals are always orthonormal

$$\langle\chi_i|\chi_j\rangle = \delta_{ij} \tag{1.11}$$

where δ_{ij} is the Kronecker delta symbol. This assumption can be made without loss of generality as the Slater determinant is invariant under linear transformations of MOs so the orbitals can always be orthonormalized.

1.3.3 Expectation values of Slater determinants

The electronic Hamiltonian can be written

$$\hat{H} = \sum_i \hat{h}_i + \sum_{i<j} \hat{v}_{ij} \tag{1.12}$$

$$\hat{h}_i = -\frac{1}{2}\nabla_i^2 - \sum_A^N \frac{Z_A}{|\mathbf{r}_i - \mathbf{r}_A|} \tag{1.13}$$

$$\hat{v}_{ij} = \frac{1}{|\mathbf{r}_i - \mathbf{r}_j|} \tag{1.14}$$

where $\hat{h}_i$ contains all one-electron terms and $\hat{v}_{ij}$ is the two-electron term. We can now compute the one- and two-electron energies as expectation values of the Slater determinant for these operators. The one-electron energy is given by

$$E_1 = \langle\Psi|\sum_i \hat{h}_i|\Psi\rangle \tag{1.15}$$

and since the orbitals χ_i are orthonormal and there are only one-electron interactions, it is straightforward to show that

$$E_1 = \sum_i \langle i|\hat{h}|i\rangle \tag{1.16}$$

where the integral is given by

$$\langle i|\hat{h}|j\rangle = \langle \chi_i|\hat{h}|\chi_j\rangle = \int \chi_i^*(\mathbf{x}_1)\left(-\frac{1}{2}\nabla^2 - \sum_A \frac{Z}{|\mathbf{r}_1 - \mathbf{r}_A|}\right)\chi_j(\mathbf{x}_1)\mathrm{d}\mathbf{x}_1 \tag{1.17}$$

The two-electron energy is given by

$$E_2 = \langle \Psi | \sum_{i<j} \hat{v}_{ij} | \Psi \rangle \tag{1.18}$$

and by similar considerations of orthonormality it can be shown that

$$E_2 = \sum_{i<j}[\langle ij|ij\rangle - \langle ij|ji\rangle] = \sum_{i<j}\langle ij||ij\rangle = \frac{1}{2}\sum_{i,j}\langle ij||ij\rangle \tag{1.19}$$

where

$$\langle ij|kl\rangle = \langle \chi_i\chi_j|\hat{v}|\chi_k\chi_l\rangle = \int \chi_i^*(\mathbf{x}_1)\chi_j^*(\mathbf{x}_2)\frac{1}{|\mathbf{r}_1 - \mathbf{r}_2|}\chi_k(\mathbf{x}_1)\chi_l(\mathbf{x}_2)\mathrm{d}\mathbf{x_1}\mathbf{x_2} \tag{1.20}$$

$$\langle ij||kl\rangle = \langle ij|kl\rangle - \langle ij|lk\rangle \tag{1.21}$$

The two integrals in eqn. (1.21) can be attributed different physical significance – the first arising from the classical Coulomb repulsion between the electrons and the second as a result of the antisymmetry of the wavefunction. It is useful to rewrite the equation to reflect this

$$E_2 = \frac{1}{2}\sum_i \langle \chi_i|\hat{J} - \hat{K}|\chi_i\rangle \tag{1.22}$$

where the total Coulomb operator $\hat{J}$ and the total exchange operator $\hat{K}$ are given by

$$\hat{J} = \sum_j \hat{J}_j f(\mathbf{x}_i) = \sum_j \left[\int \chi_j^*(\mathbf{x}_2)|\mathbf{r}_1 - \mathbf{r}_2|^{-1}\chi_j(\mathbf{x}_2)\mathrm{d}\mathbf{x}_2\right] f(\mathbf{x}_i) \tag{1.23}$$

$$\hat{K} = \sum_j \hat{K}_j f(\mathbf{x}_i) = \sum_j \left[\int \chi_j^*(\mathbf{x}_2)|\mathbf{r}_1 - \mathbf{r}_2|^{-1} f(\mathbf{x}_2)\mathrm{d}\mathbf{x}_2\right] \chi_j(\mathbf{x}_k) \tag{1.24}$$

Therefore the total energy is given by

$$E[\Psi] = \langle\Psi|\hat{H}|\Psi\rangle = \sum_i \langle i|\hat{h}|i\rangle + \frac{1}{2}\sum_i \langle i|\hat{J} - \hat{K}|i\rangle \tag{1.25}$$

1.3.4 The Hartree-Fock equations

Given the expectation value of the Hamiltonian for the Slater determinant Ψ shown in eqn. (1.25) we are now in a position to apply the variation method to obtain the best orbitals, i.e., those which minimize the energy. The energy must be minimized subject to the constraint that the orbitals remain orthonormal (1.11). Employing the method of Lagrange multipliers leads us to the following functional

$$\mathcal{L}[\Psi] = E[\Psi] - \sum_{i,j} \varepsilon_{ji} \left(\langle\chi_i|\chi_j\rangle - \delta_{ij}\right) \tag{1.26}$$

where ε_{ji} are the Lagrange multipliers. Thus, to minimize E subject to the constraints we minimize $\mathcal{L}$. This is done using the calculus of variations. If we consider an infinitesimal change in the spin orbitals $\chi_i \to \chi_i + \delta\chi_i$, which will also leads to a change $\Psi \to \Psi + \delta\Psi$,

$$\mathcal{L}[\Psi + \delta\Psi] = E[\Psi + \delta\Psi] - \sum_{i,j} \varepsilon_{ji} \left(\langle\chi_i + \delta\chi_i|\chi_j\rangle + \langle\chi_i|\chi_j + \delta\chi_j\rangle\right) \tag{1.27}$$

and $E[\Psi + \delta\Psi]$ is given by

$$\begin{aligned} E[\Psi + \delta\Psi] = &\sum_i \langle\chi_i + \delta\chi_i|\hat{h}|\chi_i + \delta\chi_i\rangle \\ &+ \frac{1}{2}\sum_{i,j} \langle(\chi_i + \delta\chi_i)(\chi_j + \delta\chi_j)|(\chi_i + \delta\chi_i)(\chi_j + \delta\chi_j)\rangle \\ &- \frac{1}{2}\sum_{i,j} \langle(\chi_i + \delta\chi_i)(\chi_j + \delta\chi_j)|(\chi_j + \delta\chi_j)(\chi_i + \delta\chi_i)\rangle \end{aligned} \tag{1.28}$$

Introducing the Fock operator

$$\hat{F} = \hat{h} + \hat{J} - \hat{K} \tag{1.29}$$

and setting the first variation in $\mathcal{L}$ equal to zero to find the minimum yields

$$\delta L[\Psi] = \sum_i \langle \delta\chi_i | \left[\hat{F}|\chi_i\rangle - \sum_j \varepsilon_{ji}|\chi_j\rangle \right] + \text{complex conjugate} = 0 \tag{1.30}$$

Since $\delta\chi_i$ is arbitrary, the quantity in square brackets must be zero. Therefore

$$\hat{F}|\chi_i\rangle = \sum_j \varepsilon_{ji}|\chi_j\rangle \tag{1.31}$$

Furthermore, since the Fock operator and the expectation values of a Slater determinant are invariant to unitary transforms which preserve orthonormality, such a transform can be applied such that the Lagrange multipliers are diagonalized, i.e., $\varepsilon_{ij} = \varepsilon_i\delta_{ij}$, yielding

$$\hat{F}|\chi_i\rangle = \varepsilon_i|\chi_i\rangle \tag{1.32}$$

This set of eigenvalue equations are the canonical Hartree-Fock equations and are used to determine the spin orbitals which yield the lowest energy.

Unrestricted and restricted orbitals

So far, the molecular orbitals considered have been spin orbitals, but now it is useful to introduce a specific form for these orbitals. We will first consider the most general case in which the spatial orbitals for electrons of one spin are not necessarily the same as those for the electrons of opposite spin. These *unrestricted* orbitals have the following form

$$\chi_j(\mathbf{x}) = \begin{cases} \psi_j^\alpha(\mathbf{r})\alpha(\omega) \\ \psi_j^\beta(\mathbf{r})\beta(\omega) \end{cases} \tag{1.33}$$

where the electrons of α spin are described by the spatial orbitals ψ_j^α and similarly for the β spin electrons. Using these expressions and the following orthonormality conditions

$$\langle\alpha|\alpha\rangle = 1 \qquad \langle\alpha|\beta\rangle = 0 \tag{1.34}$$

and integrating over spin, it is straightforward to show that

$$\hat{F}^{\alpha}\psi_i^{\alpha} = \varepsilon_i^{\alpha}\psi_i^{\alpha} \tag{1.35}$$

where

$$\hat{F}^{\alpha} = \hat{h} + \hat{J} - \hat{K}^{\alpha} \tag{1.36}$$

and K_i^{α} operates only on the n^{α} electrons of spin α. Each of these equations has a β counterpart. These are the Unrestricted Hartree-Fock (UHF) equations. Determining the orbitals is now a matter of solving these integro-differential equations. This will be addressed in the subsequent sections but first a special case of the above will be mentioned. Eqn. (1.33) places no restrictions on the form of the orbitals but in a closed shell system, where $n^{\alpha} = n^{\beta}$, it is reasonable to assume that electrons of opposite spin have the same spatial orbitals, i.e.,

$$\chi_j(\mathbf{x}) = \begin{cases} \psi_j(\mathbf{r})\alpha(\omega) \\ \psi_j(\mathbf{r})\beta(\omega) \end{cases} \tag{1.37}$$

Substituting and integrating as above leads to

$$\hat{F}\psi_i = \varepsilon_i\psi_i \tag{1.38}$$

where

$$\hat{F} = \hat{h} + 2\hat{J} - \hat{K} \tag{1.39}$$

These are the Restricted Hartree-Fock (RHF) equations. In the case where $n^{\alpha} = n^{\beta}$ the UHF equations can always yield the RHF solution but this will not necessarily be the lowest energy solution. This is particularly important in the case of stretched bonds where RHF will predict much larger energies than the UHF solution. There is another variant of HF theory known as Restricted Open Shell Hartree-Fock (ROHF) theory in which paired electrons are restricted to have the same spatial wavefunctions and the unpaired electrons are unrestricted. This is more complex to implement than UHF but has the advantage that, like RHF solutions, it is an eigenfunction of the $\hat{S}^2$ operator, which should satisfy $\hat{S}^2\Psi = S(S+1)\Psi$, where S is the total spin. The UHF solution is not necessarily an eigenfunction of this operator as it may contain higher multiplicity components and is

said to be spin contaminated. Despite this shortcoming, we favour the UHF solution as it yields a lower, and therefore variationally better, energy.

1.3.5 Linear combination of atomic orbitals

In the previous section the integro-differential equations for UHF and RHF were introduced. These equations can, in simple cases, be solved numerically [9] but in general this is not practical. Instead a further approximation is introduced in which the spatial MOs are expanded in a basis of atomic orbitals

$$\psi_i(\mathbf{r}) = \sum_{\mu=1}^{N} C_{\mu i}\phi_\mu(\mathbf{r}) \tag{1.40}$$

where $\phi_\mu(\mathbf{r})$ are the atomic orbitals. This expansion is known as a Linear Combination of Atomic Orbitals (LCAO). Expanding an unknown function in a basis of known functions is a common method in applied mathematics and here it will transform our difficult problem of coupled integro-differential equations to a more familiar and tractable one of linear algebra. This method also appeals to our chemical upbringing — molecules are made of atoms, and here molecular orbitals are made of atomic orbitals.

The resulting integrals for one- and two-electron operators for this expansion are

$$(\psi_i|\mathcal{O}_1|\psi_j) = \sum_{\mu\nu} C_{\mu i}C_{\nu j}(\phi_\mu|\mathcal{O}_1|\phi_\nu) \tag{1.41}$$

$$(\psi_i\psi_j|\mathcal{O}_2|\psi_k\psi_l) = \sum_{\mu\nu\lambda\sigma} C_{\mu i}C_{\nu j}C_{\lambda k}C_{\sigma l}(\phi_\mu\phi_\nu|\mathcal{O}_2|\phi_\lambda\phi_\sigma) \tag{1.42}$$

Although this method reduces the computational complexity and is conceptually appealing, the above expressions show that the number of one-electron integrals grows as M^2 and the number of two-electron integrals grows as M^4, where M is the number of atomic basis functions. This is not a favourable scaling but in practice not all of these integrals need be evaluated and this will be discussed later.

1.3.6 The Pople-Nesbet equations

Substituting the LCAO expansion into the UHF equations and multiplying by ϕ_μ^* and integrating leads to (considering only the α equation)

$$\sum_{\nu=1}^{N} C_{\nu i}^{\alpha} \langle \phi_\mu | \hat{F}^{\alpha} | \phi_\nu \rangle = \varepsilon_i^{\alpha} \sum_{\nu=1}^{N} C_{\nu i}^{\alpha} \langle \phi_\mu | \phi_\nu \rangle \tag{1.43}$$

Introducing the overlap matrix $\mathbf{S}$ with elements

$$S_{\mu\nu} = \langle \phi_\mu | \phi_\nu \rangle \tag{1.44}$$

and the Fock matrix $\mathbf{F}^{\alpha}$ with elements

$$F_{\mu\nu}^{\alpha} = \langle \phi_\mu | \hat{F}^{\alpha} | \phi_\nu \rangle \tag{1.45}$$

we now have

$$\sum_{\nu=1}^{N} C_{\nu i}^{\alpha} F_{\mu\nu}^{\alpha} = \varepsilon_i^{\alpha} \sum_{\nu=1}^{N} C_{\nu i}^{\alpha} S_{\mu\nu} \tag{1.46}$$

This can be written as a matrix equation and along with its β analogue, these are the Pople-Nesbet equations

$$\mathbf{F}^{\alpha}\mathbf{C}^{\alpha} = \mathbf{S}\mathbf{C}^{\alpha}\boldsymbol{\varepsilon}^{\alpha} \tag{1.47}$$

$$\mathbf{F}^{\beta}\mathbf{C}^{\beta} = \mathbf{S}\mathbf{C}^{\beta}\boldsymbol{\varepsilon}^{\beta} \tag{1.48}$$

where $\boldsymbol{\varepsilon}^{\alpha}$ is a diagonal matrix of orbital energies and $\mathbf{C}^{\alpha}$ is the matrix of LCAO expansion coefficients. To determine the MOs ψ_i^{α} and ψ_i^{β} the coefficient matrix $\mathbf{C}$ must be found by solving eqns. (1.47) and (1.48). This requires an explicit formulation for the elements of the Fock matrix. Substituting eqns (1.36), (1.23) and (1.24) into (1.45) it is straightforward to show that

$$F_{\mu\nu}^{\alpha} = H_{\mu\nu}^{\text{core}} + \sum_{\lambda\sigma} \left[P_{\lambda\sigma}(\mu\nu|\lambda\sigma) - P_{\lambda\sigma}^{\beta}(\mu\sigma|\lambda\nu) \right] \tag{1.49}$$

where

$$H_{\mu\nu}^{\text{core}} = (\mu|\hat{h}|\nu) \tag{1.50}$$

and we have introduced the concept of the density matrix

$$P^{\alpha}_{\mu\nu} = \sum_{j}^{n^{\alpha}} C^{\alpha}_{\mu j}(C^{\alpha}_{\nu j})^{*} \tag{1.51}$$

$$P^{\beta}_{\mu\nu} = \sum_{j}^{n^{\beta}} C^{\beta}_{\mu j}(C^{\beta}_{\nu j})^{*} \tag{1.52}$$

$$\mathbf{P} = \mathbf{P}^{\alpha} + \mathbf{P}^{\beta} \tag{1.53}$$

The β Fock matrix is constructed in an analogous way. The total HF energy can be written as

$$E_{\mathrm{HF}} = \sum_{\mu\nu} P_{\mu\nu} H^{\mathrm{core}}_{\mu\nu} + \sum_{\mu\nu\lambda\sigma} \left[P_{\mu\nu}P_{\lambda\sigma} - P^{\alpha}_{\mu\sigma}P^{\alpha}_{\nu\lambda} - P^{\beta}_{\mu\sigma}P^{\beta}_{\nu\lambda}) \right] (\mu\nu|\lambda\sigma) \tag{1.54}$$

As discussed earlier there is a simplification if we assume the α and β orbitals are the same. This leads to the Roothaan equations

$$\mathbf{FC} = \mathbf{SC}\varepsilon \tag{1.55}$$

where

$$F_{\mu\nu} = H^{\mathrm{core}}_{\mu\nu} + \sum_{\lambda\sigma} P_{\lambda\sigma} \left[(\mu\nu|\lambda\sigma) - \frac{1}{2}(\mu\sigma|\lambda\nu) \right] \tag{1.56}$$

$$P_{\mu\nu} = 2\sum_{i} C_{\mu i} C^{*}_{\nu i} \tag{1.57}$$

In the case where $n^{\alpha} = n^{\beta}$ solving the Pople-Nesbet equations can always lead to the restricted solution and this will depend on the method of solving the equations. Of course the Roothaan formulation is a more efficient route to this solution, however in some cases this will not be lowest energy solution.

1.3.7 The self-consistent field

In the previous section the Pople-Nesbet and the Roothaan equations were presented. These equations are a generalized eigenvalue problem in which we wish to determine the coefficient matrices and hence the molecular orbitals. The solution would be obtained by

diagonalizing a transformation of the Fock matrix (we choose a unitary transformation $\mathbf{X}$ which ensures that the orbitals are orthonormal, i.e., $\mathbf{X}^\dagger\mathbf{S}\mathbf{X} = \mathbf{1}$. The resulting equation is a normal eigenvalue equation, $\mathbf{F}'\mathbf{C}' = \mathbf{C}'\boldsymbol{\varepsilon}$). However, the Fock matrix cannot be constructed until the orbitals are known so we must start by using an initial guess for the orbitals to solve the equation. We then use the resulting orbitals to construct a new Fock operator and iterate this procedure until the the orbitals have converged to the required accuracy. The convergence criterion may be the accuracy of the resulting energy or more usually the change in density matrix elements. This iterative procedure is known as the Self-Consistent Field method (SCF). The initial guess used in this procedure will determine whether we obtain the RHF or UHF solution (if they are different) when we perform a UHF calculation.

1.4 Basis Sets

The quality of the LCAO approximation, essential to the computational simplicity of HF theory, is obviously dependent on the ability of the basis set to adopt the true form of the MOs. We know that the number of integrals grows rapidly with increasing basis set size, so a prudent choice of basis set is essential.

In 1930 Slater [10] introduced the following basis functions

$$\phi(\mathbf{r}) = (x - A_x)^{a_x}(y - A_y)^{a_y}(z - A_z)^{a_z}\mathrm{e}^{-\alpha|\mathbf{r}-\mathbf{A}|} \tag{1.58}$$

which are centred at $\mathbf{A} = (A_x, A_y, A_z)$, have angular momentum $\mathbf{a} = (a_x, a_y, a_z)$ and exponent α. These Slater-Type Orbitals (STOs) are a natural choice as for $a = 0, 1$ they are exact solutions to the hydrogenic Schrödinger equation and they have the correct cusp behaviour at the nucleus and the correct exponential decay. However, the integrals which result from STOs are very expensive to evaluate and currently this makes them an impractical choice.

In 1950 Boys [11] introduced the following basis functions

$$\phi(\mathbf{r}) = (x - A_x)^{a_x}(y - A_y)^{a_y}(z - A_z)^{a_z}\mathrm{e}^{-\alpha|\mathbf{r}-\mathbf{A}|^2} \tag{1.59}$$

Gaussian-Type Orbitals (GTOs), unlike STOs, have neither the correct cusp nor decay behaviour but the computational simplicity afforded outweighs the need to include more basis functions. GTOs also have the useful property that higher angular momentum functions are related to derivatives of lower ones. For example

$$(x - A_x)\mathrm{e}^{-\alpha|\mathbf{r}-\mathbf{A}|^2} = \frac{1}{2\alpha}\frac{\partial}{\partial A_x}\mathrm{e}^{-\alpha|\mathbf{r}-\mathbf{A}|^2} \tag{1.60}$$

This means that if we can evaluate integrals for s-type functions, all other integrals can be generated by differentiation.

Since we know before we begin a calculation what the correct short- and long-range behaviour of the orbitals should be, it is not necessary to optimize coefficients for all of the basis functions in the SCF procedure. Instead we use contracted basis functions in which an AO is approximated by a sum of GTOs

$$\phi(\mathbf{r}) = \sum_{i}^{K} D_i(x - A_x)^{a_x}(y - A_y)^{a_y}(z - A_z)^{a_z}\mathrm{e}^{-\alpha_i|\mathbf{r}-\mathbf{A}|^2} \tag{1.61}$$

where K is the degree of contraction and D_i are the contraction coefficients which are not optimized during a calculation. An example of such a basis is a STO-nG [12] basis sets which use n GTOs to approximate an STO. The most commonly used basis sets are the correlation consistent basis sets of Dunning [13] and the basis sets of Pople and co-workers [14–16].

A set of Gaussian basis functions on the same centre and with the same exponent is termed a shell. For example a p-shell consists of the three p-type functions, $\{p_x, p_y, p_z\}$. When considering two-electron integrals, we use the term class to refer to all of the integrals resulting from a shell quartet, e.g., a $(pp|ss)$ class contains 9 integrals associated with 2 p-shells and 2 s-shells.

1.4.1 Modern developments in Hartree-Fock theory

Integral evaluation

Since the development of the first quantum chemical codes in the 1960s a great deal of effort has been invested in developing efficient methods to evaluate two-electron integrals. These are the most numerous type of integral and most expensive part of a HF code. The great advantage of using GTOs is that these integrals may be performed analytically and, as mentioned above, generating higher angular momentum functions is simply a matter of differentiation. Obara and Saika showed that higher angular momentum integrals could be generated recursively from lower order integrals [17, 18] and Head-Gordon and Pople went on to introduce a second recurrence relation and show how to use the two relations efficiently [19]. Gill and co-workers went on to devise the optimum way to combine the various algorithms depending on the angular momentum and the degree of contraction of the integrals. The integrals are evaluated in an organised batch structure which makes the most efficient use of common intermediates. This is termed the PRISM algorithm [20]. These developments increased the speed of integral evaluation so much that it has become cheaper to re-evaluate the integrals on each SCF cycle rather than read them from memory or disk. This is known as a direct SCF approach.

An M^4 problem?

It is stated above that there are M^4 two-electron integrals involved in a HF calculation. However, of these integrals, how many are significant? It can be shown using Schwarz's inequality [21] that there are only $\mathcal{O}(M^2)$ significant integrals. In fact there now exist algorithms for calculating the Coulomb and exchange energies whose cost grows only linearly with size, such as the continuous fast multipole method [22] and the RI-J [23] approach for the Coulomb energy and LinK [24] for the exchange energy.

1.5 Electron Correlation

At this point we have introduced the Schrödinger equation and presented a first approximation to its solution. This independent-particle model constitutes a well defined and intuitive first approximation and it is used as a benchmark for more accurate solutions. Of course we know from the form of the Hamiltonian that the electrons do not move independently but rather the motions of the electrons are correlated. Although, HF theory accounts for $\sim$ 99% of the total energy and can sometimes provide qualitatively correct results and reasonable predictions of molecular structure, the final 1% causes it to fail in many important cases. In particular it does not account correctly for the repulsion of electrons with opposite spin. Electrons of the same spin are kept apart by the inclusion of the Pauli Principle – this is known as Fermi correlation. However, Coulomb correlation, which ensures electrons of opposite spin weave around one another in the correct way, is not accounted for and this is essential in the correct description of such phenomena as bond formation. In 1959 Löwdin defined a quantity he termed the correlation energy [25] as the difference between the exact Schrödinger eigenvalue and the restricted HF energy

$$E_{\text{Corr}} = E_{\text{Exact}} - E_{\text{RHF}} \tag{1.62}$$

Although this was the original definition of the correlation energy, throughout this work, we will define the correlation energy in a slightly different way. It is more natural to consider the difference between the exact energy and the lowest independent-electron energy, *viz.* the UHF energy, so for the remainder of this work the correlation energy is defined as

$$E_{\text{Corr}} = E_{\text{Exact}} - E_{\text{UHF}} \tag{1.63}$$

1.5.1 Static and dynamic correlation

Sometimes it can be convenient to consider electron correlation as arising from two different physical circumstances [26]. The first arises from the multideterminantal nature of wavefunctions. In many systems, especially those away from equilibrium geometry or

with nearly degenerate excited states, the addition of a few excited determinants to the wavefunction can drastically improve the results. This is termed static correlation.

The second is due to the electron-electron cusp. Hartree-Fock theory does not correctly account for the motion of electrons which are very close together - they are allowed to move too close to one another. Dynamic correlation lowers the energy by keeping electrons further apart.

Although these definitions can be conceptually useful, in practice they are not well-defined properties as it is difficult to include one and rigorously claim that the other is not being included to some degree.

1.5.2 Theoretical model chemistries

A theoretical model chemistry comprises a theoretical method and a basis set, denoted, for example, HF/6-311G for a HF calculation using the 6-311G basis set. Ideally such a model should be applicable to any system but more realistically it should be tested on as many systems as possible in order that the applicability of the model can be assessed. There are several desirable properties a model chemistry will possess. One conceptual property is that the energy should be variational. Although desirable, this is not essential, illustrated by the success of the coupled cluster methods which are not variational. Another important quality is that of size extensivity [27] which means that the energy should scale correctly with the number of electrons. A slightly looser definition is that of size consistency [28] which requires that the energy of a system of non-interacting fragments be exactly the sum of the separate fragments. The property of size extensivity has been shown to be intrinsically important in the treatment of correlation, not simply when considering fragmentation processes. HF has these scaling properties but many other methods do not. Of course a central goal for any successful model chemistry is to provide sufficiently accurate results at a feasible computational cost.

1.6 Current methods

1.6.1 Configuration interaction

The configuration interaction (CI) method (for a review see ref. [29]) is conceptually the most simple method for introducing the effects of correlation. The wavefunction is improved, and hence the energy lowered, by taking a linear combination of Slater determinants. These determinants are formed by "exciting" electrons from occupied to unoccupied orbitals in a HF determinant, Ψ_0,

$$\Psi = (1 + \hat{T}_1 + \hat{T}_2 + \ldots)\Psi_0 \tag{1.64}$$

where $\hat{T}_n$ are excitation operators which produce all determinants containing n excitations. If all possible excitations are included the exact energy, within the space spanned by the MO basis, is obtained and this is termed a full CI calculation. If the basis set used is complete, an exact solution to the problem is obtained. However, the number of determinants required increases factorially with the number of basis functions making the size of system for which a full CI calculation can be performed very small. Furthermore, the correlation energy converges at only $(l+1)^{-3}$ [30], where l is the highest angular momentum of the basis functions used. To obtain μE_h accuracy in calculating the ground state energy of He requires $l \approx 30$. Full CI calculations have been performed using modest bases on small molecules [31] which provide useful benchmark results.

There are less computationally demanding versions of the CI method. Multi-configuration self-consistent-field (MCSCF) calculations include only a small selection of all of the determinants and optimize not only the expansion coefficients but also the orbitals. MCSCF accounts primarily for non-dynamical correlation, but choosing which determinants to include is not straightforward. This ambiguity makes it more difficult to compare results and can even lead to discontinuous potential energy surfaces and dynamical correlation has been ignored. A more consistent formulation is complete-active-space self-consistent field (CASSCF) calculations which includes all valence excitations but this quickly begins to approach a full CI calculation. MCSCF or CASSCF wavefunctions can be used as

reference wavefunctions for other treatments of correlation leading to the multi-reference methods, e.g. CASPT2.

Another variant is to simply truncate the CI expansion after a given number of excitations, for example including just singly and doubly excited states is termed CI singles and doubles (CISD). These truncated expansions are not size-consistent but there are corrections such as the Davidson correction which can be used to account for this. CISD scales as M^6, where M is the size of the basis set, and typically recovers 80 – 90% of the correlation energy.

1.6.2 Møller-Plesset Perturbation Theory

Perturbation theory attempts to improve on an approximate solution based on the assumption that it differs only slightly from the exact one. In 1934 Møller and Plesset [32] applied many-body perturbation theory to the HF wavefunction to calculate the correlation energy. If the reference wavefunction is an eigenfunction of $\hat{H}_0$ then the exact Hamiltonian is given by

$$\hat{H} = \hat{H}_0 + \lambda\hat{V} \tag{1.65}$$

where λ is a parameter which will eventually be set to unity and $\hat{V}$ is the perturbation operator. The exact eigenvalues and eigenfunctions can then be expanded as a Taylor series in λ

$$E_i = E_i^{(0)} + \lambda E_i^{(1)} + \lambda^2 E_i^{(2)} + \ldots \tag{1.66}$$

$$\Psi_i = \Psi_i^{(0)} + \lambda\Psi_i^{(1)} + \lambda^2\Psi_i^{(2)} + \ldots \tag{1.67}$$

It is then straightforward to find each of the correction terms to the reference energy and wavefunction. This can be done up to arbitrary order although it has been shown that the expansion can oscillate with increasing order and sometimes even diverges [33, 34] leading to the consensus that perturbation theory beyond second order (MP2) should not be trusted. MP2 scales as M^5 and can be applied to moderately large systems. It should be noted that since perturbation theory is not variational it does not provide an upper

bound on the energy. It can be shown that perturbation theory is size consistent at any order. Typically, when the reference wavefunction is a good approximation to the exact one, MP2 theory recovers $\sim 80\%$ of the correlation energy.

1.6.3 Coupled Cluster Theory

Coupled cluster (CC) theory (for a review see ref. [35]) introduces electron correlation in the same way as CI, namely including excited determinants to variationally improve the wavefunction. However, CC theory does this using the exponential ansatz for the wavefunction

$$\Psi = \exp(\hat{T})\Psi_0 \tag{1.68}$$

$$\hat{T} = 1 + \hat{T}_1 + \hat{T}_2 + \ldots \tag{1.69}$$

where $\hat{T}_n$ are n-electron excitation operators. If the exponential is expanded in a power series it is easy to see that not only will all of the excitation operators appear separately but there will also be products of operators, so-called disconnected terms. This formulation will yield the same answer as a full CI calculation. At first blush it would seem that the problem has been made more difficult as we are now faced with the nonlinear optimisation of the expansion coefficients in comparison to the linear problem in CI. However, the advantage comes when we truncate the expansion. If $\hat{T}$ is truncated at a particular level of excitation the disconnected clusters associated with the untruncated connected terms will be retained. Thus we include higher order excitations than the truncation level and size-extensivity is ensured.

The most common CC method used is that which truncates $\hat{T}$ after single and double excitations (CCSD) and this scales as M^6. In most cases (closed shell, equilibrium geometry) CCSD recovers about $90 - 95\%$ of the exact correlation energy. For small systems higher excitations can be included; CCSDT includes triple excitations at a cost of M^8. More often triples are included perturbatively to yield the CCSD(T) method which requires a single M^7 step as opposed to the other methods which require iteration of the

most expensive part of the calculation. Truncated CC methods are not variational but the reliability of the results is such that this is not a major drawback.

1.6.4 Density Functional Theory

The three classes of method discussed for the treatment of electron correlation have all been based around the wavefunction. Density functional theory (DFT) [36] is a different class of methods based on the one-electron density

$$\rho(\mathbf{r}_1) = n \int \cdots \int \Psi(\mathbf{r}_1, \ldots, \mathbf{r}_n)\Psi^*(\mathbf{r}_1, \ldots, \mathbf{r}_n)\mathrm{d}\mathbf{r}_2 \ldots \mathrm{d}\mathbf{r}_n \tag{1.70}$$

$\rho(\mathbf{r})\mathrm{d}\mathbf{r}$ gives the probability of finding an electron in the volume element $\mathrm{d}\mathbf{r}$. Bright-Wilson's interpretation of the first Hohenberg-Kohn theorem [37] is that because the density contains cusps at the nuclei, and integrates to the number of electrons we can specify the full Schrödinger Hamiltonian and hence determine the exact energy. More formally the theorem states that the external potential is determined, within a trivial additive constant, by the electron density. The upshot of this is that the ground state energy may be written as a functional of the density

$$E = F[\rho(\mathbf{r})] \tag{1.71}$$

The second Hohenberg-Kohn theorem shows that the exact density will give the lowest energy, i.e. a variational principle for the density. Later Kohn and Sham [38] went on to introduce orbitals which provided a practical implementation of the theory. In fact in this guise, a HF code requires only minimal alteration to become a DFT code.

Although the Hohenberg-Kohn proves the existence of a functional relationship between the density and the energy it does not provide any constructive information about what this functional is. Rather than search for a functional of the total energy it easier to divide the energy into several parts

$$E[\rho] = E_V[\rho] + E_T[\rho] + E_J[\rho] + E_{XC}[\rho] \tag{1.72}$$

where the terms on the right are the nuclear potential, kinetic, Coulomb and exchange-correlation energies respectively. The nuclear potential, kinetic and Coulomb energies are usually calculated in the same was as HF. The exchange-correlation energy is often, but not always, separated further into an exchange part $E_X[\rho]$ and a correlation part $E_C[\rho]$. The first exchange-correlation functionals were considered long before the Hohenberg-Kohn theorems were stated. In 1930 Dirac derived an exchange functional based on the uniform electron gas (UEG)

$$E_X^{LDA}[\rho(\mathbf{r})] = C_X \int \rho(\mathbf{r})^{4/3} \mathrm{d}r \tag{1.73}$$

The UEG has been useful in the derivation of several other functionals such as the correlation functional of Vosko, Wilk and Nusair [39] in which they reproduce the correlation energy of the polarized electron gas as calculated by Ceperly and Alder [40]. These local density and local spin density approximations underestimate the exchange energy by approximately 10% and overestimate the correlation energy by about a factor of 2 and molecules tend to be overbound.

By far the most popular exchange functional has been that of Becke, who realized that the Dirac's exchange functional has the wrong asymptotic behaviour. He introduced the gradient of the density in a damping term and parameterized this functional using six noble gases to yield the B88 functional

$$\begin{aligned} E_X^B[\rho(\mathbf{r})] =& E_X^{LDA}[\rho(\mathbf{r})] - \beta \int \rho(\mathbf{r})^{4/3} \frac{x^2}{1 + 6\beta x \sinh^{-1} x} \\ x =& \frac{|\nabla \rho(\mathbf{r})|}{\rho(\mathbf{r})^{4/3}} \\ \beta =& 0.0042 \end{aligned} \tag{1.74}$$

The most successful correlation functional has been that of Lee, Yang and Parr which has

the following complicated form

$$
\begin{aligned}
E_C[\rho(\mathbf{r})] = &- a \int \frac{\rho(\mathbf{r})}{1 + d\rho(\mathbf{r})^{-1/3}} \mathrm{d}\mathbf{r} \\
&- ab \int \omega \rho(\mathbf{r})^2 \left[C_F \rho(\mathbf{r})^{8/3} + |\nabla \rho(\mathbf{r})|^2 \left(\frac{5}{12} - \delta \frac{7}{72} \right) - \frac{11}{24} \rho(\mathbf{r})^2 |\nabla \rho(\mathbf{r})|^2 \right] \mathrm{d}\mathbf{r} \\
\omega = &\frac{\exp(-c\rho(\mathbf{r})^{-1/3})}{1 + d\rho(\mathbf{r})^{-1/3}} \rho(\mathbf{r})^{-11/3} \qquad \delta = c\rho(\mathbf{r})^{-1/3} + \frac{d\rho(\mathbf{r})^{-1/3}}{1 + d\rho(\mathbf{r})^{-1/3}} \\
&a = 0.04918 \qquad b = 0.132 \qquad c = 0.2533 \qquad d = 0.349
\end{aligned}
\tag{1.75}
$$

and the parameters have been fitted to the helium atom.

Although DFT has solid theoretical foundations, in practice a more pragmatic stance is taken. There exist *ab initio* functionals based on model systems such as the UEG, but none of these have enjoyed the popularity of the more empirical functionals. The most successful of these are based on linear combinations of exchange-correlation functionals and Fock exchange in which the coefficients have been fitted to sets of experimental data. The inclusion of Fock exchange into the so-called hybrid functionals has made DFT the most popular tool in computational chemistry with B3LYP, which combines Fock exchange with the B88 exchange functional and the LYP correlation functional, enjoying a particularly high standing. The 8 parameters in B3LYP (one in B88, 4 in LYP and 3 coefficients for each of the functionals and Fock exchange) are optimized to reproduce various molecular properties such as heats of formation and ionisation potentials. DFT calculations can be routinely run on large systems at computational costs comparable to HF theory; another reason for its great popularity. However, the use of many functionals should be accompanied by a caveat — although they have been parameterized and assessed within certain data sets, outside of these sets they may produce erroneous and unpredictable results [41].

1.6.5 Other methods

I have mentioned just the broad classes of methods available to estimate the electron correlation energy. Of course within these there are many other variants which increase accuracy, or reduce cost, or address some other concern. There are also many other families

of methods which are being developed and I will briefly mention four.

r_{12} methods

Firstly, there are the explicitly correlated methods (for a review see ref. [42]). These methods originate from an idea of Hylleraas in 1927 [43] in which he proposed a wavefunction for helium which explicitly included a term linear in the inter-electronic distance. This is in contrast to the previous methods discussed based around one-electron MOs as now such a separation cannot be made. Others went on to extend this work for He and H_2 and such calculations provide the most accurate results to date for these small systems. The reason for the accuracy of these methods is that they explicitly account for the electron-electron cusp which MO based methods cannot. However this comes at a cost — there are very difficult three- and four-electron integrals which must be calculated. There are approximations, such as that of Kutzelnigg, which can be used to avoid these difficult integrals and these methods have been applied to larger systems ($\sim$ 10 atoms). Although, not yet broadly applicable, explicitly correlated methods have the potential to provide highly accurate results.

Quantum Monte Carlo

Secondly the Quantum Monte Carlo (QMC) methods (for a review see ref. [44]) which can in principle provide exact solutions to the Schrödinger equation. There are several flavours of QMC but I will mention only Diffusion QMC (DQMC). This formulation exploits the isomorphism of the Schrödinger equation in imaginary time and Fick's diffusion equation. The diffusion equation can then be solved by a random walk procedure, which with increasing numbers of time steps approaches a steady-state distribution which corresponds to the lowest energy wavefunction. Although DQMC can, in principle, give the exact result, in order to yield a fermionic solution the nodal structure of the wavefunction is fixed to be the same as some approximate wavefunction, often HF – this is known as the fixed-node approximation. This approximation, although usually very good, does lead to small errors in the resulting energies. Calculations in which the nodal positions are optimized are difficult and computationally prohibitive. QMC calculations have been

used to determine highly accurate energies for small first row molecules but the cost scales rapidly with increasing nuclear charge.

Reduced Density Matrix methods

The third set of methods which I will mention are the density matrix renormalization group (DMRG) methods [45]. These methods are based on a reformulation of the Schrödinger equation in which it is shown to depend not on the wavefunction but on the second-order reduced density matrix (2RDM). The problem is therefore to determine the 2RDM. However this must be done subject to the constraint of N-representability, i.e. the 2RDM must represent a realistic N-particle system. There are a hierarchy of conditions which can be enforced at increasing computational cost to do this. The development of DMRG methods in quantum chemistry is relatively recent and are not in widespread use due to the prohibitive computational cost. They do however show great promise for highly accurate calculations.

Scaled Schrödinger Equation

The final method which I will mention is that of the Scaled Schrödinger Equation (SSE) being developed by Nakatsuji [46]. In this clever formulation the Coulombic singularities do not occur and it provides a method of finding the exact wavefunction in analytic form. So far this approach has only been used on small systems such as helium and the hydrogen molecule and in these cases it provides highly accurate results. In its embryonic state it is difficult to know how extensible this will be to systems of larger size but we watch with interest as it has the potential to provide near exact solutions to the Schrödinger equation.

1.7 Outline and Aims

The goal of this research project is to develop a new theoretical model chemistry for calculating the correlation energy. The ideal outcome of such a project would be to design a robust method which can reliably estimate the correlation energy without prohibitive

computational expense. We will propose a method based around phase-space intracules which will scales in a similar manner to HF theory.

In chapter 2 the concepts of position and momentum intracules will be reviewed. These are two-electron probability distributions. The literature on the subject and some simple examples will be examined.

In chapter 3 we will introduce phase space intracules, which mark the first new area explored during this PhD. Again some simple examples will be presented.

Chapter 4 will focus on HF intracules and how they are computed, particularly the new phase-space intracules. And in chapter 5 some examples of intracules for the two-electron ions, some first row atoms, the Hooke's Law atom and some molecules will be studied to illustrate how one may draw insight from intracules.

In chapter 6 we present a data set of accurate estimates to the exact correlation energy of the neutral molecules in the G2 set which will be used to calibrate and test our new method.

Chapter 7 introduces and justifies our approach to calculating the correlation energy via phase-space intracules and some preliminary results are presented here.

Chapter 8 describes the technical detail of how this intracule based method may be cast in a self-consistent framework and the challenges faced in calculating the integrals involved. We present several approaches we have tried to do this.

In Chapter 9 results for all of the molecules in our data set, as well as all of the other G2 molecules will be analysed. All of the G2 reactions will be examined as well. From this we hope to gain insight into the strengths and weaknesses of our proposed scheme.

Chapter 10 will suggest future directions for this work and lay out the main conclusions, both positive and negative, of this research project.

Chapter 2

Distributions in position and momentum space

2.1 Position-space distributions

2.1.1 The wavefunction $\Psi(\mathbf{r}_1, \mathbf{r}_2, \ldots, \mathbf{r}_n)$

One of the most fundamental quantities in quantum chemistry is the wavefunction Ψ. Given the exact wavefunction we could extract any information about the molecule we wish. However, we very rarely have the exact wavefunction for a given system and even if we have a good approximation to it, these quantities are difficult to understand and manipulate. The wavefunction has 3-n dimensions, where n is the number of electrons and we have neglected the spin coordinates. Even for a modest sized system like methane the wavefunction has 30 dimensions - well outside any human's familiar 3-dimensional imagination. Besides the difficulty in interpreting a function of such high dimensionality, this also leads to computational overheads in handling such functions. Although many of the wavefunction based quantum chemical procedures can produce highly accurate results, this comes at comparably high computational expense.

2.1.2 The one-electron density $\rho(\mathbf{r})$

So, is there an alternative to the wavefunction? Most people who don't reside in the wavefunction camp are proponents of the one-electron density ρ. We have now gone to the other extreme – rather than consider the coordinates of all of the electrons, we now consider the coordinates of only one by integrating over all of the others

$$\rho(\mathbf{r}_1) = n \int |\Psi(\mathbf{r}_1, \mathbf{r}_2, \ldots, \mathbf{r}_n)|^2 \mathrm{d}\mathbf{r}_2 \ldots \mathrm{d}\mathbf{r}_n \tag{2.1}$$

In contrast to Ψ, ρ is quite an easy function to interpret. We can easily visualise it as it has only 3 dimensions and the interpretation is simply that $\rho(\mathbf{r})\mathrm{d}\mathbf{r}$ gives the probability of finding an electron in the volume element $\mathrm{d}\mathbf{r}$. With this reduction in dimensionality more computationally efficient methods can be developed, in particular the popular density functional theory.

2.1.3 The two-electron density $\rho_2(\mathbf{r}_1, \mathbf{r}_2)$

Have we lost too much information by limiting ourselves to looking at only one electron? Intuitively, it would seem more natural to look at electron pairs as it is these that are responsible for the formation of bonds and let us explain much of synthetic chemistry, and, more relevant to the current discussion, it seems more natural to try to explain the correlated motion of n electrons in terms of $\frac{1}{2}n(n-1)$ pairs rather than simply the probability of finding an electron at a point in space. To consider two electrons rather than one we simply omit the last integral in equation (2.1) to define the two-electron density

$$\rho_2(\mathbf{r}_1, \mathbf{r}_2) = \frac{n(n-1)}{2} \int |\Psi(\mathbf{r}_1, \mathbf{r}_2, \ldots, \mathbf{r}_n)|^2 \mathrm{d}\mathbf{r}_3 \ldots \mathrm{d}\mathbf{r}_n \tag{2.2}$$

$\rho_2(\mathbf{r}_1, \mathbf{r}_2)\mathrm{d}\mathbf{r}_1\mathrm{d}\mathbf{r}_2$ is easily interpreted as the probability of finding one electron in the volume element $\mathrm{d}\mathbf{r}_1$ and another in $\mathrm{d}\mathbf{r}_2$. Unfortunately this six-dimensional quantity is not so easy to visualise as the one electron density but is still much more comprehensible than the wavefunction.

2.1.4 Position intracules

When we consider pairs of electrons we are usually not interested in their absolute positions so much as their relative positions. In the electronic Hamiltonian, the two-electron term is concerned only with their relative positions and in explicitly correlated wavefunctions two-electron terms are again based around the relative position of the two electrons. So, perhaps, it would be useful to define a quantity which yields the probability of finding two electrons with a certain relative position. This quantity is termed the position intracule and is given by

$$P(u) = \frac{n(n-1)}{2}\langle\Psi|\delta(r_{12}-u)|\Psi\rangle = \int \rho_2(\mathbf{r}_1,\mathbf{r}_2)\delta(\mathbf{r}_{12}-\mathbf{u})\mathrm{d}\mathbf{r}_1\mathrm{d}\mathbf{r}_2\mathrm{d}\Omega_{\mathbf{u}} \qquad (2.3)$$

where $\mathbf{r}_{12} = \mathbf{r}_1 - \mathbf{r}_2$, $\Omega_{\mathbf{u}}$ is the angular part of $\mathbf{u}$ and $\delta(x)$ is the Dirac delta function. $P(u)$ gives the probability of finding two electrons separated by a distance u. We have now defined a one-dimensional quantity which retains two-electron information and is easily interpreted and visualised.

We have defined the position intracule as a spherically averaged quantity but much of the research in the field has focused on the non-spherically averaged position intracule

$$I(\mathbf{u}) = \int \rho_2(\mathbf{r}_1,\mathbf{r}_2)\delta(\mathbf{r}_{12}-\mathbf{u})\mathrm{d}\mathbf{r}_1\mathrm{d}\mathbf{r}_2 \qquad (2.4)$$

which now yields the probability of finding two electrons at a given separation and orientation $\mathbf{u}$. In much of the literature this is referred to as the position intracule but for the purpose of our work this title will always refer to the spherically averaged quantity shown in eqn (2.3). The intracule has a close relative which has also received considerable attention called the extracule which gives the distribution of the centre of mass $\frac{\mathbf{r}_1+\mathbf{r}_2}{2}$. This has not proved as useful or as insightful as the intracule and will not be discussed further in this work.

The position intracule has been discussed widely in the literature. The term intracule was introduced by Eddington in 1946 and was adopted into chemistry in 1961 in the seminal work of Coulson and Neilson [47]. Coulson and Neilson examined the position

intracule for helium using HF wavefunctions and also using progressively more correlated wavefunctions. By examining the differences between these intracules they were able to see the effect of electron correlation and visualise the Coulomb hole. This work will be reviewed further in section 5.2. In 1967 Coleman [48], in a much overlooked piece of work, strongly advocated the use of intracules and other two-electron quantities in quantum chemistry but unfortunately his suggestions were not widely adopted. He has gone on to be a strong proponent of DMRG methods.

In the last three decades position intracules have been studied extensively. Thakkar and co-workers derived electron cusp conditions for $P(u)$ [49] and examined intracules for the two-electron ions [50] and some diatomics [51]. Much of the work on intracules done by Sarasola, Ugalde, Wang, Fradera and others has focused on the comparison $I(\mathbf{u})$ derived from correlated and uncorrelated wavefunctions [52–61]. These analyses show visually and quantitatively the effects of correlation — that electron correlation lowers the energy by allowing the electrons to, on average, stay further apart. This is also borne out in the shifts in the moments of the intracules. Others have focused on the analysis, rather than comparison, of either correlated or uncorrelated intracules [56, 58, 62–65] to assess the quality of the wavefunctions and to gain insight into chemical bonding. Sarasola, Ugalde *et al.* [66–68] and Wang and Smith [69] presented formulae for the calculation of intracules, their moments and Laplacians. Cioslowski and Liu [70] developed a highly efficient algorithm to calculate $I(\mathbf{u})$ over large grids of points which also facilitated the efficient calculation of gradients and Hessians of the intracule. Lee and Gill [71] showed that, for HF wavefunctions, $P(u)$, its moments and derivatives could be calculated very efficiently using the PRISM approach [20] in an analogous way to the electron repulsion integrals. Using this approach they were able to produce intracules for large molecular systems. Koga and co-workers have published extensively [72–83], listing data pertaining to intracules and their moments, primarily for atomic systems. Much of this data is derived from highly correlated wavefunctions and may serve to test the quality of more approximate wavefunctions.

The position intracule is the generating kernel for expectation values of functions of r_{12}

$$\int_0^\infty f(u)P(u)\mathrm{d}u = \frac{n(n-1)}{2}\langle f(r_{12})\rangle \tag{2.5}$$

In particular the moments of the position intracule yield some physically significant quantities

$$\int_0^\infty u^{-1}P(u)\mathrm{d}u = E_J + E_K \tag{2.6}$$

$$\int_0^\infty u^{0}P(u)\mathrm{d}u = \frac{n(n-1)}{2} \tag{2.7}$$

where E_J and E_K are the Coulomb and exchange energies of the system respectively. If we confine ourselves to just the Coulomb contribution to the intracule, the even-order moments may be related to the multipoles of the molecule [64].

A simple example

To illustrate the interpretation of a position intracule we will consider a very simple example (further examples of all intracules will be given in chapter 5). If we consider the helium atom using a RHF wavefunction consisting of a single s-type Gaussian with exponent α (which is also the solution to the Schrödinger equation for a pair of uncoupled harmonic oscillators) the position intracule is given by

$$P(u) = \left(\frac{\alpha}{\pi}\right)^{\frac{3}{2}} 4\pi u^2 \exp(-\alpha u^2). \tag{2.8}$$

If we choose the value of the α which minimizes the HF energy of helium, $\alpha = \frac{33-8\sqrt{2}}{9\pi}$ the resulting intracule is shown in fig. 2.1. At the origin the intracule is zero as there is no probability of finding two electrons at the same point in space. It then grows quadratically until it reaches a maximum at $u = \alpha^{-1/2}$ and then decays quickly.

Figure 2.1: The position intracule for RHF/[1s] helium.

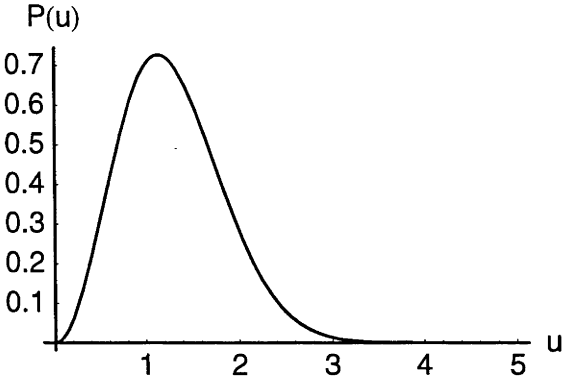

2.1.5 Momentum-space distributions

All of the quantities discussed so far, the wavefunction, the one-electron density and the two-electron densities have all been functions of the spatial coordinates of the electrons. Quantum mechanics can be equally well formulated in terms of the momenta of the particles and each of the distributions considered in the previous section have momentum space analogues. The wavefunctions in position and momentum space are related by a Fourier transform

$$\Phi(\mathbf{p}_1,\ldots,\mathbf{p}_n) = \left(\frac{1}{2\pi}\right)^{\frac{3n}{2}} \int \Psi(\mathbf{r}_1,\ldots,\mathbf{r}_n)\exp(i\mathbf{p}_1.\mathbf{r}_1+\ldots+i\mathbf{p}_n.\mathbf{r}_n)\mathrm{d}\mathbf{r}_1\ldots\mathrm{d}\mathbf{r}_n \qquad (2.9)$$

where the $\mathbf{p}_i$ are the coordinates of the electrons in momentum space. The one- and two-electron densities in momentum space can now be defined in the same way as their position-space analogues.

$$\pi(\mathbf{p}_1) = n\int |\Phi(\mathbf{p}_1,\mathbf{p}_2,\ldots,\mathbf{p}_n)|^2\mathrm{d}\mathbf{p}_2\ldots\mathrm{d}\mathbf{p}_n \qquad (2.10)$$

$$\pi_2(\mathbf{p}_1,\mathbf{p}_2) = \frac{n(n-1)}{2}\int |\Phi(\mathbf{p}_1,\mathbf{p}_2,\ldots,\mathbf{p}_n)|^2\mathrm{d}\mathbf{p}_3\ldots\mathrm{d}\mathbf{p}_n \qquad (2.11)$$

where $\pi(\mathbf{p})$ gives the probability of finding an electron with momentum $\mathbf{p}$ and $\pi_2(\mathbf{p}_1,\mathbf{p}_2)$ gives the probability of finding one electron with momentum $\mathbf{p}_1$ and another with $\mathbf{p}_2$.

2.1.6 Momentum intracules

Just as the position intracule gives the probability of finding two-electrons with a given separation we can define a momentum intracule which yields the probability of finding two electrons with a given relative momentum. It is given by

$$M(v) = \frac{n(n-1)}{2}\langle\Phi|\delta(p_{12}-v)|\Phi\rangle = \int \pi_2(\mathbf{p}_1,\mathbf{p}_2)\delta(\mathbf{p}_{12}-\mathbf{v})\mathrm{d}\mathbf{p}_1\mathrm{d}\mathbf{p}_2\mathrm{d}\Omega_{\mathbf{v}} \tag{2.12}$$

where $\mathbf{p}_{12} = \mathbf{p}_1 - \mathbf{p}_2$, $\Omega_{\mathbf{v}}$ is the angular part of $\mathbf{v}$, the relative momentum of the two electrons.

The momentum intracule has received less attention than its spatial counterpart. It was first studied by Banyard and Reed in 1978 [84] in work relating it to Compton scattering experiments. Banyard and co-workers [85–92] have examined the effect of correlation and the Coulomb hole in momentum space for small atoms in ground and excited states. Ugalde [93] and others [55,94] examined the effect of correlation on the momentum space distributions of some diatomics. Koga and co-workers have published prolificly [74, 75, 80–82,95–104], listing accurate values of the intracule and its moments for correlated and uncorrelated wavefunctions. Besley *et al.* [105] showed that for HF wavefunctions, the momentum intracule can be efficiently calculated for large molecules using the PRISM algorithm.

The momentum intracule is the generating kernel for expectation values of functions of p_{12}

$$\int_0^\infty f(v)M(v)\mathrm{d}v = \frac{n(n-1)}{2}\langle f(p_{12})\rangle \tag{2.13}$$

In particular the moments of the momentum intracule yield some useful quantities

$$\int_0^\infty v^0 M(v)\mathrm{d}v = \frac{n(n-1)}{2} \tag{2.14}$$

$$\int_0^\infty v^2 M(v)\mathrm{d}v = 2(n-1)E_T \tag{2.15}$$

where E_T is the electronic kinetic energy of the system.

Figure 2.2: The momentum intracule for RHF/[1s] helium.

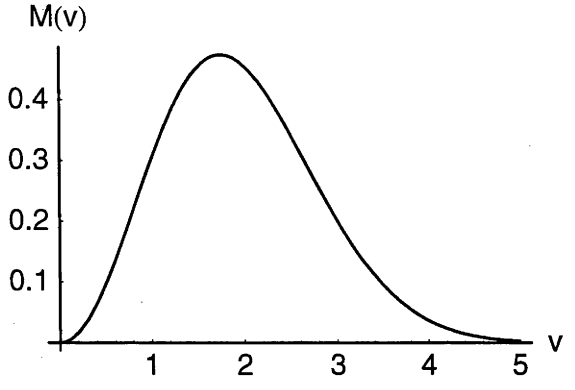

A simple example

Again we will consider the example of RHF/[1s] helium. The momentum intracule is given by

$$M(v) = \left(\frac{1}{4\pi\alpha}\right)^{\frac{3}{2}} 4\pi v^2 \exp\left(-\frac{v^2}{4\alpha}\right) \tag{2.16}$$

This is shown in fig. 2.2. The momentum intracule vanishes at the origin indicating that there is no chance of finding two electrons with identical momenta. It then grows quadratically to a maximum at $u = 2\alpha^{1/2}$ and then decays with increasing v. However it does so more slowly than in the position intracule indicating that the two electrons in helium can adopt a broader range of relative momenta than relative positions.

Chapter 3

Distributions in phase space

3.1 Phase space probability distributions

In the previous chapter we discussed position and momentum wavefunctions and densities and used them to define intracules in these two spaces. However, as can be gleaned from the moments of the two types of intracules they contain different information. This will become clearer in chapter 5 when some examples of intracules for simple systems are presented. With this in mind we ask whether it is possible to define a quantity which contains information about both the position *and* momentum of the electrons and yields more than either the position or momentum intracules alone?

When we began discussing intracules, we first introduced the wavefunctions and densities in position and momentum space. If we wish to investigate a joint position and momentum distribution must we first define a phase-space wavefunction? This, of course, is not possible due to Heisenberg's Uncertainty principle. We cannot write down a function which simultaneously gives the position and momentum of an electron. However it is possible to define a distribution which will have many of the properties one would expect from a phase-space wavefunction. For example, it will yield the correct expectation values with respect to any operators of position or momentum, and one should be able to extract from it both the correct position and momentum probability distributions. It should also be the

exact phase-space distribution when applied to classical mechanics. In 1932 Wigner [106] formulated such a distribution for application to a statistical mechanics problem. There are, in fact, an infinite number of such distributions but the simplest is known as Wigner's distribution and is given by

$$\begin{aligned} W(\mathbf{r}_1,\ldots,\mathbf{r}_n;\mathbf{p}_1,\ldots,\mathbf{p}_n) = &\frac{1}{\pi^{3n}}\int \Psi(\mathbf{r}_1+\mathbf{q}_1,\ldots,\mathbf{r}_n+\mathbf{q}_n;\sigma_1,\ldots,\sigma_2) \\ &\times \Psi^*(\mathbf{r}_1-\mathbf{q}_1,\ldots,\mathbf{r}_n-\mathbf{q}_n;\sigma_1,\ldots,\sigma_2)\mathrm{e}^{-2i(\mathbf{p}_1\cdot\mathbf{q}_1+\cdots+\mathbf{p}_n\cdot\mathbf{q}_n)} \\ &\times \mathrm{d}\mathbf{q}_1\ldots\mathrm{d}\mathbf{q}_n\mathrm{d}\sigma_1\ldots\mathrm{d}\sigma_2 \end{aligned} \tag{3.1}$$

where σ_i is the spin on electron i. The expression can be viewed as a "half"-Fourier transform, so that instead of transforming a position-space function all the way into a momentum-space function as a normal Fourier transform does, this leaves us with a function straddling both spaces. This distribution cannot be interpreted as a probability as it is not everywhere positive. However, we do not let this deter us from its usefulness — as mentioned earlier it has many of the properties one would expect if a true phase-space distribution existed. Also, the Wigner phase-space function contains neither more nor less information than the wavefunction [107] and the familiar position or momentum based quantum mechanics can be reformulated in terms of these phase space functions*.

Taking the Wigner distribution as our starting point we can now follow the same logic as in position and momentum space. First, let us define the reduced Wigner density as given by [107,108]

$$W_k(\mathbf{r}_1,\mathbf{p}_1,\ldots,\mathbf{r}_k,\mathbf{p}_k) = \int W(\mathbf{r}_1,\ldots,\mathbf{r}_n;\mathbf{p}_1,\ldots,\mathbf{p}_n)\mathrm{d}\mathbf{r}_{k+1}\ldots\mathrm{d}\mathbf{r}_n\mathrm{d}\mathbf{p}_{k+1}\ldots\mathrm{d}\mathbf{p}_n \tag{3.2}$$

Springborg and Dahl calculated the first-order Wigner density, $W_1(\mathbf{r},\mathbf{p})$ for the hydrogen atom [109] and then for other closed shell atoms [107] using HF wavefunctions. By reducing this function further to a function of r, p and u, the angle between $\mathbf{r}$ and $\mathbf{p}$, the function could be visualised at various u. These were shown to have large positive regions close to the origin and damped oscillations as r and p increase.

*It is noted that this is not the case for all phase-space distributions. For example the Husimi function is made everywhere positive by convolution with Gaussian functions. In this process, information is lost.

The distribution of interest in this work is the second-order, reduced Wigner function which can be written in terms of the second-order reduced density matrix

$$W_2(\mathbf{r}_1,\mathbf{p}_1,\mathbf{r}_2,\mathbf{p}_2) = \frac{1}{\pi^6}\int \rho_2(\mathbf{r}_1+\mathbf{q}_1,\mathbf{r}_1-\mathbf{q}_1,\mathbf{r}_2+\mathbf{q}_2,\mathbf{r}_2-\mathbf{q}_2)\mathrm{e}^{-2i(\mathbf{p}_1\cdot\mathbf{q}_1+\mathbf{p}_2\cdot\mathbf{q}_2)}\mathrm{d}\mathbf{q}_1\mathrm{d}\mathbf{q}_2 \quad (3.3)$$

This could equally be written in terms of the second-order reduced density matrix in momentum space $\pi_2(\mathbf{p}_1,\mathbf{p}_2)$.

3.2 The Wigner intracule

We now have a two-electron, phase-space distribution so this allows us to define a phase-space intracule. We define the Wigner intracule as

$$W(u,v) = \int W_2(\mathbf{r}_1,\mathbf{p}_1,\mathbf{r}_2,\mathbf{p}_2)\delta(\mathbf{r}_{12}-\mathbf{u})\delta(\mathbf{p}_{12}-\mathbf{v})\mathrm{d}\mathbf{r}_1\mathrm{d}\mathbf{r}_2\mathrm{d}\mathbf{p}_1\mathrm{d}\mathbf{p}_2\mathrm{d}\Omega_{\mathbf{u}}\mathrm{d}\Omega_{\mathbf{v}} \quad (3.4)$$

Like its parent distribution, the Wigner intracule is not everywhere positive and cannot rigorously be interpreted as a probability. Instead it is generally interpreted as the "quasi-probability" of finding two electrons separated by a distance u with relative momentum v. This formal lack of rigour should not dissuade us, however. On projection the Wigner intracule immediately yields the position and momentum intracules

$$P(u) = \int W(u,v)\mathrm{d}u \quad (3.5)$$

$$M(v) = \int W(u,v)\mathrm{d}v \quad (3.6)$$

and hence can also be used to extract the u^n and v^n moments of the position and momentum intracules. It is also a generating kernel for expectation values of functions of (r_{12},p_{12})

$$\int_0^\infty f(u,v)W(u,v)\mathrm{d}u\mathrm{d}v = \frac{n(n-1)}{2}\langle f(r_{12},p_{12})\rangle \quad (3.7)$$

Figure 3.1: The Wigner intracule for RHF/[1s] helium

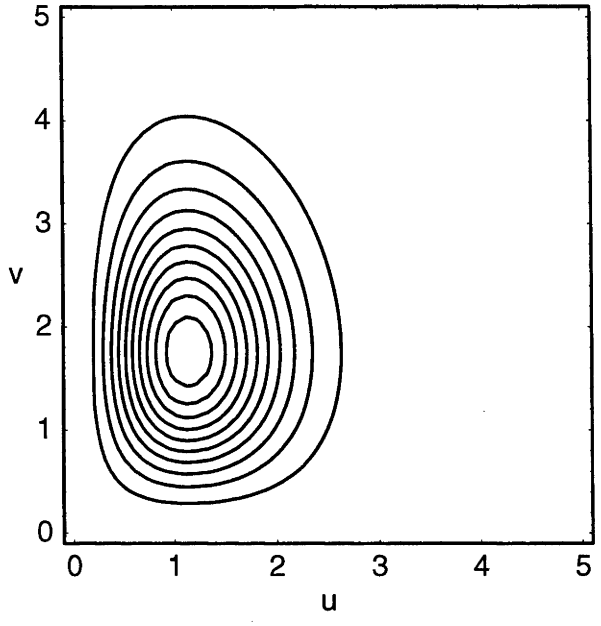

A simple example

Again we consider the RHF/[1s] helium atom. The Wigner intracule is given by

$$W(u,v) = \frac{2u^2v^2}{\pi} \exp\left(-\alpha u^2 - \frac{v^2}{4\alpha}\right) \tag{3.8}$$

This is shown in fig. 3.1. This simple example exhibits two atypical properties of the Wigner intracule. Firstly, it is simply the product of $P(u)$ and $M(v)$ and in all but the simplest cases this will not be so. Secondly, it is everywhere positive, and this is only the case when considering contributions to the HF intracule from electrons of opposite spin. So, in the case of singlet HF helium the Wigner intracule will be everywhere positive but triplet helium will contain negative regions. It is easy to see mathematically and diagrammatically that the marginal distributions are the position and momentum intracules. The Wigner intracule vanishes along the axes and has a single maximum at $(\alpha^{-1/2}, 2\alpha^{-1/2})$. As α is varied the maximum will trace out the hyperbola $uv = 2$.

Figure 3.2: The action intracule for RHF/[1s] helium.

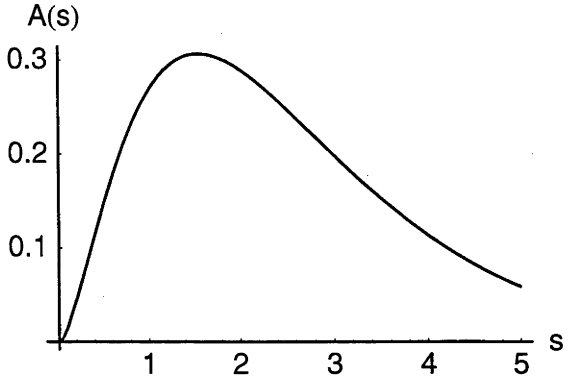

3.3 Action intracules

Finally, we define one more type of intracule. The coordinate of the action intracule is the product of the relative position and the relative momentum, $s = uv$ and by the appropriate substitution and integration is given by

$$A(s) = \int \frac{1}{u} W(u, \frac{s}{u}) \mathrm{d}u \tag{3.9}$$

Action intracules are generally rather featureless and the product of position and momentum is a less familiar quantity to us, so as a results they can be difficult to gain insight from. However, they will be of great importance later in this work. The action intracule is the generating kernel for expectation values of functions of $r_{12}p_{12}$

$$\int_0^\infty f(s)A(s)\mathrm{d}s = \frac{n(n-1)}{2}\langle f(r_{12}p_{12})\rangle \tag{3.10}$$

A simple example

The action intracule for RHF/[1s] helium is given by

$$A(s) = \frac{2s^2}{\pi} K_0(s) \tag{3.11}$$

where $K_0(s)$ is the zeroth-order modified Bessel function of the second kind. The action intracule is shown in fig. 3.2. It is interesting to observe that the action intracule is independent of α meaning that all of the two-electron ions, in this simple basis, will have identical action intracules. This makes physical sense because as the nuclear charge increases, the electrons are forced closer together, u decreases, and they must move faster relative to one another, v increases, but the product uv remains constant. The intracule vanishes at the origin and initially increases as $s^2 \log s$. There is a single maximum at $s \approx 1.55$ after which it decreases exponentially with s.

Chapter 4

Hartree-Fock intracules

So far the discussion has been limited to intracules derived from any given wavefunction, with some simple examples using minimal basis HF wavefunctions, but now we shall focus only on the one of primary interest to us, namely the HF wavefunction. Starting from eqn. (1.19) and integrating over spin it is easy to write the HF two-electron energy as

$$E_J + E_K = \frac{1}{2}\left(\sum_a^n \sum_b^n (\psi_a\psi_a|\psi_b\psi_b) - \sum_a^{n^\alpha} \sum_b^{n^\alpha} (\psi_a^\alpha\psi_b^\alpha|\psi_b^\alpha\psi_a^\alpha) - \sum_a^{n^\beta} \sum_b^{n^\beta} (\psi_a^\beta\psi_b^\beta|\psi_b^\beta\psi_a^\beta)\right) \tag{4.1}$$

where ψ_i^σ are the MOs of spin σ, n^σ is the number of electrons of spin σ, n is the total number of electrons and $(\psi_i\psi_j|\psi_k\psi_l)$ are the electron repulsion integrals. We define the HF intracule in an analogous way

$$Z = \frac{1}{2}\left(\sum_a^n \sum_b^n (\psi_a\psi_a\psi_b\psi_b)_Z - \sum_a^{n^\alpha} \sum_b^{n^\alpha} (\psi_a^\alpha\psi_b^\alpha\psi_b^\alpha\psi_a^\alpha)_Z - \sum_a^{n^\beta} \sum_b^{n^\beta} (\psi_a^\beta\psi_b^\beta\psi_b^\beta\psi_a^\beta)_Z\right) \tag{4.2}$$

where Z is the intracule of interest and $(\psi_i\psi_j\psi_k\psi_l)_Z$ is the associated MO integral. As usual, we expand the MOs in a basis of AOs

$$\psi_a(\mathbf{r}) = \sum_\mu C_{\mu a}\phi_\mu(\mathbf{r}) \tag{4.3}$$

which lets us express the MO integrals as

$$(\psi_a\psi_a\psi_b\psi_b)_Z = \sum_{\mu\nu\lambda\sigma} C^*_{\mu a}C^*_{\nu a}C_{\lambda b}C_{\sigma b}(\mu\nu\lambda\sigma)_Z \tag{4.4}$$

where $(\mu\nu\lambda\sigma)_Z$ are the integrals over the atomic basis functions for the required intracule. These will be discussed later for each of the intracules. Finally this gives us

$$Z = \frac{1}{2}\sum_{\mu\nu\lambda\sigma}\left[P_{\mu\nu}P_{\lambda\sigma} - P^{\alpha}_{\mu\sigma}P^{\alpha}_{\nu\lambda} - P^{\beta}_{\mu\sigma}P^{\beta}_{\nu\lambda}\right](\mu\nu\lambda\sigma)_Z \tag{4.5}$$

We note that this formulation can be generalized to arbitrary wavefunctions

$$Z = \sum_{\mu\nu\lambda\sigma}\Gamma_{\mu\nu\lambda\sigma}(\mu\nu\lambda\sigma)_Z \tag{4.6}$$

where $\Gamma_{\mu\nu\lambda\sigma}$ is the two-particle density matrix.

4.1 Partitioning HF intracules

Although we usually consider the intracule as a whole it is sometimes useful to analyse the different components of the intracule separately. A simple decomposition is that into parallel and anti-parallel spin components

$$Z = Z^{\alpha\beta} + Z^{\alpha\alpha} + Z^{\beta\beta} = Z^{\alpha\beta} + Z^{||} \tag{4.7}$$

where $Z^{\alpha\beta}$ is the anti-parallel component and $Z^{||} = Z^{\alpha\alpha} + Z^{\beta\beta}$ is the parallel component. These are easy to express in terms of the density matrices

$$Z^{\alpha\beta} = \sum_{\mu\nu\lambda\sigma} P^{\alpha}_{\mu\nu}P^{\beta}_{\lambda\sigma}(\mu\nu\lambda\sigma)_Z \tag{4.8}$$

$$Z^{\alpha\alpha} = \frac{1}{2}\sum_{\mu\nu\lambda\sigma}\left[P^{\alpha}_{\mu\nu}P^{\alpha}_{\lambda\sigma} - P^{\alpha}_{\mu\sigma}P^{\alpha}_{\nu\lambda}\right](\mu\nu\lambda\sigma)_Z \tag{4.9}$$

$$Z^{\beta\beta} = \frac{1}{2}\sum_{\mu\nu\lambda\sigma}\left[P^{\beta}_{\mu\nu}P^{\beta}_{\lambda\sigma} - P^{\beta}_{\mu\sigma}P^{\beta}_{\nu\lambda}\right](\mu\nu\lambda\sigma)_Z \tag{4.10}$$

4.2 Position Intracules

As mentioned in section 2.1.4, Lee and Gill [71] have described a method to rapidly evaluate position intracules derived from HF wavefunctions. It can be shown that for any operator which can be written as a function of r_{12} the PRISM algorithm can be invoked to evaluate the required integrals and this is exploited in the evaluation of the intracule.

The position integral over atomic basis functions is given by

$$(\mu\nu\lambda\sigma)_P = \int \phi^*_\mu(\mathbf{r})\phi^*_\nu(\mathbf{r})\phi_\lambda(\mathbf{r}+\mathbf{u})\phi_\sigma(\mathbf{r}+\mathbf{u})\mathrm{d}\mathbf{r}\mathrm{d}\Omega_\mathbf{u} \tag{4.11}$$

For four Gaussian s-type basis functions this is straightforward to evaluate in closed form and higher angular momentum integrals are generated recursively. As with electron repulsion integrals, position integrals have eight-fold permutational symmetry

$$\begin{aligned}(\mu\nu\lambda\sigma)_P = (\mu\nu\sigma\lambda)_P = (\nu\mu\lambda\sigma)_P = (\nu\mu\sigma\lambda)_P \\ = (\lambda\sigma\mu\nu)_P = (\lambda\sigma\nu\mu)_P = (\sigma\lambda\mu\nu)_P = (\sigma\lambda\nu\mu)_P\end{aligned} \tag{4.12}$$

4.3 Momentum Intracules

In an analogous way to the position intracule, Besley, *et al.* [105] have shown that momentum intracules derived from HF wavefunctions can be rapidly evaluated using the PRISM algorithm. The momentum integrals over atomic basis functions are given by

$$(\mu\nu\lambda\sigma)_M = \frac{v^2}{2\pi^2}\int \phi^*_\mu(\mathbf{r})\phi^*_\nu(\mathbf{r}+\mathbf{q})\phi_\lambda(\mathbf{u}+\mathbf{q})\phi_\sigma(\mathbf{u})j_0(qv)\mathrm{d}\mathbf{r}\mathrm{d}\mathbf{q}\mathrm{d}\mathbf{u} \tag{4.13}$$

where $j_0(z)$ is the zeroth-order spherical Bessel function. For four s-type Gaussian functions this is straightforward to evaluate in closed form and higher angular momentum integrals are evaluated recursively. Momentum integrals, unlike position integrals, do not

possess eight-fold symmetry, but only four-fold

$$\begin{aligned}(\mu\nu\lambda\sigma)_M &= (\mu\nu\sigma\lambda)_M = (\nu\mu\lambda\sigma)_M = (\nu\mu\sigma\lambda)_M \\ (\lambda\sigma\mu\nu)_M &= (\lambda\sigma\nu\mu)_M = (\sigma\lambda\mu\nu)_M = (\sigma\lambda\nu\mu)_M\end{aligned} \tag{4.14}$$

Hence, the cost of computing a momentum intracule will be approximately twice that of computing a position intracule.

4.4 Wigner Intracules

Recalling from section 3.2 that the Wigner intracule is given by

$$W(u,v) = \int W_2(\mathbf{r}_1,\mathbf{p}_1,\mathbf{r}_2,\mathbf{p}_2)\delta(\mathbf{r}_{12}-\mathbf{u})\delta(\mathbf{p}_{12}-\mathbf{v})\mathrm{d}\mathbf{r}_1\mathrm{d}\mathbf{r}_2\mathrm{d}\mathbf{p}_1\mathrm{d}\mathbf{p}_2\mathrm{d}\Omega_{\mathbf{u}}\mathrm{d}\Omega_{\mathbf{v}} \tag{4.15}$$

$$\begin{aligned}= \frac{1}{\pi^6}\int \rho_2(\mathbf{r}_1+\mathbf{q}_1,\mathbf{r}_1-\mathbf{q}_1,\mathbf{r}_2+\mathbf{q}_2,\mathbf{r}_2-\mathbf{q}_2)\mathrm{e}^{-2i(\mathbf{p}_1\cdot\mathbf{q}_1+\mathbf{p}_2\cdot\mathbf{q}_2)} \\ \times\delta(\mathbf{r}_{12}-\mathbf{u})\delta(\mathbf{p}_{12}-\mathbf{v})\mathrm{d}\mathbf{q}_1\mathrm{d}\mathbf{q}_2\mathrm{d}\mathbf{r}_1\mathrm{d}\mathbf{r}_2\mathrm{d}\mathbf{p}_1\mathrm{d}\mathbf{p}_2\mathrm{d}\Omega_{\mathbf{u}}\mathrm{d}\Omega_{\mathbf{v}}\end{aligned} \tag{4.16}$$

Starting with the integral

$$\begin{aligned}&\int \mathrm{e}^{-2\mathrm{i}(\mathbf{p}_1\cdot\mathbf{q}_1+\mathbf{p}_2\cdot\mathbf{q}_2)}\delta(\mathbf{p}_{12}-\mathbf{v})\mathrm{d}\mathbf{p}_1\mathrm{d}\mathbf{p}_2\mathrm{d}\Omega_{\mathbf{v}} \\ &\qquad = \left(\int \mathrm{e}^{-2\mathrm{i}\mathbf{p}_1\cdot(\mathbf{q}_1+\mathbf{q}_2)}\mathrm{d}\mathbf{p}_1\right)\left(\int \mathrm{e}^{-2\mathrm{i}\mathbf{v}\cdot\mathbf{q}_2}\mathrm{d}\Omega_{\mathbf{v}}\right) \\ &\qquad = 4\pi^4 v^2 j_0(2q_1v)\delta(\mathbf{q}_1+\mathbf{q}_2)\end{aligned} \tag{4.17}$$

which when inserted into eqn. (4.16) leads to

$$W(u,v) = \frac{v^2}{2\pi^2}\int \rho_2(\mathbf{r},\mathbf{r}+\mathbf{q},\mathbf{r}+\mathbf{q}+\mathbf{u},\mathbf{r}+\mathbf{u})j_0(qv)\mathrm{d}\mathbf{r}\mathrm{d}\mathbf{q}\mathrm{d}\Omega_{\mathbf{u}} \tag{4.18}$$

The Wigner integral for four atomic basis functions is given by

$$(\mu\nu\lambda\sigma)_W = \frac{v^2}{2\pi^2}\int \phi^*_\mu(\mathbf{r})\phi^*_\nu(\mathbf{r}+\mathbf{q})\phi_\lambda(\mathbf{r}+\mathbf{q}+\mathbf{u})\phi_\sigma(\mathbf{r}+\mathbf{u})j_0(qv)\mathrm{d}\mathbf{r}\mathrm{d}\mathbf{q}\mathrm{d}\Omega_{\mathbf{u}} \tag{4.19}$$

Given four unnormalized s-type Gaussian functions on centres **A**, **B**, **C** and **D** with exponents α, β, γ and δ respectively the $[ssss]_W$ integral is

$$[ssss]_W = \frac{v^2}{2\pi^2}\iiint \exp\big(-\alpha|\mathbf{r}-\mathbf{A}|^2-\beta|\mathbf{r}+\mathbf{q}-\mathbf{B}|^2 - \gamma|\mathbf{r}+\mathbf{q}+\mathbf{u}-\mathbf{C}|^2-\delta|\mathbf{r}+\mathbf{u}-\mathbf{D}|^2\big)\, j_0(qv)\mathrm{d}\mathbf{r}\mathrm{d}\mathbf{q}\mathrm{d}\Omega_{\mathbf{u}} \tag{4.20}$$

Introducing

$$\lambda^2 = \frac{\alpha\delta}{\alpha+\delta}+\frac{\beta\gamma}{\beta+\gamma} \tag{4.21}$$

$$\mu^2 = \frac{1}{4}\left(\frac{1}{\alpha+\delta}+\frac{1}{\beta+\gamma}\right) \tag{4.22}$$

$$\eta = \frac{\alpha}{\alpha+\delta}-\frac{\beta}{\beta+\gamma} \tag{4.23}$$

$$\mathbf{P} = \frac{2\alpha\delta}{\alpha+\delta}(\mathbf{A}-\mathbf{D})+\frac{2\beta\gamma}{\beta+\gamma}(\mathbf{B}-\mathbf{C}) \tag{4.24}$$

$$\mathbf{Q} = \frac{\alpha\mathbf{A}+\delta\mathbf{D}}{\alpha+\delta}-\frac{\beta\mathbf{B}+\gamma\mathbf{C}}{\beta+\gamma} \tag{4.25}$$

$$R = \frac{\alpha\delta}{\alpha+\delta}|\mathbf{A}-\mathbf{D}|^2+\frac{\beta\gamma}{\beta+\gamma}|\mathbf{B}-\mathbf{C}|^2 \tag{4.26}$$

$$\mathbf{V} = \frac{(\gamma+\delta)\mathbf{u}+(\beta+\gamma)\mathbf{q}-(\alpha\mathbf{A}+\beta\mathbf{B}+\gamma\mathbf{C}+\delta\mathbf{D})}{\alpha+\beta+\gamma+\delta} \tag{4.27}$$

leads to

$$[ssss]_W = \frac{v^2\mathrm{e}^{-(R+\lambda^2u^2)}}{2\pi^2}\int \mathrm{e}^{-\mathbf{P}.\mathbf{u}}\exp\left(-\frac{|\mathbf{q}-(\mathbf{Q}+\eta\mathbf{u})|^2}{4\mu^2}-(\alpha+\beta+\gamma+\delta)|\mathbf{r}+\mathbf{V}|^2\right) \times j_0(qv)\mathrm{d}\mathbf{r}\mathrm{d}\mathbf{q}\mathrm{d}\Omega_{\mathbf{u}} \tag{4.28}$$

Integrating over **r** and **q** is straightforward and yields

$$[ssss]_W = \frac{\pi v^2\mathrm{e}^{-(R+\lambda^2u^2+\mu^2v^2)}}{2(\alpha+\delta)^{3/2}(\beta+\gamma)^{3/2}}\int \mathrm{e}^{-\mathbf{P}.\mathbf{u}} j_0(|\mathbf{Q}+\eta\mathbf{u}|v)\mathrm{d}\Omega_{\mathbf{u}} \tag{4.29}$$

These integrals can be performed by quadrature and this will be discussed in section 4.5. If **Q** is chosen to lie on the z-axis and **P** to lie in the yz-plane and $\angle\mathbf{QOP} = \omega$ then

$$\mathbf{P}.\mathbf{u} = Pu(\cos\omega\cos\theta+\sin\omega\sin\theta\sin\phi) \tag{4.30}$$

$$|\mathbf{Q}+\eta\mathbf{u}| = \sqrt{Q^2+\eta^2u^2+2\eta Qu\cos\theta} \tag{4.31}$$

where θ and ϕ are the angular dimensions of $\mathbf{u}$. The integral over ϕ is straightforward

$$\int_0^{2\pi} \exp(Pu\sin\omega\sin\theta\sin\phi)\mathrm{d}\phi = 2\pi I_0\left(Pu\sin\omega\sin\theta\right) \tag{4.32}$$

where $I_0(z)$ is the zeroth-order modified Bessel function [21]. The final integral can be performed using the Addition Theorem [21]

$$j_0(\lambda|\mathbf{A}-\mathbf{B}|) = \sum_{n=0}^{\infty}(2n+1)j_n(\lambda A)j_n(\lambda B)P_n\left(\frac{\mathbf{A}.\mathbf{B}}{AB}\right) \tag{4.33}$$

and the following integral

$$\begin{aligned}\int_0^{\pi} \exp\left(Pu\cos\omega\cos\theta\right) I_0\left(Pu\sin\omega\sin\theta\right)P_n(\cos\theta)\sin\theta\mathrm{d}\theta \\ = (-1)^n 2i_n(Pu)P_n(\cos\omega)\end{aligned} \tag{4.34}$$

where $P_n(z)$ is the nth Legendre polynomial [21], not to be confused with the vector $\mathbf{P}$. This yields

$$[ssss]_W = \frac{2\pi^2 v^2 \mathrm{e}^{-(R+\lambda^2u^2+\mu^2v^2)}}{(\alpha+\delta)^{3/2}(\beta+\gamma)^{3/2}}\sum_{n=0}^{\infty}(2n+1)i_n(Pu)j_n(Qv)j_n(\eta uv)P_n\left(\frac{\mathbf{P}.\mathbf{Q}}{PQ}\right) \tag{4.35}$$

Besley [110] has implemented this for s- and p-functions in Q-CHEM [111].

In the case where $\mathbf{P}$ or $\mathbf{Q}$ are equal to zero the following form should be used

$$\begin{aligned}[ssss]_W =& \frac{2\pi^2 v^2 \mathrm{e}^{-(R+\lambda^2u^2+\mu^2v^2)}}{(\alpha+\delta)^{3/2}(\beta+\gamma)^{3/2}} \\ &\times\sum_{n=0}^{\infty}(2n+1)u^n v^n \frac{i_n(Pu)}{(Pu)^n}\frac{j_n(Qv)}{(Qv)^n}j_n(\eta uv)\left[(PQ)^n P_n\left(\frac{\mathbf{P}.\mathbf{Q}}{PQ}\right)\right]\end{aligned} \tag{4.36}$$

to avoid division by zero. In the case were $P = 0$ or $Q = 0$ the infinite series truncates after $(L+1)$ terms, where L is the total angular momentum of the integral. Even with this simplification, the integrals are tedious to generate. For example a $[p_x sss]$ integral is

given by

$$
\begin{aligned}
[p_x sss]_W &= \frac{1}{2\alpha}\Big\{ -\frac{\alpha\delta}{\alpha+\delta}(A_x - D_x)[0] + u^2\frac{2\alpha\delta}{\alpha+\delta}P_x[1]_i \\
&\quad -v^2\frac{\alpha}{\alpha+\delta}Q_x[1]_j + \left(\frac{\alpha}{\alpha+\delta}P_x + \frac{2\alpha\delta}{\alpha+\delta}Q_x\right)[1]_P\Big\} \qquad (4.37)\\
[0] &= \frac{2\pi^2u^2v^2\mathrm{e}^{-(R+\lambda^2u^2+\mu^2v^2)}}{(\alpha+\delta)^{3/2}(\beta+\gamma)^{3/2}} i_0(Pu)j_0(Qv)j_0(\eta uv) \qquad (4.38)\\
[1]_i &= \frac{2\pi^2u^2v^2\mathrm{e}^{-(R+\lambda^2u^2+\mu^2v^2)}}{(\alpha+\delta)^{3/2}(\beta+\gamma)^{3/2}} \frac{i_1(Pu)}{Pu} j_0(Qv)j_0(\eta uv) \qquad (4.39)\\
[1]_j &= \frac{2\pi^2u^2v^2\mathrm{e}^{-(R+\lambda^2u^2+\mu^2v^2)}}{(\alpha+\delta)^{3/2}(\beta+\gamma)^{3/2}} i_0(Pu)\frac{j_0(Qv)}{Qv} j_0(\eta uv) \qquad (4.40)\\
[1]_P &= \frac{2\pi^2u^2v^2\mathrm{e}^{-(R+\lambda^2u^2+\mu^2v^2)}}{(\alpha+\delta)^{3/2}(\beta+\gamma)^{3/2}} \frac{i_1(Pu)}{Pu}\frac{j_1(Qv)}{Qv}(3uv)j_1(\eta uv) \qquad (4.41)
\end{aligned}
$$

As part of this work this has been implemented for s- and p-type functions in Q-CHEM.

Wigner integrals, like momentum integrals, have only four-fold permutational symmetry

$$
\begin{aligned}
(\mu\nu\lambda\sigma)_W &= (\mu\nu\sigma\lambda)_W = (\nu\mu\lambda\sigma)_W = (\nu\mu\sigma\lambda)_W \\
(\lambda\sigma\mu\nu)_W &= (\lambda\sigma\nu\mu)_W = (\sigma\lambda\mu\nu)_W = (\sigma\lambda\nu\mu)_W
\end{aligned} \qquad (4.42)
$$

4.5 Evaluating Wigner integrals using quadrature

To evaluate numerically an integral of the form

$$
I = \int_0^{2\pi} \mathrm{d}\phi \int_0^{\pi} \mathrm{d}\theta f(\theta,\phi)\sin\theta, \qquad (4.43)
$$

where θ is the polar angle and ϕ the azimuthal angle in spherical polar coordinates, an angular quadrature rule is used. In a similar way to one-dimensional Gaussian quadrature, which is characterized by the highest degree of a particular orthogonal polynomial which it can integrate exactly, angular quadrature is characterized by the highest degree L of spherical harmonic $Y_l^m(\theta,\phi)$ up to which it obtains the exact result. The two angular grids available in the Q-CHEM package are the Lebedev [112–114] grids and the Gauss-Legendre grids.

Lebedev grids have been devised specifically for this type of quadrature using the octahedral group. They have been computed up to degree $L = 125$ (5294 points). Gauss-Legendre grids are the product of separate θ and ϕ grids. The former being derived from a Gaussian quadrature rule using the Legendre polynomials and the latter being an equally spaced grid. The advantage of the Gauss-Legendre scheme is that any grid size can be specified whereas we are limited to the Lebedev grids which have been constructed previously. However, Lebedev quadrature is known to require approximately two-thirds as many points as Gauss-Legendre to obtain similar accuracy, and with the large grids available in Q-CHEM we have used only Lebedev quadrature in the evaluation of integrals. This type of angular grid, in combination with a radial grid, is also used in the three-dimensional molecular quadrature required in DFT.

The Wigner integral can be written in the above form where

$$\begin{aligned} f(\theta,\phi) &= \frac{\pi u^2 v^2 \mathrm{e}^{-(R+\lambda^2 u^2+\mu^2 v^2)}}{2(\alpha+\delta)^{3/2}(\beta+\gamma)^{3/2}} \mathrm{e}^{-(P_x u_x+P_y u_y+P_z u_z)} \\ &\quad \times j_0\left(\sqrt{(Q_x+\eta u_x)^2+(Q_y+\eta u_y)^2+(Q_z+\eta u_z)^2}\right) \qquad (4.44) \\ u_x &= u\cos\phi\sin\theta \qquad (4.45) \\ u_y &= u\sin\phi\sin\theta \qquad (4.46) \\ u_z &= u\cos\theta \qquad (4.47) \end{aligned}$$

The major advantage of writing the Wigner integral in this form is in the generation of integrals of higher angular momentum. The infinite series formulation leads to successively more complicated and tedious expressions as the geometrical parameters appear inside square roots. However, the above expression is much less complicated due to the following differential property of Bessel functions

$$\begin{aligned} \frac{\partial}{\partial x} g_n\left(\sqrt{f(x)}\right) &= -\frac{g_{n+1}\left(\sqrt{f(x)}\right)}{2}\frac{\partial}{\partial x} f(x) \qquad (4.48) \\ g_n(x) &= \frac{j_n(x)}{x^n} \qquad (4.49) \end{aligned}$$

Hence the square roots must never be differentiated explicitly. Using this expression,

Table 4.1: Convergence of four points on the HF/6-311G intracule for ethene with increasing Lebedev grid size. The exact results are obtained from the series expansion

Grid	$W(1,1)$	$W(1,4)$	$W(4,1)$	$W(4,4)$
6	1.428210792	2.315903870	12.050144049	3.330809610
74	1.415070359	2.644503481	7.940815642	2.024274600
194	1.415070336	2.264503426	7.952388673	1.847231337
302	1.415070336	2.264503426	7.951761663	1.839467059
590	1.415070336	2.264503426	7.952573144	1.849946553
974	1.415070336	2.264503426	7.952532473	1.849439804
1454	1.415070336	2.264503426	7.952521929	1.849294392
2030	1.415070336	2.264503426	7.952529619	1.849395320
5294	1.415070336	2.264503426	7.952527680	1.849370626
Exact	1.415070336	2.264503426	7.952527682	1.849370666

integrals of higher angular momentum are greatly simplified in comparison with those from the infinite series [105] and all required integrals for s- and p-functions have been generated and implemented in Q-CHEM. For example the following is a $[p_x sss]$ type integral (with all of the non-geometric terms omitted for conciseness)

$$\begin{aligned}\frac{1}{2\alpha}\frac{\partial}{\partial A_x}\left\{\mathrm{e}^{-R}\int \mathrm{e}^{-\mathbf{P}.\mathbf{u}} j_0(|\mathbf{Q}+\eta\mathbf{u}|)\mathrm{d}\Omega_{\mathbf{u}}\right\} = \\ -\frac{\delta}{\alpha+\delta}(A_x-D_x)\mathrm{e}^{-R}\int \mathrm{e}^{-\mathbf{P}.\mathbf{u}} j_0(|\mathbf{Q}+\eta\mathbf{u}|)\mathrm{d}\Omega_{\mathbf{u}} \\ -\frac{\delta}{\alpha+\delta}P_x\mathrm{e}^{-R}\int u_x \mathrm{e}^{-\mathbf{P}.\mathbf{u}} j_0(|\mathbf{Q}+\eta\mathbf{u}|)\mathrm{d}\Omega_{\mathbf{u}} \\ -\frac{1}{\alpha+\delta}v^2 Q_x \mathrm{e}^{-R}\int \mathrm{e}^{-\mathbf{P}.\mathbf{u}}\frac{j_1(|\mathbf{Q}+\eta\mathbf{u}|}{2|\mathbf{Q}+\eta\mathbf{u}|v}\mathrm{d}\Omega_{\mathbf{u}}\end{aligned} \tag{4.50}$$

Even though these integrals are more straightforward, generating them for arbitrary angular momentum is tedious and error-prone and this has not been done. The ideal solution to this would be to find a recurrence relation to generate higher order integrals but as of yet we have been unable to find such a relation.

Although quadrature often provides a practical and simple route to addressing difficult integrals it suffers from two serious downfalls. The first is accuracy. Table 4.1 shows how four (u,v) points on the HF/6311G intracule for ethene converge with grid size. At the points $(1,1)$ and $(1,4)$ convergence to ten significant figures is achieved using the relatively modest 194-point grid. However, at the points $(4,1)$ and $(4,4)$ the highest

accuracy which can be achieved is nine and eight significant figures respectively. The source of the problem can be traced to increasing values of u. The term $e^{\mathbf{P}.\mathbf{u}} = e^{Pu\cos\theta}$ cannot easily be represented by spherical harmonics of low degree as P and/or u become large. Hence, to obtain accurate results large grids are required.

The second problem from which quadrature suffers is efficiency. At every point across the grid the integrand must be evaluated. In the simplest case, an $[ssss]$-type integral, this requires the evaluation of several trigonometric functions, an exponential, a square root, several arithmetic operations and, computationally most intensive, a spherical Bessel function. Depending on the value of the argument [115, 116], the Bessel function is evaluated by series expansion or the trigonometric form of the function. Higher order Bessel functions are calculated via recurrence. Integrals of higher angular momentum require far more function evaluations. If results of high accuracy are required using large grids and basis sets, the time to evaluate the Wigner intracule will be prohibitive. In practice the 302-point grid is used and any errors in the resulting Wigner intracules are visually undetectable when the intracule is plotted but numerical analysis is treated with caution.

4.5.1 Efficiency

In the implementation of the position and momentum integrals the loop structure, i.e., locating the loop over u or v points inside or outside the loop over shell quartets, is vital to the performance of the algorithm. Locating the loop over u or v points inside the loop over shell-quartets has been shown to be optimal [70, 71, 105]. However, in the case of calculating Wigner intracules using quadrature this is less of a concern. The expense of calculating a single integral is so overwhelming that the savings gained from an optimal loop structure are negligible. A similar loop structure to that used for position and momentum intracules would be favourable but in the case of the infinite series formulation this requires a prohibitive amount of memory [110]. Both loop structures have been implemented within Q-CHEM.

A more plausible method of increasing the efficiency of evaluating the Wigner intracule is to attempt to avoid the calculation integrals which have a negligible contribution. Starting

Figure 4.1: The first three members of the graphene series

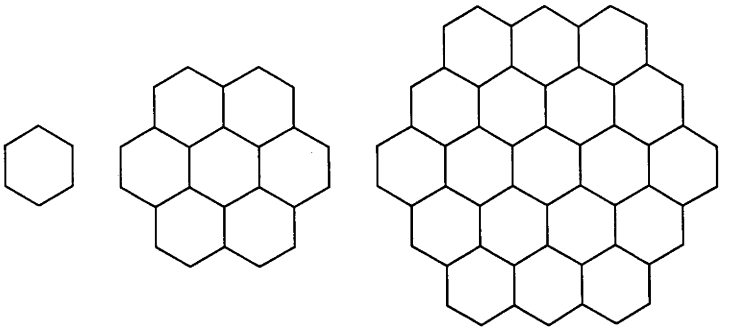

(a) (b) (c)

from eqn. (4.29) and noting that $|j_0(x)| \leq 1$, it follows that

$$\begin{aligned}
[ssss]_W &\leq \frac{\pi u^2 v^2}{2(\alpha+\delta)^{3/2}(\beta+\gamma)^{3/2}} e^{-R-\lambda^2u^2-\mu^2v^2} \int e^{\mathbf{P}.\mathbf{u}} d\Omega_{\mathbf{u}} \\
&= \frac{\pi^2 u^2 v^2}{(\alpha+\delta)^{3/2}(\beta+\gamma)^{3/2}} e^{-R-\lambda^2u^2-\mu^2v^2} \left(\frac{e^{Pu}-e^{-Pu}}{Pu}\right) \\
&\leq \frac{\pi^2 u^2 v^2}{2(\alpha+\delta)^{3/2}(\beta+\gamma)^{3/2}} \\
&\quad \exp\left(-\frac{\alpha\delta}{\alpha+\delta}(|\mathbf{A}-\mathbf{D}|-u)^2 - \frac{\beta\gamma}{\beta+\gamma}(|\mathbf{B}-\mathbf{C}|-u)^2 - \frac{v^2}{4(\alpha+\delta)} - \frac{v^2}{4(\beta+\gamma)}\right)
\end{aligned} \tag{4.51}$$

This upper bound shows that there are $\mathcal{O}(M^2)$ significant integrals which must be calculated.

More useful than this theoretical scaling is to know how the method will scale in practice. By looking at a selection of graphenes (graphitic fragments of formula $C_{6n^2}H_{6n}$ with D_{6h} symmetry. See figure 4.1) we can see how the number of significant integrals scales with the size of the molecule. We note that these planar systems will show more favourable scaling than 3-dimensional systems but they serve to illustrate the point. 11 and 5 primitive s-type basis functions have been placed on each carbon and hydrogen respectively. The exponents have been taken from all of the functions in the 6-31++G basis set [117, 118]. The C-C and C-H bond lengths are 1.38Å and 1.08Å respectively. Integrals which have a magnitude greater than 10^{-8} are considered non-negligible.

Figure 4.2 shows logarithmically how the number of significant integrals behaves with

Figure 4.2: To examine the number of significant integrals I with the size of basis set M. The number of significant integrals is averaged over 25 (u, v) points

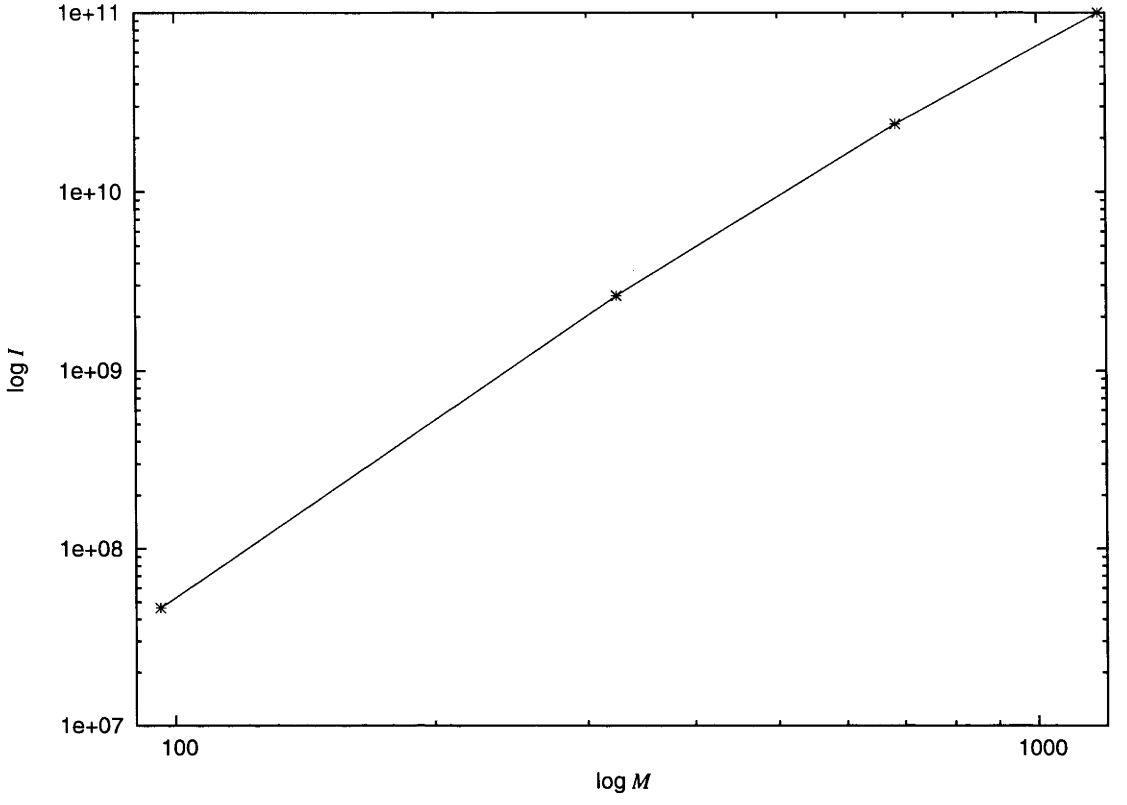

basis set size. The first segment of the plot has slope 3.3 compared to the last which has slope 2.6, suggesting that the M^2 scaling is being approached. By comparing the value of the bound to the exact integral we can estimate the strength of the bound. For benzene the bound predicts that there are 4.62×10^7 integrals which must be evaluated whereas there are actually only 1.96×10^7, so the bound is causing the calculation of $\sim 135\%$ extra integrals.

4.6 Action intracules

Evaluating the action intracule directly has proven a difficult task. In fact for the case of the action integral for four s-type Gaussians, a practical formula has not been obtained. In the special case of concentric integrals, Gill has derived formulae in terms of modified Bessel functions of the second kind $K_n(z)$ and these have been used to generate intracules

for atoms. For example, for four concentric s-functions

$$[ssss]_A = \frac{2\pi^2 s^2}{(\alpha+\delta)^{3/2}(\beta+\gamma)^{3/2}} K_0(2\lambda\mu s) j_0(\eta s) \tag{4.52}$$

In the more general case we must resort to integrating the Wigner intracule numerically.

$$A(s) = \int W(u, \frac{s}{u}) \frac{1}{u} \mathrm{d}u \tag{4.53}$$

To evaluate this integral accurately a carefully selected grid of (u, v) points should be chosen such that the spacings along the hyperbola uv correspond to an appropriate quadrature scheme. We have been interested only in the qualitative features of the action intracule and so used MATHEMATICA [119] to interpolate and numerically integrate the Wigner intracule to obtain the action intracule. Some examples of action intracules generated this way are shown in chapter 5. The numerics of such an approach should not be relied on.

Chapter 5

Some examples of intracules

5.1 Atomic intracules

5.1.1 Two-electron ions

In figure 5.1.1 the HF Wigner intracules for the two-electron ions from $Z = 2 - 10$ are shown. Each one possesses a single peak corresponding to relative position and momentum at which there is the highest probability of finding the electron pair. There are several other noteworthy observations. Firstly these intracules are everywhere positive. This is the case in all intracules which contain only contributions from electrons of opposite spin. Secondly, as the nuclear charge increases the peak moves to larger v and smaller u as the electrons are brought closer together but move more rapidly. There is also an elongation of the peak that can be attributed to the Heisenberg Uncertainty principle — as the position of the two electrons becomes more defined, the momentum is less well defined. Finally, it is worth noting that the position of the maxima lie approximately along the hyperbola $uv = 1.8$. Each of the ions will have almost identical action intracules.

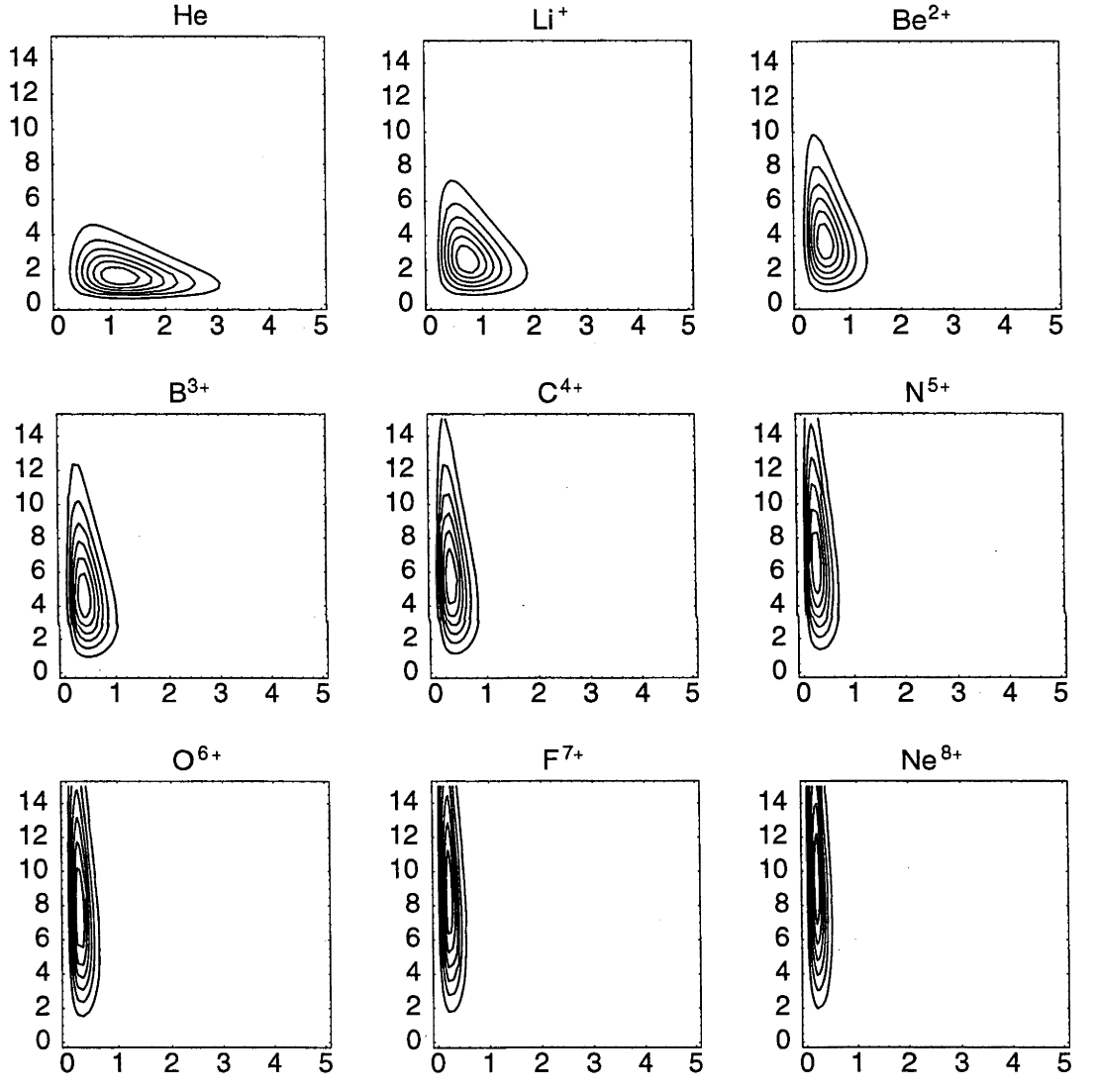

Figure 5.1: The HF/6-311G Wigner intracules for the two-electron ions from He to Ne^{8+}

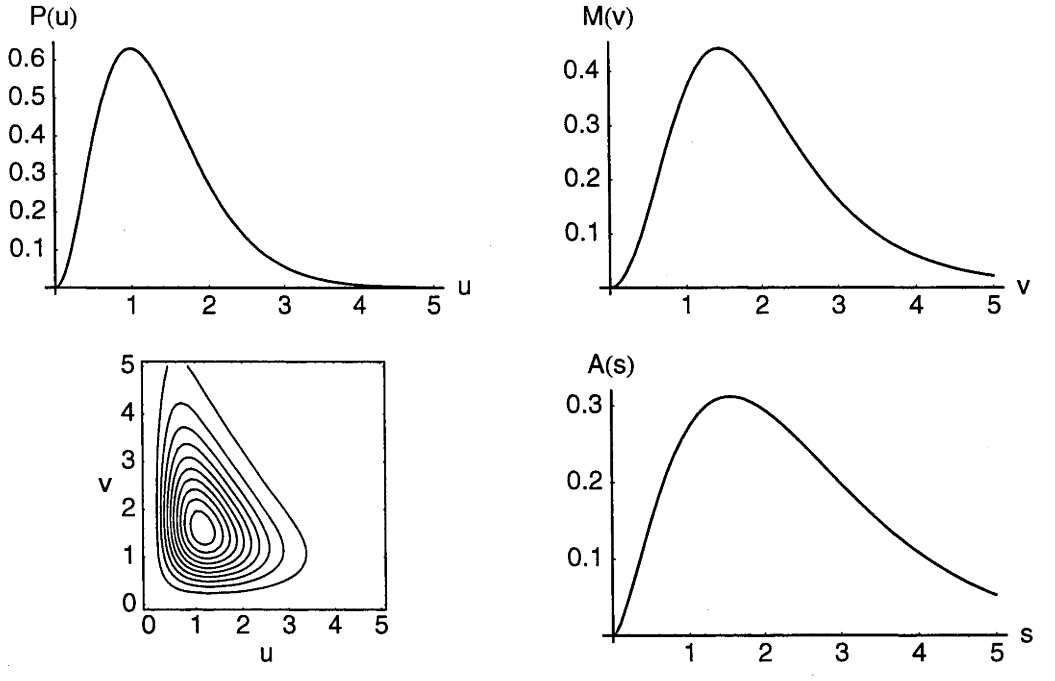

Figure 5.2: The HF/6-311G position, momentum, Wigner and action intracules for He

5.1.2 Helium, Lithium, Beryllium and Neon

Helium

Figure 5.2 shows the position, momentum, Wigner and action intracules for the helium atom. Each of the intracules exhibits a single peak corresponding to the highest likelihood of finding the two electrons at $u \approx 1.0$, $v \approx 1.5$, $(u, v) \approx (1.1, 1.6)$ and $s \approx 1.5$. It is also easy to see that the Wigner intracule will yield the position or momentum intracule when integrated with respect to v or u.

Lithium

Figure 5.3 shows the four intracules for the lithium atom. The position intracule shows two clear peaks – the peak at $u \approx 0.6$ corresponds to the two electrons in the small inner $1s$ orbital. The second peak at $u \approx 3.1$ is due to one of the electrons in the $1s$ orbital and the single electron in the $2s$ orbital. The momentum intracule has less features and we can only say that $v \approx 1.6$ is the most likely relative momentum that two electrons will

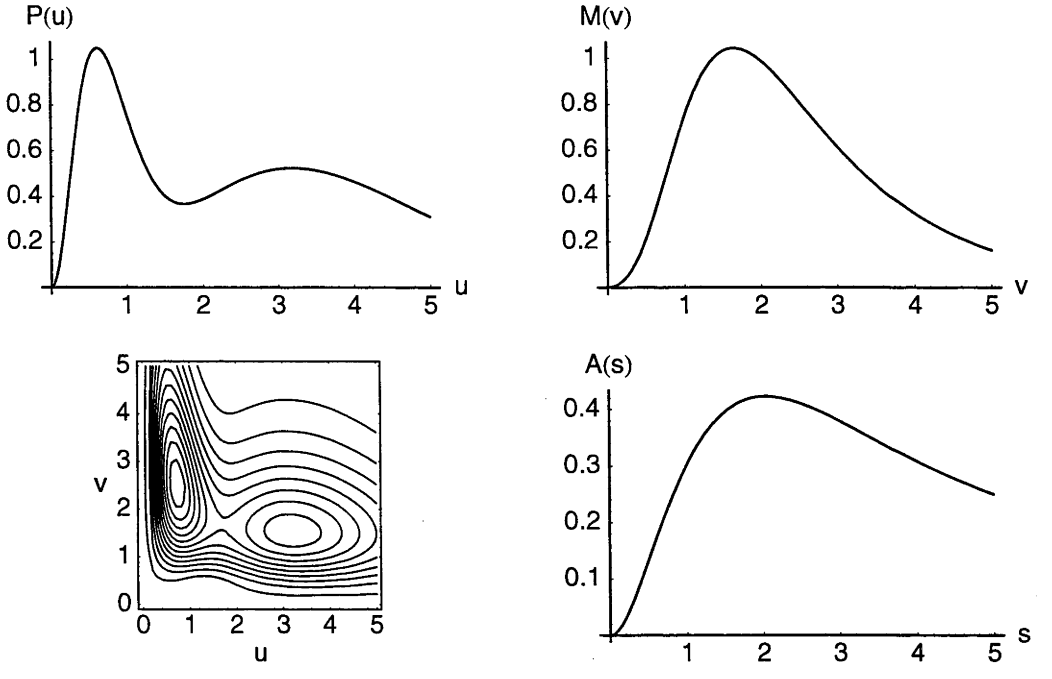

Figure 5.3: The HF/6-311G position, momentum, Wigner and action intracules for Li

have. The Wigner intracule, however, is seen to contain more information than either the position or momentum intracules. There are two peaks – the peak at $(0.8, 2.6)$ is from the $1s$ electron pair which are very close together and moving rapidly around the nucleus. The second peak at $(3.2, 1.4)$ is due to likelihood of finding one of the electrons in the $1s$ orbital and the electron in the $2s$ orbital at this relative position in phase space. The volume under the second peak is twice that under the first for statistical reasons. The action intracule is characteristically featureless and possesses a single maximum followed by a slowly decaying tail.

Beryllium

Figure 5.4 shows the four intracules for the beryllium atom. The position intracule shows two peaks – the smaller inner peak at $u \approx 0.5$ results from the two electrons in the small $1s$ orbital. The second larger peak is more difficult to assign. The momentum intracule also exhibits two peaks – the inner peak at $v \approx 0.7$ is due to the two electrons in the outer $2s$ orbital which are moving quite slowly relative to each other. Again the outer peak cannot easily be attributed to an electron pair. The Wigner intracule gives us more information

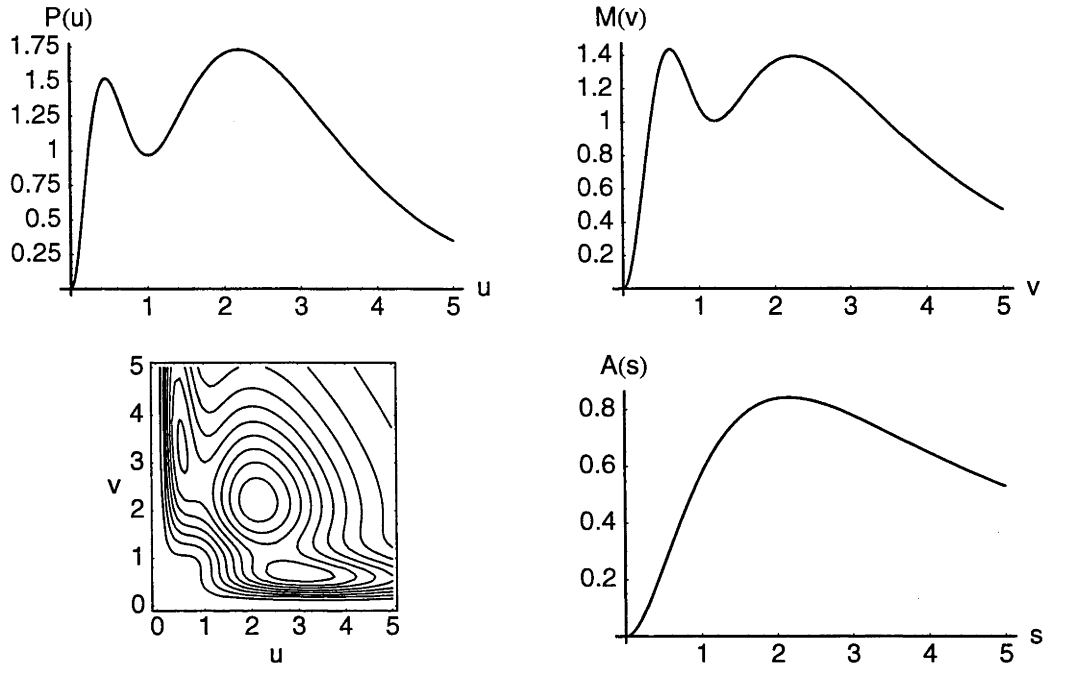

Figure 5.4: The HF/6-311G position, momentum, Wigner and action intracules for Be

and explains the two broad outer peaks in the position and momentum intracules. The first peak at $(0.8, 3.4)$ results from the two electrons in the $1s$ orbital which are very close together and moving very quickly to keep away from each other. The second peak at $(3.0, 2.7)$ is explained by the electron pair in the more diffuse $2s$ orbital which are relatively far apart and move slowly relative to one another. Finally the central peak is due to finding one electron in the $1s$ orbital and one in the $2s$ orbital at $(2.1, 2.2)$. This central peak has four times the content than either of the others for statistical reasons. The outer peaks in the position and momentum intracules can now be explained by the merging of the central peak with one of the other peaks when the Wigner intracule is integrated with respect to u or v. Finally the action intracule again does not provide much insight only to say the most likely value of the product of relative position and momentum that two electrons in Be will have is $s \approx 2.1$.

Neon

Fig. 5.5 shows just the HF/6-311G Wigner and action intracules for the neon atom. Both have less features than the previous intracules studied as with the increasing number of

Figure 5.5: The HF/6-311G Wigner and action intracules for Ne.

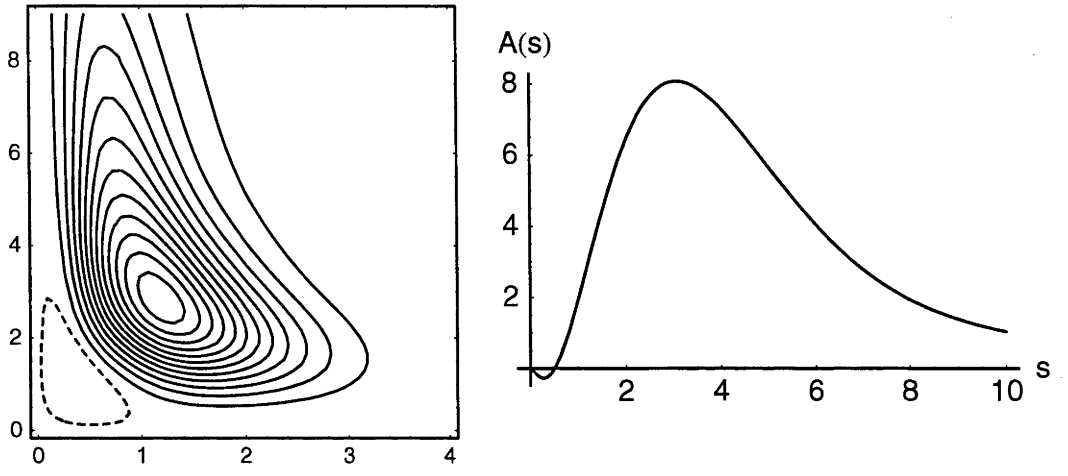

electron pairs (*cf.* 6 in Be and 45 in Ne) there are many more overlapping peaks leading to one large peak. It can be seen that with increasing nuclear charge the intracule is sliding up towards higher v. The action intracule is similarly lacking in features with the exception of a visible negative region near the origin which is also present on the Wigner intracule.

5.2 Wavefunctions and two-electron probability distributions of the Hooke's-law atom and helium*

5.2.1 Introduction

Contrary to the claims of most textbooks, systems with two electrons do not inevitably have intractable Schrödinger equations. This is exemplified by a curious "atom" wherein two electrons repel Coulombically but are bound to a nucleus by a harmonic potential and is governed by the Hamiltonian

$$\hat{H} = -\frac{1}{2}\nabla_1^2 - \frac{1}{2}\nabla_1^2 + \frac{1}{2}kr_1^2 + \frac{1}{2}kr_2^2 + \frac{1}{r_{12}} \tag{5.1}$$

*Taken directly from ref. [120]

It was first considered forty years ago by Kestner and Sinanoglu [121] but it was not until 1989 that Kais *et al.* discovered [122] that, if the harmonic force constant is $k = 1/4$, its *exact* ground-state wavefunction can be written in closed from and the associated energy is $E = 2$. Since then, interest in this unusual system has grown steadily [31,123–141] and its study has shed light on the behaviour of strongly correlated electrons.

A consensus on a name for the "atom" has not yet been reached. It has been variously termed the Hooke's Law model, Hooke's atom, the Hookean atom, harmonium and the harmonic quantum dot. However in this paper, we will use the term "hookium" to refer specifically to the ($k = 1/4$, $E = 2$) system.

If the harmonic potential is replaced by a coulombic one, the Hamiltonian becomes

$$\hat{H} = -\frac{1}{2}\nabla_1^2 - \frac{1}{2}\nabla_1^2 - \frac{2}{r_1} - \frac{2}{r_2} + \frac{1}{r_{12}} \tag{5.2}$$

and hookium is transformed into helium. Unfortunately, no exact helium wavefunctions are known but a number of simple near-exact wavefunctions were developed by Hylleraas in the early days of quantum mechanics [43]. Although hookium and helium are quantitatively different — hookium being a more diffuse species, and the overlap of the two wavefunctions being ~ 0.6 — meaningful qualitative comparisons can be made between the two.

We have recently commenced a systematic study of position, momentum, and Wigner intracules of atoms and molecules. The position intracule, $P(u)$, which gives the probability of finding two electrons separated by a distance u, is given by [64]

$$P(u) = \iiint |\Psi(\mathbf{r}_1, \mathbf{r}_2)|^2 \, \delta(\mathbf{r_{12}} - \mathbf{u}) \mathrm{d}\mathbf{r}_1 \mathrm{d}\mathbf{r}_2 \mathrm{d}\Omega_{\mathbf{u}} \tag{5.3}$$

where $\mathbf{r}_1$ and $\mathbf{r}_2$ are the positions of electrons 1 and 2, $\mathbf{r}_{12} = \mathbf{r}_1 - \mathbf{r}_2$, and $\Omega_{\mathbf{u}}$ is the angular component of $\mathbf{u}$.

The momentum intracule, $M(v)$, which gives the probability of finding two electrons

moving with a relative momentum v, is given by [105]

$$M(v) = \iiint |\Phi(\mathbf{p}_1, \mathbf{p}_2)|^2 \, \delta(\mathbf{p_{12}} - \mathbf{v}) \mathrm{d}\mathbf{p}_1 \mathrm{d}\mathbf{p}_2 \mathrm{d}\Omega_{\mathbf{v}} \tag{5.4}$$

where $\Phi(\mathbf{p}_1, \mathbf{p}_2)$ is the momentum wavefunction, $\mathbf{p}_1$ and $\mathbf{p}_2$ are the momenta of electrons 1 and 2, $\mathbf{p}_{12} = \mathbf{p}_1 - \mathbf{p}_2$, and $\Omega_{\mathbf{v}}$ is the angular component of $\mathbf{v}$.

Finally the Wigner intracule, $W(u, v)$ [142], which gives the quasi-probability of finding two electrons at a distance u and moving with relative momentum v, is given for a two-electron singlet by

$$W(u, v) = \frac{v^2}{2\pi^2} \iiint \Psi(\mathbf{r}, \mathbf{r} + \mathbf{q} + \mathbf{u}) \Psi(\mathbf{r} + \mathbf{q}, \mathbf{r} + \mathbf{u}) j_0(qv) \mathrm{d}\mathbf{r} \mathrm{d}\mathbf{q} \mathrm{d}\Omega_{\mathbf{u}} \tag{5.5}$$

where $j_0(x)$ is the zeroth order spherical Bessel function [21].

In this paper, we present and discuss intracules for hookium and helium, using both (near-) exact and Hartree-Fock (HF) wavefunctions.

5.2.2 Correlated wavefunctions and intracules

Hookium

The normalized exact position wavefunction [31] for hookium is given by

$$\Psi(\mathbf{r}_1, \mathbf{r}_2) = \frac{1}{2\sqrt{8\pi^{5/2} + 5\pi^3}} \left(1 + \frac{r_{12}}{2}\right) \exp\left(-\frac{r_1^2 + r_2^2}{4}\right) \tag{5.6}$$

The position intracule derived from this [140] is given by

$$P(u) = \frac{1}{8 + 5\pi^{1/2}} u^2 \left(1 + \frac{u}{2}\right)^2 \exp\left(-\frac{u^2}{4}\right) \tag{5.7}$$

To derive the analogous momentum intracule, the normalized momentum wavefunction for hookium, which is related to the position wavefunction via a Fourier transform must

be determined

$$\Phi(\mathbf{p}_1,\mathbf{p}_2)=\frac{1}{2\sqrt{8\pi^{5/2}+5\pi^3}}\frac{1}{8\pi^3}\iint\left(1+\frac{r_{12}}{2}\right)\exp\left(-\frac{r_1^2+r_2^2}{4}+\mathrm{i}(\mathbf{p}_1.\mathbf{r}_1+\mathbf{p}_2.\mathbf{r}_2)\right)\mathrm{d}\mathbf{r}_1\mathrm{d}\mathbf{r}_2 \tag{5.8}$$

The first term which does not contain r_{12} is a straightforward Fourier transform of a pair of Gaussians

$$\frac{1}{8\pi^3}\iint\exp\left(-\frac{r_1^2+r_2^2}{4}+\mathrm{i}(\mathbf{p}_1.\mathbf{r}_1+\mathbf{p}_2.\mathbf{r}_2)\right)\mathrm{d}\mathbf{r}_1\mathrm{d}\mathbf{r}_2=8\mathrm{e}^{-\mathbf{p}_1^2-\mathbf{p}_2^2} \tag{5.9}$$

The second term which is linear in r_{12} is not so straightforward. We start by introducing the following Fourier integral

$$r_{12}=\frac{r_{12}^2}{r_{12}}=r_{12}^2\int\frac{4\pi}{k^2}\mathrm{e}^{\mathrm{i}\mathbf{k}.\mathbf{r}_{12}}\mathrm{d}\mathbf{k} \tag{5.10}$$

This allows us to expand the factor r_{12}^2 to yield

$$\begin{aligned}&\frac{1}{8\pi^3}\iint\frac{r_{12}}{2}\exp\left(-\frac{r_1^2+r_2^2}{4}+\mathrm{i}(\mathbf{p}_1.\mathbf{r}_1+\mathbf{p}_2.\mathbf{r}_2)\right)\mathrm{d}\mathbf{r}_1\mathrm{d}\mathbf{r}_2\\&=\frac{1}{32\pi^5}\iiint\frac{r_{12}^2}{k^2}\exp\left(-\frac{r_1^2+r_2^2}{4}+\mathrm{i}(\mathbf{p}_1.\mathbf{r}_1+\mathbf{p}_2.\mathbf{r}_2+\mathbf{k}.\mathbf{r}_{12})\right)\mathrm{d}\mathbf{r}_1\mathrm{d}\mathbf{r}_2\mathrm{d}\mathbf{k} \qquad (5.11)\\&=\frac{1}{32\pi^5}\int\frac{1}{k^2}(f_2^xf_0^yf_0^z+f_0^xf_2^yf_0^z+f_0^xf_0^yf_2^z)\mathrm{d}\mathbf{k} \qquad (5.12)\end{aligned}$$

where we have used $r_{12}^2=(x_1-x_2)^2+(y_1-y_2)^2+(z_1-z_2)^2$ and we define the following functions

$$\begin{aligned}f_n^x&=\int_{-\infty}^{\infty}\int_{-\infty}^{\infty}(x_1-x_2)^n\exp\left(-\frac{x_1^2+x_2^2}{4}\right)\\&\qquad\times\exp(\mathrm{i}(p_{1x}.x_1+p_{2x}.x_2+k_x.(x_1-x_2)))\mathrm{d}x_1\mathrm{d}x_2 \qquad (5.13)\\f_0^x&=4\pi\exp(-2k_x^2-p_{1x}^2-p_{2x}^2+2k_xp_{12x}) \qquad (5.14)\\f_2^x&=-16\pi\exp(-2k_x^2-p_{1x}^2-p_{2x}^2+2k_xp_{12x})((2k_x-p_{12x})^2-1) \qquad (5.15)\end{aligned}$$

and $\mathbf{p}_1=(p_{1x},p_{1y},p_{1z})$, $\mathbf{p}_2=(p_{2x},p_{2y},p_{2z})$, $\mathbf{p}_{12}=\mathbf{p}_1-\mathbf{p}_2=(p_{12x},p_{12y},p_{12z})$. Putting everything back together yields an integral in $\mathbf{k}$ which is relatively straightforward to

perform term wise in polar coordinates

$$\frac{8\mathrm{e}^{-p_1^2-p_2^2}}{\pi^2}\int \mathrm{e}^{-2k^2-2\mathbf{k}.\mathbf{p}_{12}}(3-4k^2-p_{12}^2-4\mathbf{k}.\mathbf{p}_{12})\mathrm{d}\mathbf{k}$$
$$= 8\mathrm{e}^{-p_1^2-p_2^2}\left[\sqrt{\frac{2}{\pi}}\exp\left(\frac{p_{12}^2}{2}\right)+\left(\frac{1}{p_{12}}-p_{12}\right)\mathrm{erfi}\left(\frac{p_{12}}{\sqrt{2}}\right)\right] \quad (5.16)$$

Finally, combining the eqns. (5.9) and (5.16) yields the momentum wavefunction

$$\Phi(\mathbf{p}_1,\mathbf{p}_2)=\frac{4\exp\left(-p_1^2-p_2^2\right)}{\sqrt{8\pi^{5/2}+5\pi^3}}\left[1+\sqrt{\frac{2}{\pi}}\exp\left(\frac{p_{12}^2}{2}\right)+\left(\frac{1}{p_{12}}-p_{12}\right)\mathrm{erfi}\left(\frac{p_{12}}{\sqrt{2}}\right)\right] \quad (5.17)$$

where $\mathrm{erfi}(z)=\mathrm{erf}(iz)/i$ and $\mathrm{erf}(z)$ is the error function [21]. Inserting this expression into eqn. (5.4) gives the exact momentum intracule for hookium

$$M(v) = \frac{64\pi}{8+5\sqrt{\pi}}\left[1+\sqrt{\frac{2}{\pi}}\exp\left(\frac{v^2}{2}\right)+\left(\frac{1}{v}-v\right)\mathrm{erfi}\left(\frac{v}{\sqrt{2}}\right)\right]^2$$
$$\times\int_0^\infty 2\pi p_1^2\mathrm{e}^{-2p_1^2}\int_0^\pi \mathrm{e}^{-2p_1^2-2v^2+4vp_1\cos\theta}v^2\sin\theta\mathrm{d}\theta\mathrm{d}p_1 \quad (5.18)$$
$$= \frac{8v^2}{8+5\sqrt{\pi}}\left[\sqrt{\frac{2}{\pi}}+\exp\left(-\frac{v^2}{2}\right)+\left(\frac{1}{v}-v\right)\exp\left(-\frac{v^2}{2}\right)\mathrm{erfi}\left(\frac{v}{\sqrt{2}}\right)\right]^2 \quad (5.19)$$

Inserting the expression for the wavefunction into eqn. (5.5) to give the Wigner intracule for hookium yields, with some rearrangement,

$$W(u,v)=\frac{v^2}{8\pi^{9/2}(8+5\sqrt{\pi})}\iint\left(1+\frac{|\mathbf{q}+\mathbf{u}|}{2}\right)\left(1+\frac{|\mathbf{q}-\mathbf{u}|}{2}\right)\mathrm{e}^{-\frac{q^2}{4}}j_0(qv)$$
$$\times\int \mathrm{e}^{-|\mathbf{r}+\frac{\mathbf{u}+\mathbf{q}}{2}|^2}\mathrm{d}\mathbf{r}\mathrm{d}\mathbf{q}\mathrm{d}\Omega_{\mathbf{u}} \quad (5.20)$$

The integral over $\mathbf{r}$ is trivial and if we allow $\mathbf{u}$ to lie along the z-axis the integral over $\Omega_{\mathbf{u}}$ is simply $4\pi u^2$ which leaves us with

$$W(u,v)=\frac{u^2v^2\mathrm{e}^{-u^2/4}}{\pi(8+5\sqrt{\pi})}\int_0^\infty q^2\mathrm{e}^{-q^2/4}j_0(qv)f(q,u)\mathrm{d}q \quad (5.21)$$

where

$$f(q,u)=\int_0^\pi\left(1+\frac{1}{2}\sqrt{q^2+u^2+2qu\cos\theta}\right)\left(1+\frac{1}{2}\sqrt{q^2+u^2-2qu\cos\theta}\right)\sin\theta\mathrm{d}\theta \quad (5.22)$$

and expanding the parentheses and integrating term wise leads to

$$f(q,u) = \begin{cases} 2 + 2u + \frac{2q^2}{3u} + \frac{u^2-q^2}{4} + \frac{(q^2+u^2)^2}{4qu} \arctan(\frac{q}{u}) & (q \leq u) \\ 2 + 2q + \frac{2u^2}{3q} + \frac{q^2-u^2}{4} + \frac{(q^2+u^2)^2}{4qu} \arctan(\frac{u}{q}) & (q > u) \end{cases} \tag{5.23}$$

The final integral over q has not been obtained analytically and we use the Quadpack numerical integration subroutines [143] to perform this integral using highly accurate adaptive quadrature.

Helium

The near-exact wavefunction we have chosen is that of Hylleraas [43] and is given by

$$\Psi(\mathbf{r}_1, \mathbf{r}_2) = \frac{4\alpha^4}{\pi\sqrt{16\alpha^2 + 70\alpha c + 96c^2}}(1 + c\, r_{12})\mathrm{e}^{-\alpha(r_1+r_2)} \tag{5.24}$$

where c and α are such that they minimize the energy. The position intracule is then given by

$$P(u) = \frac{4\alpha^5 u^2(1+cu)^2(3+6u\alpha+4u^2\alpha^2)}{3(8\alpha^2+35\alpha c+48c^2)}\mathrm{e}^{-2\alpha u} \tag{5.25}$$

The momentum wavefunction proves to be too difficult to derive so to obtain the momentum and Wigner intracules we expand the position wavefunction using a set of GTOs to represent the STOs

$$\Psi(\mathbf{r}_1, \mathbf{r}_2) = M(1 + c\, r_{12}) \sum_{i=1}^{n} a_i \phi_i(\zeta_i, \mathbf{r}_1) \sum_{j=1}^{n} a_j \phi_j(\zeta_j, \mathbf{r}_2) \tag{5.26}$$

where the $\phi_i(\mathbf{r})$ are Gaussian functions with contraction coefficients a_i and exponents ζ_i, and M is a normalisation constant. Using this expansion, the Wigner intracule can be reduced to a one-dimensional integral, analogous to that of hookium, and the momentum intracule is then calculated from this by integrating over u using 50-point Euler-Maclaurin [144] quadrature.

An energy of $-2.891121\ E_\mathrm{h}$ is achieved using $c = 0.365796$ and $\alpha = 1.849685$. Using an appropriately scaled STO-6G expansion in (5.26) yields an energy of $-2.889978\ E_\mathrm{h}$.

5.2.3 Hartree-Fock wavefunctions and intracules

Hookium

Whereas the exact wavefunction of hookium (5.6) is known in closed form, the corresponding HF wavefunction is known only from numerical calculation. The normalized HF orbital $\psi(r)$ satisfies the integro-differential equation

$$\left[-\frac{1}{2}\frac{\mathrm{d}^2}{\mathrm{d}r^2}-\frac{1}{r}\frac{\mathrm{d}}{\mathrm{d}r}+\frac{r^2}{8}+\frac{1}{r}\int_0^r 4\pi x^2\Psi^2(x)\mathrm{d}x+\int_r^\infty 4\pi x\Psi^2(x)\mathrm{d}x\right]\Psi(r)=\epsilon\Psi(r) \quad (5.27)$$

and the HF energy is $E_{\mathrm{HF}}=E_1+E_2$ where

$$E_1 = 2\int\psi(r)\left[-\frac{1}{2}\frac{\mathrm{d}^2}{\mathrm{d}r^2}-\frac{1}{r}\frac{\mathrm{d}}{\mathrm{d}r}+\frac{r^2}{8}\right]\psi(r)\mathrm{d}\mathbf{r} \quad (5.28)$$

$$E_2 = \iint\psi^2(r_1)\frac{1}{r_{12}}\psi^2(r_2)\mathrm{d}\mathbf{r}_1\mathrm{d}\mathbf{r}_2 \quad (5.29)$$

It is difficult to solve (5.27) directly but, if we expand $\psi(r)$ in an orthonormal basis

$$\psi(r)\approx\psi_N(r)=\sum_{k=1}^{N}c_k\phi_k(r) \quad (5.30)$$

and choose the appropriate basis functions all of the required integrals can be evaluated in closed form. We choose the basis functions to be the harmonic oscillator eigenfunctions

$$\phi_k(r)=\frac{H_{2k-1}(r/\sqrt{2})}{2^k\sqrt{(2k-1)!}\,r/\sqrt{2}}\frac{\exp(-r^2/4)}{(2\pi)^{3/4}} \quad (5.31)$$

(where H_k is the k^{th} Hermite polynomial) and the expansion converges very rapidly, as Table 5.1 shows. We observe that the expansion coefficients c_k decay roughly exponentially. Our limiting energy (2.03843887 E_{h}) is significantly lower than that reported by Kais *et al.* [31] (2.039325 E_{h}) but the reason for this discrepancy is not clear [145]. Using an expansion of eight Gaussian basis functions [146] an energy of 2.0384390 E_{h} can be achieved. This is slightly lower than the energy of 2.03851 E_{h} achieved by Amovilli *et al.* [141] using ten Gaussians.

By subtracting our lowest HF energy from the exact energy ($E=2$), we deduce that the

Table 5.1: Convergence of the Hartree-Fock energy with Hermite basis set size

N	E_N	$E_N - E_{N-1}$	c_2	c_3	c_4	c_5
1	2.06418958					
2	2.03878780	-0.02540178	0.10994405			
3	2.03845337	-0.00033443	0.10833978	-0.00951451		
4	2.03843949	-0.00001388	0.10825043	-0.00940132	0.00157574	
5	2.03843889	-0.00000061	0.10824442	-0.00939263	0.00156292	-0.000284251
6	2.03843887	-0.00000001	0.10824412	-0.00939209	0.00156212	-0.000283023
7	2.03843887	-0.00000000	0.10824414	-0.00939212	0.00156212	-0.000283102

exact correlation energy of hookium is -38.4388733 mE_h. This is a little smaller than the correlation energy of helium (-42.044 mE_h) and supports the assertion by Kestner and Sinanoglu that the correlation energies of two-electron systems are remarkably insensitive to the nature or magnitude of the external field [121].

Although it is straightforward to calculate the position and momentum intracules using the basis set in (5.31), the Wigner intracule proves more difficult. For this reason we use the eight-Gaussian basis set mentioned above to calculate all of the intracules. The quality of this Gaussian basis set is such that we do not see any differences in the intracules derived from it as compared to those derived using the Hermite basis set.

Helium

We expand the HF wavefunction for helium as a linear combination of 10 s-type Gaussians. In particular the exponents are taken from the s-functions used in the cc-pV6Z basis set [147] for helium, uncontracting the contracted basis function. This basis yields an energy of -2.861673 E_h, almost reaching the HF limit (-2.86168 E_h). Subtracting this from the energy resulting from the near-exact wavefunction gives a correlation energy of 29.45 mE_h, which is 70% of the true correlation energy for helium.

5.2.4 Effect of correlation on the intracules

To examine the effect that the inclusion of electron correlation has on the intracules for hookium and helium, each of the position, momentum and Wigner intracules will be

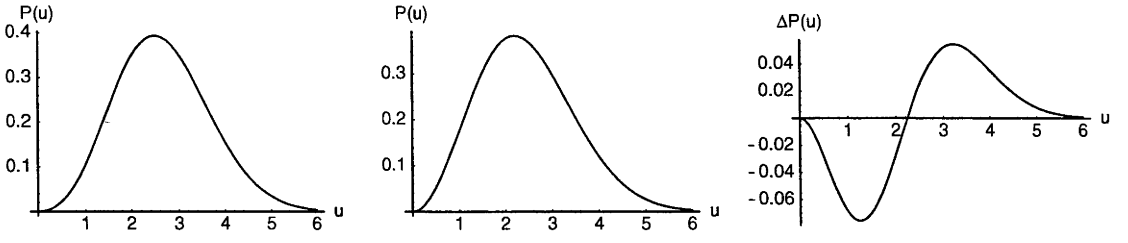

(a) (b) (c)

Figure 5.6: The exact and HF position intracules and the corresponding Coulomb hole for hookium (u in a.u.).

examined for both the (near-)exact and HF cases and also the Coulomb hole [47], ΔZ, where

$$\Delta Z = Z_{Exact} - Z_{HF} \tag{5.32}$$

where Z is $P(u)$, $M(v)$ or $W(u,v)$.

Hookium

Position Intracule

Figure 5.6(a) shows the exact position intracule for hookium. At $u = 0$ the intracule vanishes, indicating that there is no probability of finding the two electrons at the same point in space. Near the origin it grows quadratically and reaches a maximum at $u \approx 2.494$ and then decays away as u increases. Figure 5.6(b) shows the corresponding HF intracule. Again, it vanishes at the origin and grows to a maximum, this time at $u \approx 2.204$, before decaying away. As expected, the effect of correlation is to keep the two electrons further apart, and this is clearly shown in the Coulomb hole in Figure 5.6(c). The radius of the Coulomb hole, as defined by Coulson and Nielson [47], for hookium is approximately 2.25.

Momentum Intracule

Figure 5.7(a) shows the exact momentum intracule for hookium. Like the position intracule, it vanishes at the origin indicating that there is no probability of finding the two electrons with zero relative momentum. It then grows quadratically to a maximum

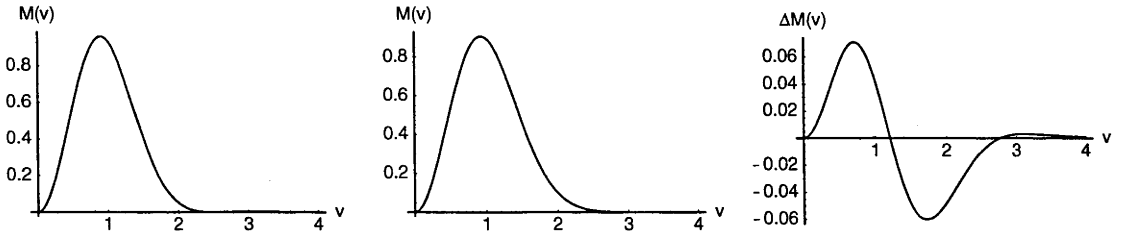

(a) (b) (c)

Figure 5.7: The exact and HF momentum intracules and the corresponding Coulomb hole for hookium (v in a.u.).

at $v \approx 0.897$ followed by a rapid decay back to zero at $v \approx 2.506$, indicating that there is no probability of the two electrons having this relative momentum. Another much smaller maximum then occurs at $v \approx 3.086$. Figure 5.7(b) shows the HF momentum intracule. Again, it vanishes at the origin and grows to maximum at $v \approx 0.926$, before decaying away. The second peak does not appear on the HF intracule indicating that correlation also favours electrons moving with high relative momentum. Figure 5.7(c) shows the Coulomb hole for hookium in momentum space. It is considerably more complex than its position space counterpart, with correlation favouring both lower and higher relative momenta.

Wigner Intracule

Figure 5.8(a) shows the exact Wigner intracule for hookium. The intracule vanishes along the axes $u = 0$ and $v = 0$ indicating that there is no probability of finding two electrons at the same point in either position or momentum space. From the origin it grows quadratically in both u and v and reaches a maximum at $(u, v) \approx (2.378, 0.899)$. We also note the presence of a shallow negative region at $(u, v) \approx (1.109, 2.048)$. Whereas the position and momentum intracules are everywhere positive, this is not the case for the Wigner intracule which reflects its interpretation as a quasi-probability. Figure 5.8(b) shows the HF Wigner intracule. Again, it vanishes at the origin and along the axes and it grows to a maximum at $(u, v) \approx (2.187, 0.923)$. The negative region present in the exact intracule is no longer present. Figure 5.8(c) shows the Coulomb hole in phase space. It combines the results of the two previous sections and shows that, in hookium, correlation

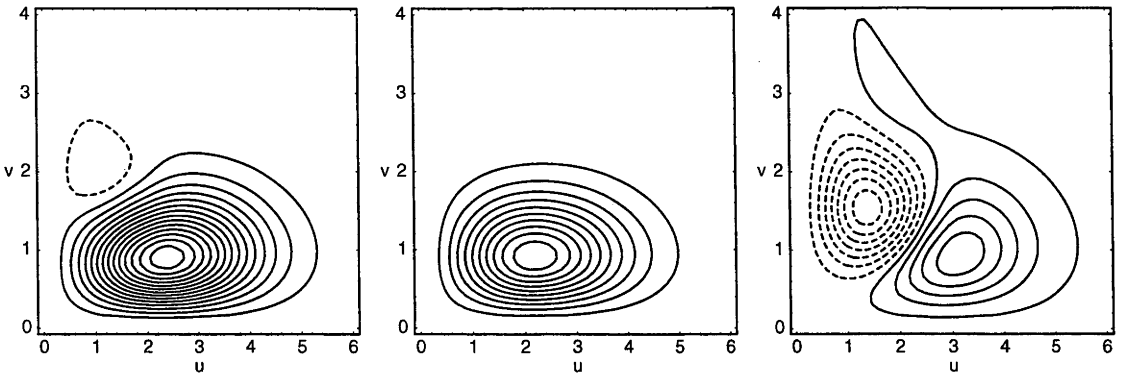

(a) (b) (c)

Figure 5.8: The exact and HF Wigner intracules and the corresponding Coulomb hole for hookium (u and v in a.u.).

favours a larger inter-electronic separation and lower relative momentum and to a much lesser extent higher relative momentum.

Helium

Position Intracule

Figure 5.9(a) shows the near-exact position intracule for helium. At $u = 0$ the intracule vanishes, indicating that there is no probability of finding the two electrons at the same point in space. Near the origin it grows quadratically and reaches a maximum at $u \approx 1.0765$ and then decays away as u increases. Figure 5.9(b) shows the corresponding HF intracule. Again, it vanishes at the origin and grows to a maximum, this time at $u \approx 0.995$, before decaying away. As expected, the effect of correlation is to keep the two electrons further apart, and this is clearly shown in the Coulomb hole in Figure 5.9(c). The radius of the Coulomb hole for helium is approximately 0.95. This is significantly less than 1.1 quoted by Coulson and Nielson and we attribute this difference to the inferior quality of our correlated wavefunction. We also note the presence of a second node in the Coulomb hole and again believe that this is due to our choice of wavefunction rather than having physical significance. Comparing these results with those of hookium, we see qualitatively the same features but quantitatively hookium's Coulomb hole is much larger reflecting its diffuseness relative to helium.

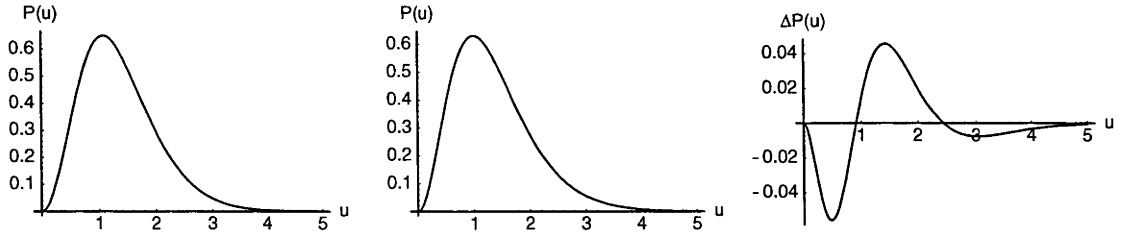

(a) (b) (c)

Figure 5.9: The near-exact and HF position intracules and the corresponding Coulomb hole for helium (u in a.u.).

Momentum Intracule

Figure 5.10(a) shows the near-exact momentum intracule for helium. Like the position intracule, it vanishes at the origin indicating that there is no probability of finding the two electrons with zero relative momentum. It then grows quadratically to a maximum at $v \approx 1.498$ and decays away with v. Figure 5.10(b) shows the HF momentum intracule. Again, it vanishes at the origin and grows to maximum at $v \approx 1.447$, before decaying away. The shifting of this maximum shows that correlation favours electrons moving with lower relative momentum. Figure 5.10(c) shows the Coulomb hole for helium in momentum space. It is considerably more complex than its position space counterpart, with correlation disfavouring both lower and higher relative momenta. The Coulomb hole in momentum space has been studied previously [84, 148–151] using CI, MCHF and explicitly correlated position wavefunctions to derive the correlated intracule. We are not aware of any studies using a wavefunction linear in r_{12}. Comparing our results with those of Gálvez *et al.* [150], we obtain qualitatively the same result although quantitatively the magnitude of our peaks are too large. Again this reflects the relatively poor quality of our choice of wavefunction.

The Coulomb hole for helium is very different to that of hookium. Whereas in helium (and the hydride ion [84]) correlation disfavours both low and high relative momenta, in hookium the opposite is true. The physical significance for this is not clear, though it does reflect the fact that although hookium is often used as a model for helium in some respects they are very different.

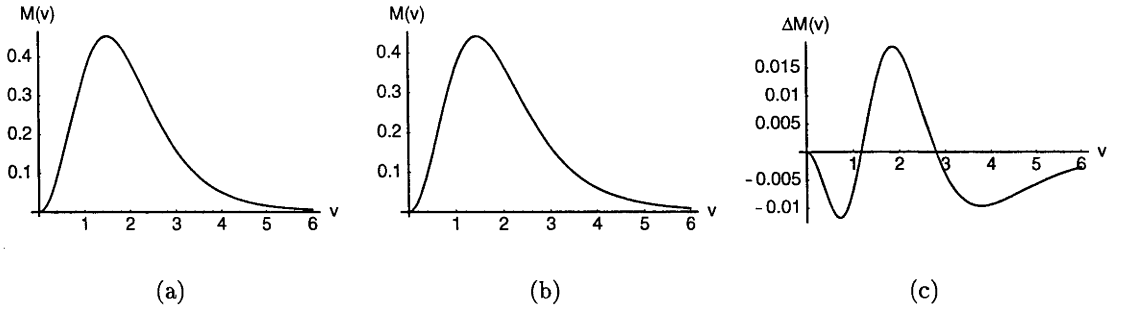

(a) (b) (c)

Figure 5.10: The near-exact and HF momentum intracules and the corresponding Coulomb hole for helium (v in a.u.).

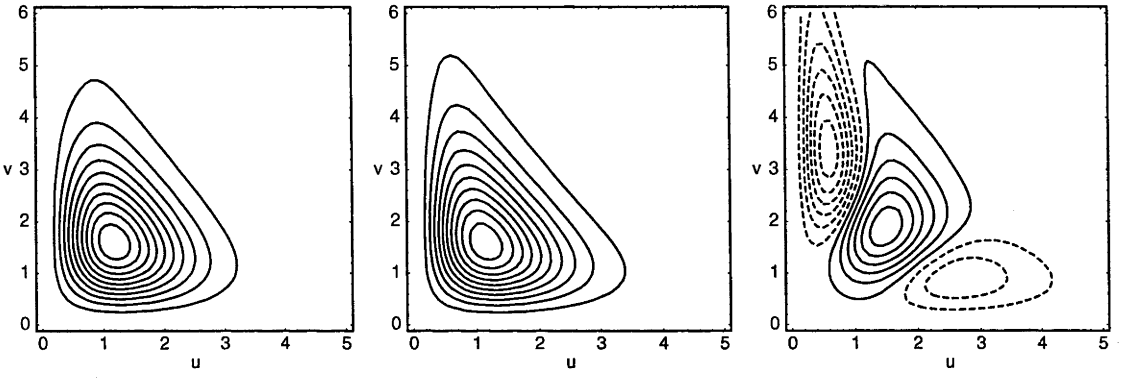

(a) (b) (c)

Figure 5.11: The near-exact and HF Wigner intracules and the corresponding Coulomb hole for helium (u and v in a.u.).

Wigner Intracule

Figure 5.11(a) shows the near-exact Wigner intracule for helium. The intracule vanishes at the origin and along the axes $u = 0$ and $v = 0$ indicating that there is no probability of finding two electrons with either or both the same position in space and zero relative momentum. From the origin it grows quadratically in both u and v and reaches a maximum at $(u, v) \approx (1.170, 1.589)$. Figure 5.11(b) shows the HF Wigner intracule. Again, it vanishes at the origin and along the axes and it grows to a maximum at $(u, v) \approx (1.316, 1.589)$. Figure 5.11(c) shows the Coulomb hole in phase space. It combines the results of the two previous sections and shows that, in helium, correlation favours a larger inter-electronic separation and lower relative momentum.

5.2.5 Conclusions

Although there has been interest in the position-space properties of hookium over the last four decades, its momentum-space properties have not been considered. Here we have presented the momentum-space wavefunction, the corresponding momentum intracule, and also the Wigner intracule for hookium. The momentum intracule exhibits two maxima and a value $v \approx 2.506$ of the relative momentum, p_{12}, that can never occur. We have not observed such nodes in $M(v)$ before. The Wigner intracule allows us to look at the position- and momentum-space properties of hookium simultaneously.

The position and momentum space properties of helium have been studied extensively. In this paper we use a simple explicitly correlated wavefunction, which is linear in r_{12} to look at the effects of correlation in helium. Qualitatively we reproduce the results of previous work, such as Coulson and Nielson, and Gálvez *et al.*, although quantitatively our results are not as accurate. These could be improved by the use of a more sophisticated wavefunction. By expanding the slater part of our wavefunction in terms of Gaussians we were able to look at the momentum intracule for a wavefunction which depended explicitly on r_{12}, and this approach could easily be extended to more accurate wavefunctions.

In both hookium and helium the effect of correlation is to keep the electrons further apart. They differ, however, in the effect that correlation has on their momentum distributions. Correlation favours lower relative momentum and, to a much lesser extent, higher relative momentum in hookium, whereas the analogous Coulomb hole in helium shows the opposite preferences, disfavouring both lower and higher relative momentum. Looking at the Coulomb hole in phase space again shows us both the similarities and differences between hookium and helium.

Figure 5.12: The Wigner intracule for H_2 using the RHF/6-311G (top row) and UHF/6-311G (bottom row) wavefunctions at increasing values of the bond length, R

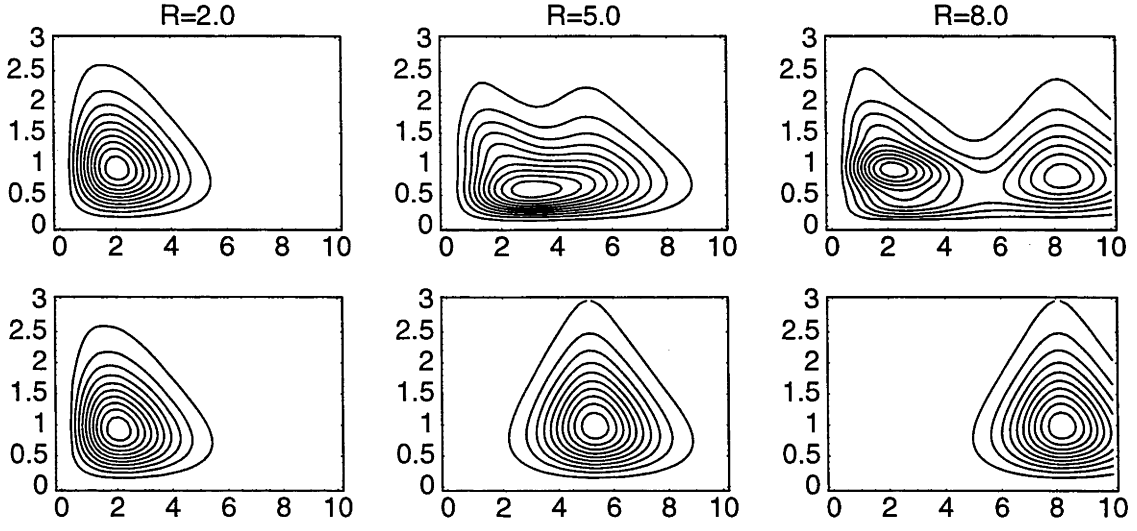

5.3 Molecular intracules

5.3.1 Dissociation of the H_2 molecule

Fig. 5.12 shows the RHF/6-311G and UHF/6-311G Wigner intracules for the hydrogen molecule at various bond lengths. At the smallest bond length, both RHF and UHF intracules exhibit a single peak. However as the bond is stretched the two intracules begin to differ with a second peak appearing on the RHF intracule but the UHF intracule retaining a single peak. This is a very clear manifestation of the shortcomings of the RHF description of a stretched bond. RHF dissociates H_2 incorrectly into an ionic and a covalent contribution, the first corresponding to the inner peak in which the two electrons are localized around a single nucleus and the second corresponding to the outer peak in which there is an electron localized around each nucleus. However, the UHF intracule contains only a single peak due to the physically correct covalent contributions.

Figure 5.13: The total-, antiparallel- and parallel-spin components of the HF/6-311G Wigner intracule for H_2O.

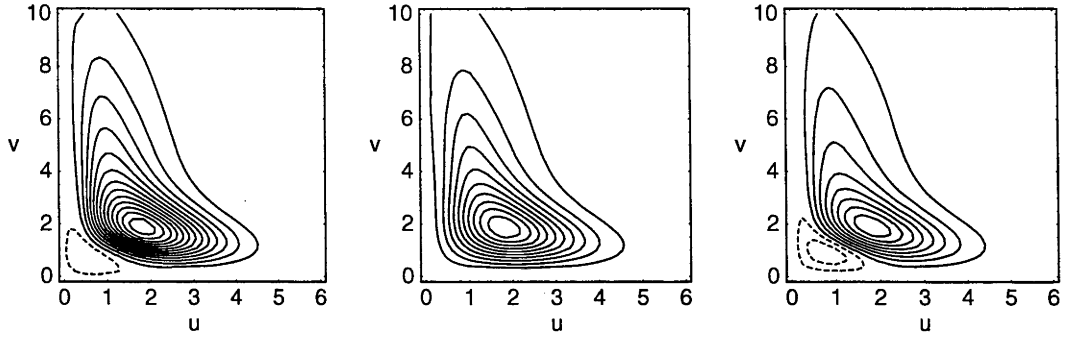

5.3.2 Spin intracules for H_2O and F_2

Figure 5.13 shows the contributions to the HF/6-311G Wigner intracule from all of the electrons, from electrons of opposite spin (antiparallel) and from electrons of the same spin (parallel) for the water molecule. The total intracule possesses a shallow negative region at the origin and a single maximum. This 10-electron species is similar to the Ne atom but more diffuse. If we compare the intracule with that of Ne, we see that their features are very similar, with the intracule for water being at slightly lower v and larger u as would be expected with the decrease in nuclear charge. The antiparallel intracule is everywhere positive and possesses a single maximum. The parallel intracule has a negative region close to the origin and a single maximum.

Figure 5.14 shows the HF/6-311G spin intracules for F_2. F_2 has quite a long bond which results in there being two distinct peaks on the intracule — the inner one arising from atomic electron pairs and the outer from intra-atomic pairs. Since there are 72 atomic pairs and only 48 intra-atomic pairs, the inner peak is larger than the outer. The antiparallel and parallel intracules exhibit similar features with the exception of the negative region which is only present in the total and parallel intracules.

Figure 5.14: The total-, antiparallel- and parallel-spin components of the HF/6-311G Wigner intracule for F_2.

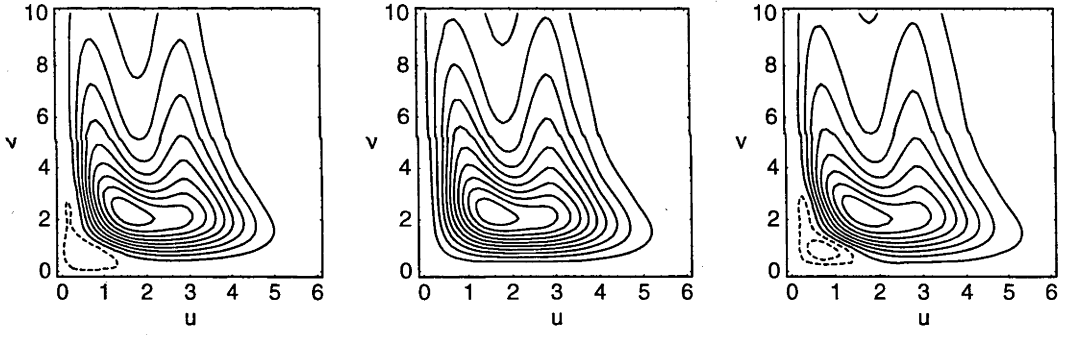

Chapter 6

Benchmark correlation energies for small molecules*

6.1 Introduction

The prediction of thermochemical quantities to high accuracy ($\sim$ 1 kcal/mol) is an important and challenging goal in quantum chemistry and a purely *ab initio* approach requires the use of highly accurate and computationally expensive treatments of electron correlation and relativistic effects. Many of the popular, more computationally accessible, but more empirical quantum chemical models, such as B3LYP [153] or the Gaussian-n methods [154–157], are parameterized to reproduce such thermochemical data and while this is clearly a desirable quality in any method, an even more satisfying target is to reproduce accurately atomic and molecular total energies: this too would lead to accurate thermochemistry but without depending upon unphysical error cancellation. Clearly to parameterize or to assess the performance of a method requires an accurate data set. Although there are papers [158–163] which contain estimates of the total energy of one or several small molecules, we are not aware of a large systematic set of such data in the chemical physics literature. In this article we use a combination of accurately determined experimental and theoretical quantities to do so for 56 small molecules, *viz.* the 55 neutral

*Taken directly from ref. [152]

molecules in the G1 set [154, 155] and H_2. In particular we list the non-relativistic (NR) total and electronic energies, the restricted and unrestricted Hartree-Fock (HF) energies and the corresponding correlation energies. We aim to determine these quantities to within a millihartree (mE_h).

6.2 Method

The atomisation energy, ΣD_0, of an N-atom molecule M is calculated using

$$\Sigma D_0 = \sum_i^N E_e^i - E_0^M + \Delta E_{Rel} \tag{6.1}$$

where E_e^i is the total NR electronic energy of the i^{th} atom in M, E_0^M is the NR energy of the lowest vibronic state of the molecule, and ΔE_{Rel} corrects the calculated atomisation energy for the effects of relativity. E_0^M is given by

$$E_0^M = E_e^M + E_{ZPVE}^M, \tag{6.2}$$

where E_e^M is the total NR electronic energy of M if the nuclei were held fixed at positions corresponding to the potential minimum and E_{ZPVE}^M is the zero-point vibrational energy. E_e^M can be written as

$$E_e^M = E_{HF}^M + E_{corr}^M \tag{6.3}$$

where E_{HF}^M is the HF energy and E_{corr}^M the correlation energy of M. Given the atomisation energies, the relativistic corrections, the zero-point corrections, the total atomic energies and the HF energies, we can now determine E_0^M, E_e^M and E_{corr}^M,

$$E_0^M = \sum_i^N E_e^i + \Delta E_{Rel} - \Sigma D_0, \tag{6.4}$$

$$E_e^M = E_0^M - E_{ZPVE}^M, \tag{6.5}$$

$$E_{corr}^M = E_e^M - E_{HF}^M. \tag{6.6}$$

6.3 Results

The quality of the results we obtain using eqns 6.4-6.6 is clearly dependent on the accuracy of the data we use. The methods used to obtain these data are summarized in table 6.1. We obtain the atomisation energy from experiment, specifically we take those listed in [156] for the G1 molecules (correcting the value for CN to that quoted in [130]) and the value for H_2 from [164]. The majority of these have error-bars less than one mE_h and we assume they are accurate for our purposes.

The zero-point vibrational energies are obtained by scaling the ZPVE from a MP2/6-31G* harmonic frequency calculation by 0.9661 [165] and are taken from [166]. The RMS error of this method with the 39 molecules used to parameterize it is approximately 0.3 mE_h.

We use the relativistic corrections to the atomisation energies listed by Feller and Peterson [167] which consist of scalar relativistic corrections (one-electron Darwin and mass-velocity terms in the Breit-Pauli Hamiltonian) obtained using a CISD(FC)/cc-pVTZ//CCSD(T)(FC)/aug-cc-pVTZ wavefunction, and also a spin-orbit correction based on experimental results. The scalar relativistic corrections are expected to be within one mE_h of four-component or Douglas-Kroll results. Although the geometries, at which the relativistic corrections are calculated, are not the experimental geometries, the differences are expected to be negligible and furthermore it has been shown that these corrections have a very weak dependence on geometry [168].

The NR electronic energies of the atoms are taken from [169] and are taken to have errors of less than one mE_h. The molecular HF energies are calculated using experimental r_e structures (taken from [164] and [170]) which are available for 42 of the species under investigation. The remaining 14 HF energies are calculated at the QCISD/G3MP2Large [171–173] geometries. The HF results are obtained using the cc-pV5Z [13, 174] basis set with the h-functions removed (cc-pV5Z-h). Halkier *et al* have studied the convergence of the HF energy using correlation consistent basis sets and report that using the cc-pV5Z basis yield energies within one mE_h of the HF-limit [175]. All HF energies are calculated using the Q-CHEM package [111].

Table 6.1: Methods used to derive required quantities

Quantity	Method
ΣD_0	Experimental
E_{ZPVE}	MP2/6-31G* ZPVE scaled by 0.9661
E_{HF}	HF/cc-pV5Z$-h$//(Exp. or QCISD/G3MP2Large)
ΔE_{Rel}	CISD(FC)/cc-pVTZ//CCSD(T)(FC)/aug-cc-pVTZ for one-electron scalar relativistic corrections. Spin-orbit corrections from experiment.
E_{e}	Total atomic energies from [169]

In table 6.2 we present all of the quantities described above. The correlation energy depends upon whether a restricted (RHF) or unrestricted (UHF) wavefunction is used and we therefore list both. We note that the atomic correlation energies given here are different to those given by Chakravorty *et al* [169] as they have used numerical HF energies [9] which are symmetry restricted and therefore higher than either the RHF or UHF energies shown here. We would recommend, when assessing a post-HF method using a RHF/UHF wavefunction to estimate the correlation energy, the use of the energies listed here rather than those of [169].

Ideally we would like to be able to compare our results to exact solutions (within an infinite basis set) of the Schrödinger equation but in the two decades since this was done for water [31] (within a double-zeta basis set) we have not moved much closer to this goal. Although quantum Monte Carlo offers estimates to the exact energy, quantifying the error due to the fixed node approximation requires the use of experimentally derived energies like the ones listed in the table above. We hope that the data listed here will not only be useful but also highlight the need for theoretical methods which can produce benchmark data like these without approximation or experimental data.

Table 6.2: Geometry[a], Atomisation energy ΣD_0[b], Zero-point vibrational energy E_{ZPVE}[c], relativistic correction ΔE_{Rel}[d], non-relativistic energy of lowest vibronic state E_0, non-relativistic electronic energy E_e[e], HF energy E_{HF}[f], and correlation energy E_{Corr} for atoms and molecules. All energies are in Hartrees.

							E_{HF}		$E_{\mathrm{Corr}}\times10^3$	
Species	Geom.	$\Sigma D_0\times10^3$	$E_{\mathrm{ZPVE}}\times10^3$	$\Delta E_{\mathrm{Rel}}\times10^3$	E_0	E_e	UHF	RHF	UHF	RHF
H	–	–	–	–	–	−0.5000	−0.5000	−0.5000	-0	-0
He	–	–	–	–	–	−2.9037	−2.8616	−2.8616	-42	-42
Li	–	–	–	–	–	−7.4781	−7.4327	−7.4327	-45	-45
Be	–	–	–	–	–	−14.6674	−14.5730	−14.5730	-94	-94
B	–	–	–	–	–	−24.6539	−24.5331	−24.5291	-121	-125
C	–	–	–	–	–	−37.8450	−37.6937	−37.6886	-151	-156
N	–	–	–	–	–	−54.5892	−54.4045	−54.4009	-185	-188
O	–	–	–	–	–	−75.0673	−74.8188	−74.8122	-249	-255
F	–	–	–	–	–	−99.7339	−99.4161	−99.4112	-318	-323
Ne	–	–	–	–	–	−128.9376	−128.5468	−128.5468	-391	-391
Na	–	–	–	–	–	−162.2546	−161.8587	−161.8587	-396	-396
Mg	–	–	–	–	–	−200.0530	−199.6146	−199.6146	-438	-438
Al	–	–	–	–	–	−242.3460	−241.8808	−241.8768	-465	-469
Si	–	–	–	–	–	−289.3590	−288.8588	−288.8544	-500	-505
P	–	–	–	–	–	−341.2590	−340.7192	−340.7187	-540	-540
S	–	–	–	–	–	−398.1100	−397.5132	−397.5071	-597	-603
Cl	–	–	–	–	–	−460.1480	−459.4897	−459.4838	-658	-664
Ar	–	–	–	–	–	−527.5400	−526.8173	−526.8173	-723	-723
H_2	HH	164.6	9.8	0.0	−1.1646	−1.1745	−1.1336	−1.1336	-41	-41
LiH	HH	89.2	3.1	0.0	−8.0673	−8.0704	−7.9873	−7.9873	-83	-83
BeH	HH	74.7	4.7	0.0	−15.2421	−15.2468	−15.1536	−15.1532	-93	-94

Table 6.2: (*continued*)

Species	Geom.	$\Sigma D_0 \times 10^3$	$E_{\mathrm{ZPVE}} \times 10^3$	$\Delta E_{\mathrm{Rel}} \times 10^3$	E_0	E_e	E_{HF}		$E_{\mathrm{Corr}} \times 10^3$	
							UHF	RHF	UHF	RHF
CH	HH	127.3	6.5	0.0	−38.4723	−38.4788	−38.2844	−38.2798	-194	-199
$CH_2(^3B_1)$	KU	286.2	16.7	−0.5	−39.1317	−39.1484	−38.9408	−38.9353	-208	-213
$CH_2(^1A_1)$	KU	271.9	17.4	−0.3	−39.1172	−39.1346	−38.8959	−38.8959	-239	-239
CH_3	KU	460.9	29.5	−0.2	−39.8060	−39.8355	−39.5811	−39.5766	-254	-259
CH_4	KU	625.5	44.8	−0.5	−40.4710	−40.5158	−40.2170	−40.2170	-299	-299
NH	HH	125.9	7.4	−0.2	−55.2153	−55.2227	−54.9862	−54.9783	-236	-244
NH_2	KU	270.9	18.9	−0.3	−55.8604	−55.8794	−55.5920	−55.5870	-287	-292
NH_3	QCI	440.9	34.1	−0.5	−56.5306	−56.5647	−56.2249	−56.2249	-340	-340
OH	HH	161.4	8.2	−0.2	−75.7289	−75.7371	−75.4278	−75.4228	-309	-314
OH_2	KU	349.5	20.8	−0.8	−76.4176	−76.4383	−76.0672	−76.0672	-371	-371
FH	HH	215.5	8.9	−1.0	−100.4503	−100.4592	−100.0706	−100.0706	-389	-389
$SiH_2(^1A_1)$	QCI	230.1	11.8	−1.0	−290.5901	−290.6019	−290.0352	−290.0352	-567	-567
$SiH_2(^3B_1)$	KU	196.7	12.2	−1.3	−290.5569	−290.5692	−290.0288	−290.0268	-540	-542
SiH_3	QCI	341.0	20.4	−1.3	−291.2013	−291.2217	−290.6467	−290.6451	-575	-577
SiH_4	QCI	482.5	31.3	−1.6	−291.8431	−291.8744	−291.2682	−291.2682	-606	-606
PH_2	QCI	230.6	13.6	−0.3	−342.4899	−342.5035	−341.8929	−341.8872	-611	-616
PH_3	KU	362.4	24.2	−0.6	−343.1220	−343.1462	−342.4943	−342.4943	-652	-652
SH_2	KU	276.0	15.2	−1.4	−399.3874	−399.4026	−398.7198	−398.7198	-683	-683
ClH	HH	162.9	6.7	−1.6	−460.8125	−460.8192	−460.1125	−460.1125	-707	-707
Li_2	HH	38.2	0.8	0.0	−14.9944	−14.9951	−14.8716	−14.8716	-124	-124
LiF	HH	219.3	2.2	−1.0	−107.4322	−107.4344	−106.9931	−106.9931	-441	-441
HCCH	QCI	619.8	25.0	−0.8	−77.3105	−77.3355	−76.8555	−76.8555	-480	-480
H_2CCH_2	QCI	847.6	50.3	−0.8	−78.5384	−78.5888	−78.0706	−78.0706	-518	-518
H_3CCH_3	QCI	1061.8	74.6	−1.0	−79.7528	−79.8274	−79.2665	−79.2665	-561	-561

Table 6.2: (*continued*)

Species	Geom.	$\Sigma D_0 \times 10^3$	$E_{\mathrm{ZPVE}} \times 10^3$	$\Delta E_{\mathrm{Rel}} \times 10^3$	E_0	E_e	E_{HF}		$E_{\mathrm{Corr}} \times 10^3$	
							UHF	RHF	UHF	RHF
CN	HH	284.3	6.3	−0.2	−92.7187	−92.7250	−92.2422	−92.2250	-483	-500
HCN	KU	480.9	15.5	−0.5	−93.4156	−93.4311	−92.9157	−92.9157	-515	-515
CO	HH	408.3	4.7	−0.8	−113.3214	−113.3261	−112.7907	−112.7907	-535	-535
HCO	KU	430.8	13.0	−1.0	−113.8440	−113.8570	−113.3035	−113.2981	-553	-559
H_2CO	QCI	569.2	26.4	−1.1	−114.4826	−114.5090	−113.9231	−113.9231	-586	-586
H_3COH	QCI	766.2	50.8	−1.3	−115.6798	−115.7306	−115.1017	−115.1017	-629	-629
N_2	HH	358.7	4.8	−0.2	−109.5373	−109.5421	−108.9929	−108.9929	-549	-549
H_2NNH_2	QCI	646.0	52.9	−0.3	−111.8248	−111.8776	−111.2364	−111.2364	-641	-641
NO	HH	239.2	8.6	−0.5	−129.8962	−129.9047	−129.3087	−129.3009	-596	-604
O_2	HH	188.0	3.1	−1.0	−150.3236	−150.3267	−149.6908	−149.6672	-636	-660
HOOH	QCI	402.1	25.4	−1.4	−151.5381	−151.5635	−150.8528	−150.8528	-711	-711
F_2	HH	58.8	2.2	−1.4	−199.5280	−199.5303	−198.7729	−198.7729	-757	-757
CO_2	KU	608.6	11.2	−1.8	−188.5899	−188.6011	−187.7250	−187.7250	-876	-876
Na_2	HH	26.5	0.4	0.0	−324.5357	−324.5360	−323.7165	−323.7165	-819	-819
Si_2	HH	117.9	1.1	−1.6	−578.8375	−578.8386	−577.7615	−577.7549	-1077	-1084
P_2	HH	185.0	1.6	0.3	−682.7027	−682.7043	−681.4995	−681.4995	-1205	-1205
S_2	HH	160.5	1.5	−2.2	−796.3827	−796.3842	−795.1090	−795.0933	-1275	-1291
Cl_2	HH	91.2	1.2	−1.6	−920.3887	−920.3899	−919.0101	−919.0101	-1380	-1380
NaCl	HH	155.4	0.8	−1.8	−622.5597	−622.5605	−621.4600	−621.4600	-1101	-1101
SiO	HH	303.6	2.6	−1.3	−364.7312	−364.7337	−363.8545	−363.8545	-879	-879
SC	HH	270.1	2.9	−1.1	−436.2262	−436.2291	−435.3618	−435.3618	-867	-867
SO	HH	196.8	2.4	−1.8	−473.3759	−473.3783	−472.4210	−472.4039	-957	-974
ClO	HH	100.9	1.9	−2.1	−535.3182	−535.3201	−534.3183	−534.3106	-1002	-1009
ClF	HH	96.1	1.8	−2.2	−559.9802	−559.9820	−558.9194	−558.9194	-1063	-1063

Table 6.2: (*continued*)

Species	Geom.	$\Sigma D_0 \times 10^3$	$E_{\mathrm{ZPVE}} \times 10^3$	$\Delta E_{\mathrm{Rel}} \times 10^3$	E_0	E_e	E_{HF}		$E_{\mathrm{Corr}} \times 10^3$	
							UHF	RHF	UHF	RHF
Si_2H_6	QCI	797.0	49.1	−3.2	−582.5181	−582.5672	−581.3842	−581.3842	-1183	-1183
CH_3Cl	KU	591.2	37.8	−2.2	−500.0865	−500.1243	−499.1564	−499.1564	-968	-968
CH_3SH	QCI	709.3	46.2	−1.9	−438.6662	−438.7124	−437.7665	−437.7665	-946	-946
HOCl	KU	249.1	12.7	−2.4	−535.9668	−535.9795	−534.9340	−534.9340	-1045	-1045
SO_2	KU	404.8	6.3	−3.0	−548.6524	−548.6588	−547.3250	−547.3250	-1334	-1334

[a]Geometries are denoted by HH=Huber and Herzberg (experimental r_e from [164]), KU=Kuchitsu (experimental r_e from [170]) and QCI=geometry calculated using QCISD/G3MP2Large.

[b]Taken from [156], with the exception of CN from [130] and H_2 from [164].

[c]MP2/6-31G* ZPVE scaled by 0.9661 [165] taken from [166].

[d]Scalar relativistic and spin-orbit corrections taken from [167].

[e]Atomic total energies taken from [169]

[f]Calculated using cc-pV5Z-*h*.

Chapter 7

A new way to understand electron correlation*

Coulomb's law seems straightforward: particles of the same charge repel; opposites attract. But the deceptive simplicity of inverse-square laws yields surprising complexity even in very small systems. The classical three-body problem defeated the brightest minds of the 19th century and the quantum analogue proved equally resistant in the 20th. In the helium atom, for example, the two electrons dodge and weave as they seek to remain close to the nucleus but far from each other and, despite 80 years of work, an exact mathematical description of their motion still remains undiscovered.

Although an exact solution to the electronic Schrödinger equation [5] appears unlikely, the development of effective approximations brings rich rewards since the ability to calculate molecular energies accurately allows the *ab initio* determination of structure, bonding and reactivity and will have ramifications within biochemistry, material science and medicine.

In the early days of quantum theory, Hartree introduced the orbital approximation [7] wherein each electron is assumed to move independently in the mean field of all others and this was subsequently modified by Fock [8] to accommodate the requirements of the Pauli Principle. Though the Hartree-Fock (HF) model is simpler than the Schrödinger

*Taken directly from ref. [176]

formulation, the associated integro-differential equations are still difficult to solve in polyatomic systems. However, if the orbitals are expanded in a finite basis set, the more tractable Roothaan-Hall eigenvalue equations emerge [177, 178] and intensive efforts over the last thirty years have led to algorithms [179] whose computational cost grows only linearly with the size of the basis set. Using such methods and a standard PC, one can now perform a finite-basis HF calculation on a system with a few hundred atoms in a few hours [111]. HF theory often yields fairly accurate predictions of molecular structure but it is less satisfactory for most other properties. In particular, its mean-field treatment of electron motion cannot account properly for the formation of an electron pair during bond formation. It is therefore usually necessary to go beyond the HF model and explicitly include the fact that the motions of the electrons are correlated. Allowing the electrons to avoid one another stabilizes the system and the difference between the exact many-body energy of a system and its unrestricted HF energy is known as the correlation energy E_{Corr}. The task of calculating it is known as "the correlation problem" and has been the single greatest challenge to the progress of quantum chemistry since the subject's inception in 1927.

Models of electron correlation fall into two broad classes. Those in the first class, which include configuration interaction, Møller-Plesset perturbation theory and coupled cluster theory [6], are based on the mathematical observation that an improved wavefunction can be formed by taking a sum of HF-like wavefunctions, the latter being generated by the "substitution" of electrons from occupied to unoccupied orbitals in the HF wavefunction. Although in the limit these methods provide exact results, they are intrinsically inefficient [180] and, as a consequence, their computational cost becomes prohibitive even for quite small systems. This is the price that one pays for using a mathematically, rather than physically, motivated model.

The second class of models constitute the density-functional theories (DFT) and are based on the Hohenberg-Kohn theorem [37] which states that the exact energy of the ground state of a system is a unique functional of the exact electron density $\rho(\mathbf{r})$. Because $\rho(\mathbf{r})$ is a much simpler object than the wavefunction, DFT calculations are relatively inexpensive and have become the most popular tools in quantum chemistry. However, although the

existence of the unique Hohenberg-Kohn functional is proven, its form is unknown and the search for useful surrogates continues and has become increasingly empirical in recent years [41]. Many functionals are now available, each with its own strengths and weaknesses, but none entirely satisfactory. Moreover, it appears unlikely that the one-electron DFT models will ever be able to treat intrinsically two-electron phenomena such as dispersion energies [181].

Although the pursuit of more accurate functionals is unlikely to cease for some time, it is worth pausing to ask whether $\rho(\mathbf{r})$ is really the best starting point for calculations of electron correlation. After all, $\rho(\mathbf{r})$ measures the probability of finding one electron at the point $\mathbf{r}$ and yet electron correlation is concerned with the stabilization achieved when *two* electrons manage to avoid each other. Isn't it more natural, as emphasized by Hylleraas' famous work [43] on helium, to base an electron correlation model on the two-electron density? The answer is that, although this is certainly an attractive idea, a mechanism must be found by which two-electron information can be included without significantly degrading the computational advantages enjoyed by DFT. This has proven to be a major challenge but in this article we present a two-electron treatment of electron correlation which retains the favourable scaling of HF theory.

If it is agreed that information about pairs of electrons is valuable, we must then ask which property of the two electrons should be included and how this is best incorporated. The most obvious candidate is the inter-electronic distance $u = |\mathbf{r}_1 - \mathbf{r}_2|$ for one instinctively expects electrons that are close together to be strongly correlated. However, the naïvety of this expectation becomes clear when one considers the sequence of ground-state helium-like ions H^-, He, Li^+, whose exact and HF energies (in atomic units) are known [182,183] to be

$$E_{\text{exact}} = -Z^2 + \tfrac{5}{8}Z - 0.15767 + O(Z^{-1}) \tag{7.1}$$

$$E_{\text{HF}} = -Z^2 + \tfrac{5}{8}Z - 0.11100 + O(Z^{-1}) \tag{7.2}$$

where Z is the nuclear charge of the ion. It follows from these that $E_{\text{Corr}} = -0.04667 + O(Z^{-1})$ and the correlation energy therefore tends toward a constant as the nuclear charge

Figure 7.1: Wigner intracule for a beryllium atom

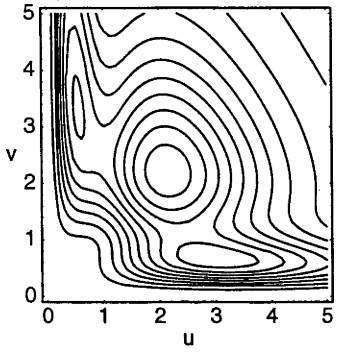

increases. Thus, for example, although the two electrons in the U^{90+} ion are generally much closer together than those in the Ne^{8+} ion, the resulting correlation energies are almost equal. This counterintuitive discovery clearly illustrates the insufficiency of u as a correlation indicator.

A few years ago, Rassolov argued [184] that not only the separation u, but also the relative momentum $v = |\mathbf{p}_1 - \mathbf{p}_2|$, of two electrons are crucial in determining their correlation. Rassolov's insight provides a simple explanation for the similarity in the correlation energies of the helium-like ions: as Z increases, the mean separation $\langle u \rangle$ decreases as $1/Z$, but the mean relative momentum $\langle v \rangle$ grows as Z and, evidently, these two effects cancel. We will return to this observation later.

In this article we develop Rassolov's idea into a general approach for estimating the correlation energy in any system. Our model is based on the Wigner intracule, a function that measures the distribution of u and v values in a system. In what follows, we introduce intracules, propose a connection between the Wigner intracule and the correlation energy, and present some preliminary results. We conclude by comparing our approach to existing methods and discussing how it may develop in the future. Atomic units are used throughout and all intracules and correlation energies are derived from the HF/6-311G wavefunction [185].

An intracule is the probability density function for the distance between two electrons in a certain space [186]. The position intracule $P(u)$, which gives the probability of finding two electrons separated by a distance u, was first utilized in theoretical chemistry by Coulson

and Nielson [47]. The momentum intracule $M(v)$, which gives the probability of finding two electrons with relative momentum v, was introduced by Banyard and Reed [84] but has received less attention than its position analogue. We recently introduced [105,186] the Wigner intracule

$$W(u,v) = \int W_2(\mathbf{r}_1\mathbf{p}_1\mathbf{r}_2\mathbf{p}_2)\delta(|\mathbf{r}_1 - \mathbf{r}_2| - u)\delta(|\mathbf{p}_1 - \mathbf{p}_2| - v)\mathrm{d}\mathbf{r}_1\mathrm{d}\mathbf{r}_2\mathrm{d}\mathbf{p}_1\mathrm{d}\mathbf{p}_2 \qquad (7.3)$$

which can be interpreted as the probability of finding two electrons at a distance u and with relative momentum v. However, since neither $W(u,v)$ nor the parent Wigner distribution $W_2(\mathbf{r}_1\mathbf{p}_1\mathbf{r}_2\mathbf{p}_2)$ is rigorously non-negative, neither is a proper probability distribution [106, 187] and $W(u,v)$ is termed a "quasi-probability". Nevertheless, the Wigner intracule yields the position and momentum intracules after projection

$$P(u) = \int_0^\infty W(u,v)\mathrm{d}v \qquad M(v) = \int_0^\infty W(u,v)\mathrm{d}u,$$

both of which are rigorous probability distributions. Furthermore it contains information that cannot easily be extracted from $P(u)$ and $M(v)$. We have previously reported the Wigner intracules for various atoms and molecules, in ground and excited states [120,186, 188,189], but an illustration at this point may be helpful. Fig. 7.1 shows the Wigner intracule for a ground-state beryllium atom [186] whose small $1s$ orbital and larger $2s$ orbital are each doubly occupied. Suppose that two of the electrons are observed. If both are in the $1s$ orbital, they will tend to be close together and moving rapidly, yielding the peak at low u and high v. If both are in the $2s$ orbital, they will tend to be further apart and moving relatively slowly, yielding the peak at large u and small v. If one is in the $1s$ orbital and the other is in the $2s$ orbital, intermediate u and v values arise, giving the central peak. For statistical reasons, this last peak is four times as large as the others.

The Wigner intracule is a versatile function and easily yields several components of the total energy. For example, in a n-electron system, the sum of the coulomb and exchange

energies, and the kinetic energy

$$E_J + E_K = \iint_0^\infty W(u,v)u^{-1}\mathrm{d}u\mathrm{d}v, \tag{7.4}$$

$$E_T = \iint_0^\infty W(u,v)\frac{v^2}{2(n-1)}\mathrm{d}u\mathrm{d}v, \tag{7.5}$$

are both linear functionals of the Wigner intracule contracted with a suitable kernel.

The purpose of this article is to suggest that the correlation energy can be obtained in a similar way. Specifically, we propose that

$$E_c = \iint_0^\infty W(u,v)G(u,v)\mathrm{d}u\mathrm{d}v \tag{7.6}$$

where $G(u,v)$ is a universal correlation kernel, analogous to the exchange-correlation functional of DFT.

Electron correlation is a measure of the error in the HF model and it is plausible that its assumption of independent motion is poorest for two electrons that are close together and have low relative momentum. Thus, we conjecture that situations in which both u and v are small make the largest contributions to the correlation energy. We expect a smaller contribution when one variable is small but the other is large, and we anticipate the least correlation when both are large. Contemplating this and the helium-like ions, mentioned above, led us to focus our initial efforts on correlation kernels that depend only on the product uv.

We have shown previously [105] that the Wigner intracule from a HF wavefunction is

$$W(u,v) = \frac{1}{2}\sum_{\mu\nu\lambda\sigma}\left[P_{\mu\nu}P_{\lambda\sigma} - P^\alpha_{\mu\sigma}P^\alpha_{\nu\lambda} - P^\beta_{\mu\sigma}P^\beta_{\nu\lambda}\right](\mu\nu\lambda\sigma)_W \tag{7.7}$$

where $\mathbf{P}$, $\mathbf{P}^\alpha$ and $\mathbf{P}^\beta$ are the usual total, alpha and beta density matrices [6] and $(\mu\nu\lambda\sigma)_W$

is a Wigner integral. This immediately yields a practical formula for the correlation energy

$$E_c^W = \frac{1}{2}\sum_{\mu\nu\lambda\sigma}\left[P_{\mu\nu}P_{\lambda\sigma} - P^{\alpha}_{\mu\sigma}P^{\alpha}_{\nu\lambda} - P^{\beta}_{\mu\sigma}P^{\beta}_{\nu\lambda}\right](\mu\nu\lambda\sigma)_G \tag{7.8}$$

$$(\mu\nu\lambda\sigma)_G = (2\pi)^{-3}\int \phi_\mu(\mathbf{r})\phi_\nu(\mathbf{r}+\mathbf{q})\phi_\lambda(\mathbf{r}+\mathbf{q}+\mathbf{u})\phi_\sigma(\mathbf{r}+\mathbf{u}) \times G(u,v)j_0(qv)\mathbf{drdqdudv} \tag{7.9}$$

where $j_0(z) = (\sin z)/z$ and the ϕ_i are basis functions. The good news is that this expression for E_c^W is conformal with the HF energy expression, indicating that the time to evaluate E_c^W will increase only as fast as that of a HF or DFT calculation. The bad news, on the other hand, is that the $(\mu\nu\lambda\sigma)_G$ appear to be much more challenging than the integrals normally encountered in quantum chemistry. However, for certain correlation kernels, we have developed a method to accurately determine these integrals as outlined below.

How can we determine the correlation kernel $G(u,v)$? A reasonable approach often taken by those who design exchange-correlation functionals for DFT, is to select a functional form with parameters that can be tuned to reproduce benchmark data. For the sake of simplicity we have restricted ourselves to two-parameter functions fitted to the known correlation energies [152] of the first and second row atoms.

DFT benefits from years of research which has uncovered many properties the exact functional must satisfy, but with little such theoretical guidance [190] as to the functional form of $G(u,v)$ we began by exploring linear combinations of elementary functions. This led us to discover that $G(u,v) = G_0 j_0(\zeta uv)$ (where the two parameters are $G_0 = -0.107$ and $\zeta = 0.902$) works remarkably well and is shown in fig. 7.2. Although the oscillatory nature of $G(u,v)$ may appear surprising, it can be shown that [191] the resulting $(ssss)_G$ integrals are always negative. We evaluate the correlation integrals (Eq. (7.9)) for this kernel using a convergent infinite series of positive terms, which can be summed to high accuracy. Each term in the series is given by an integral of the form

$$\langle m\rangle = \frac{\alpha^{2m}}{(2m+1)!}\int |\mathbf{r}-\mathbf{A}|^{2m}|\mathbf{r}-\mathbf{B}|^{2m}e^{-r^2}d\mathbf{r} \tag{7.10}$$

Figure 7.2: The correlation kernel $G(u,v) = -0.107 j_0(0.902uv)$

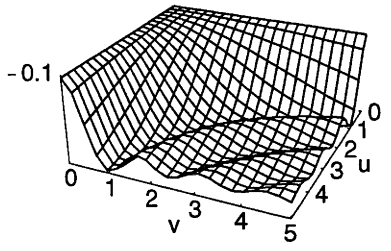

and these reduce to polynomials in A^2, B^2 and $|\mathbf{A}-\mathbf{B}|^2$. The $\langle m \rangle$ are computed using a five-term recurrence relation and has been implemented in a modified version of the Q-CHEM package [111].

To gauge the performance of our method, we compare our results to one of the most popular density functionals for calculating the correlation energy, the LYP functional [192]. For the atoms of the first and second rows (Table 7.1) the mean absolute deviations (MAD) from the exact correlation energies [152] are 1.5% for our method and 5.0% for LYP. Of course most chemists are interested in molecular properties so we have also examined how the the two methods reproduce the exact correlation energies [152] of the 73 neutral atoms and molecules from the G1 data set [154, 155]. Our method (Table 7.1) has a MAD of 5.6% compared to LYP's MAD of 5.2%. Remarkably, using a very simple $G(u,v)$, we have achieved comparable results to the much more complicated LYP functional. Moreover, examining the deviations in our method reveals systematic errors in isoelectronic species, which we believe can be exploited to improve accuracy in the near future.

The calculation of correlation energies at a low computational cost is one of the major goals of molecular physics. In this article, we have introduced a radical approach that is distinguished from conventional post-Hartree-Fock and density functional methods by its explicit dependence on two-electron phase-space information. It requires the computation of four-index integrals of a novel type but, apart from this, can be easily appended to a HF calculation. The method is conceptually simple and provides a powerful new perspective on the phenomenon of electron correlation. Preliminary results, obtained using a simple correlation kernel whose two parameters are fitted to the known correlation energies of the He and Ne atoms, are encouraging and we are confident that the accuracy of the method

Table 7.1: Exact correlation energies E_c^{ex} and deviations of the calculated values for the new method $\Delta_W = E_c^{ex} - E_c^W$ and for the LYP functional $\Delta_{LYP} = E_c^{ex} - E_c^{LYP}$ (all in millihartrees). † Maximum deviation.

Atom	$-E_c^{ex}$	Δ_W	Δ_{LYP}	Mol.	$-E_c^{ex}$	Δ_W	Δ_{LYP}
He	42	0	2	H_2	41	1	-3
Li	45	2	8	CH_4	299	53	-5
Be	94	-5	1	NH_3	340	23	-23
B	121	-2	5	H_2O	371	-2	-31
C	151	2	9	HF	371	-11	-16
N	185	6	7	C_2H_2	480	14	-37
O	249	1	9	C_2H_4	518	55	-21
F	318	5	4	C_2H_6	561	98	-10
Ne	391	-11	-7	N_2	549	-45	-67
Na	396	-7	12	O_2	636	-57	-67
Mg	438	-3	21	F_2	757	-80	-82
Al	465	1	30	HCN	515	-20	-52
Si	500	1	31	CO_2	876	-52	-87†
P	540	-1	26	HCl	707	15	19
S	597	3	33	Si_2H_6	1183	124	76
Cl	658	6	33	SO_2	1334	-206†	-81
Ar	723	10	28	NaCl	1101	19	31

can be improved further by refinement of the correlation kernel. We are extending this work in a number of directions: (1) The entire procedure can be performed self-consistently by absorbing the expression for E_c^W into the HF equations; (2) The methodology, unlike conventional DFT, can be used to treat dispersion energies; and (3) We are developing a more rigorous derivation of this approach.

7.1 Addendum

The preceding section is taken directly from ref. [176]. Due to the nature of the article some detail has been omitted. Some of the more important points should be expanded on further.

7.1.1 Rassolov's Idea

Rassolov proposed that the correlation energy should be expressible as the expectation value of a linear operator — one based on position and momentum [184]. He justified this using two physically very different systems: the first was the highly localized two-electrons ions of high nuclear charge, which we have mentioned above, and the second was the dense electron gas which is distributed over all space. In this second system it is possible to relate the correlation hole to the correlation operator and show that the proposed operator yields a pair correlation function which, although functionally different from the true form, has the correct dependence on the Wigner-Seitz radius and hence the density. Using these systems he was able to "derive" a general form which the correlation operator should take and show that the relative momentum was essential in the correct description of electron correlation. The form of the operator is given by

$$\hat{C} = -\frac{C_0}{r_{12}^2 p_{12}^2} \tag{7.11}$$

and by imposing constraints of hermiticity and symmetry with respect to permutation of basis functions within a $\langle ij|$ or $|kl\rangle$ (a constraint we do not apply) he was able to choose two operators, one analogous to the above equation and a second based on the Wigner distribution. Although Rassolov acknowledged limitations in both formulations, they were shown to give remarkably good results in the case of atoms and outperformed the LYP functional when mixed together using a single semi-empirical parameter. The concepts outlined in this paper mark the start of the work which has been continued in this thesis.

7.1.2 Determining a correlation kernel

In determining the form of a correlation kernel there are of course a myriad of possibilities. With no theoretical guidance as to what form this should take initial efforts focused on allowing the kernel to take any form. This was achieved by taking a linear combination of of well-tempered Gaussians and optimizing their coefficients to reproduce atomic correlation energies. At first this was done with the restriction that the correlation kernel should

Figure 7.3: Four-Gaussian correlation kernel

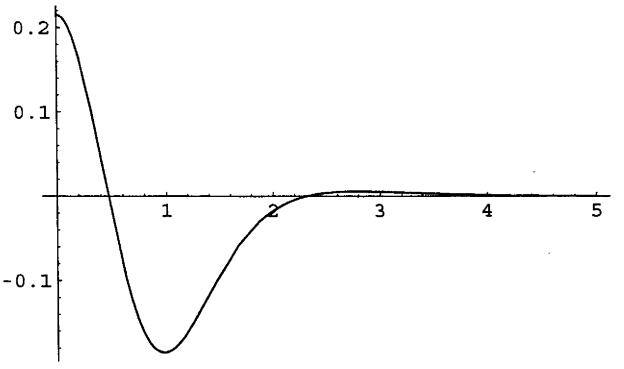

be everywhere negative as the notion of a positive correlation energy is physically unreasonable. However, it was quickly realised that such a function yields significantly inferior results to one which contains positive regions. A four Gaussian expansion optimized using the first row atoms is given by

$$G(s) = 1.00518\mathrm{e}^{-2s^2} - 0.60662\mathrm{e}^{-s^2} - 0.26209\mathrm{e}^{-\frac{s^2}{2}} + 0.07855\mathrm{e}^{-\frac{s^2}{4}} \qquad (7.12)$$

and is shown in fig. 7.3. The seemingly necessary negative regions in the correlation kernel led us to investigate oscillatory functions such as damped trigonometric functions and subsequently the zeroth-order spherical Bessel function which has been shown to work remarkably well. The Bessel function also has the attractive property that the $[ssss]_G$ integral is provably negative and in section 8.4.5 it will be shown that this choice of correlation kernel seems to lead to integrals which take on a simpler form than those of other kernels.

Chapter 8

Hartree-Fock-Wigner Theory

8.1 Introduction

The Hartree-Fock self-consistent field procedure forms the cornerstone of most quantum chemical calculations [6]. This independent particle model is the first approximation to the solution of the electronic Schrödinger equation and provides the starting point for more sophisticated treatments of the problem as a reference function for the multi-configurational methods. However, usually these methods apply corrections to the Hartree-Fock energy rather than solving the whole problem in a self-consistent manner. A self-consistent solution is more desirable, not only conceptually, but also from a computational point of view. Often the goal of a quantum chemical calculation is not to ascertain the energy but to determine some property such as the geometry, nuclear shielding constants, vibrational frequencies or countless others. Molecular properties like these are written in terms of derivatives of the energy with respect to the nuclear coordinates or some external field, and the calculation of such quantities is made much more straightforward when dealing with a self-consistent solution. The notable exception to this statement is, of course, Kohn-Sham density functional theory (DFT) which provides a self-consistent solution while incorporating electron correlation [36].

8.2 Hartree-Fock-Wigner theory

We have proposed [176] that the correlation energy can be estimated by

$$E_{\mathrm{C}} = \iint_0^\infty W_{\mathrm{HF}}(u,v) G_{\mathrm{HF}}(u,v)\, \mathrm{d}u\mathrm{d}v \tag{8.1}$$

where $W_{\mathrm{HF}}(u,v)$ is the Wigner intracule derived from a HF wavefunction and $G_{\mathrm{HF}}(u,v)$ is a correlation kernel. If the MOs are expanded within a basis set, the correlation energy is given by

$$E_{\mathrm{C}} = \frac{1}{2} \sum_{\mu\nu\lambda\sigma} \left[P_{\mu\nu}P_{\lambda\sigma} - P^{\alpha}_{\mu\sigma}P^{\alpha}_{\nu\lambda} - P^{\beta}_{\mu\sigma}P^{\beta}_{\nu\lambda} \right] (\mu\nu\lambda\sigma)_{\mathrm{G}} \tag{8.2}$$

where $P^{\alpha}_{\mu\nu}$ and $P^{\beta}_{\mu\nu}$ are elements of the α and β HF density matrices, $P_{\mu\nu}$ is an element of the total HF density matrix and $(\mu\nu\lambda\sigma)_{\mathrm{G}}$ is the 10-dimensional correlation integral for four AOs

$$(\mu\nu\lambda\sigma)_{\mathrm{G}} = \frac{1}{2\pi^2} \int \phi_\mu(\mathbf{r})\phi_\nu(\mathbf{r}+\mathbf{q})\phi_\lambda(\mathbf{r}+\mathbf{q}+\mathbf{u})\phi_\sigma(\mathbf{r}+\mathbf{u}) v^2 j_0(qv)\, G(u,v)\, \mathrm{d}\mathbf{r}\, \mathrm{d}\mathbf{q}\, \mathrm{d}\mathbf{u}\, \mathrm{d}v \tag{8.3}$$

The HF energy is given by

$$E_{\mathrm{HF}} = \sum_{\mu\nu} P_{\mu\nu}H_{\mu\nu} + \frac{1}{2} \sum_{\mu\nu\lambda\sigma} \left[P_{\mu\nu}P_{\lambda\sigma} - P^{\alpha}_{\mu\sigma}P^{\alpha}_{\nu\lambda} - P^{\beta}_{\mu\sigma}P^{\beta}_{\nu\lambda} \right] (\mu\nu|\lambda\sigma) \tag{8.4}$$

where $(\mu\nu|\lambda\sigma)$ are the usual Coulomb integrals. This expression may be combined with equation (8.2) to yield the Hartree-Fock-Wigner (HFW) energy

$$\begin{aligned} E_{\mathrm{HFW}} = & \sum_{\mu\nu} P_{\mu\nu}H_{\mu\nu} \\ & + \frac{1}{2} \sum_{\mu\nu\lambda\sigma} \left[P_{\mu\nu}P_{\lambda\sigma} - P^{\alpha}_{\mu\sigma}P^{\alpha}_{\nu\lambda} - P^{\beta}_{\mu\sigma}P^{\beta}_{\nu\lambda} \right] (\mu\nu\lambda\sigma)_{\mathrm{HFW}} \end{aligned} \tag{8.5}$$

where $(\mu\nu|\lambda\sigma)_{\mathrm{HFW}} = (\mu\nu|\lambda\sigma) + (\mu\nu\lambda\sigma)_{\mathrm{G}}$ and $P_{\mu\nu}$ is no longer a HF density matrix element but rather a density matrix element obtained when a self-consistent calculation is performed with the inclusion of the Wigner correlation energy.

8.3 The Fock matrix

Of course, the addition of correlation to the HF method does not come without a price. Although the formal scaling of HFW and HF are the same, both the computation and digestion of HFW integrals are more expensive. HFW integrals, like the integrals required in the calculation of momentum and Wigner intracules, have only four-fold permutational symmetry [110]

$$\begin{aligned}(\mu\nu\lambda\sigma)_{\mathrm{G}} &= (\nu\mu\sigma\lambda)_{\mathrm{G}} = (\sigma\lambda\nu\mu)_{\mathrm{G}} = (\lambda\sigma\mu\nu)_{\mathrm{G}} \\ (\mu\nu\sigma\lambda)_{\mathrm{G}} &= (\nu\mu\lambda\sigma)_{\mathrm{G}} = (\sigma\lambda\mu\nu)_{\mathrm{G}} = (\lambda\sigma\nu\mu)_{\mathrm{G}}\end{aligned} \tag{8.6}$$

This reduction in symmetry means that care must be taken to calculate all required HFW integrals without computing any extra Coulomb integrals. In Q-CHEM the HFW integrals are calculated by running over the list of Coulomb shell-quartets twice — the first time calculating all of the integrals and the second time calculating only ones for which $(\mu\nu\lambda\sigma)_{\mathrm{G}} \neq (\mu\nu\sigma\lambda)_{\mathrm{G}}$. Currently we must also switch off the cut-off schemes which are invoked to discard negligible Coulomb integrals as the corresponding correlation integral is not necessarily negligible. This procedure is not optimal but significant changes must be made to the shell-pair formation code and the integral batching system to remedy this. However, the speed-up from such optimisation would be negligible in comparison to improving the integral evaluation itself. Following the integral evaluation the next step in the SCF procedure is the construction of the Fock matrix. The Fock matrices in an unrestricted HFW calculation are exactly analogous to those in HF theory and are given by

$$F^{\alpha}_{\mu\nu} = H^{\mathrm{core}}_{\mu\nu} + \sum_{\lambda\sigma} P_{\lambda\sigma}\,(\mu\nu\lambda\sigma)_{\mathrm{HFW}} - P^{\alpha}_{\lambda\sigma}\,(\mu\lambda\nu\sigma)_{\mathrm{HFW}} \tag{8.7}$$

$$F^{\beta}_{\mu\nu} = H^{\mathrm{core}}_{\mu\nu} + \sum_{\lambda\sigma} P_{\lambda\sigma}\,(\mu\nu\lambda\sigma)_{\mathrm{HFW}} - P^{\beta}_{\lambda\sigma}\,(\mu\lambda\nu\sigma)_{\mathrm{HFW}} \tag{8.8}$$

Due to the difference in integral permutational symmetry, the construction of the HFW Fock matrices differs in that each integral contributes to only *four*, elements of the Fock matrix as compared to six in HF. Assuming for simplicity that all labels are different, each

integral contributes to the following elements of the α Fock matrix

$$\begin{aligned} F^{\alpha}_{\mu\nu} &= F^{\alpha}_{\mu\nu} + P_{\lambda\sigma}\,(\mu\nu\lambda\sigma)_{\mathrm{HFW}} \\ F^{\alpha}_{\lambda\sigma} &= F^{\alpha}_{\lambda\sigma} + P_{\mu\nu}\,(\mu\nu\lambda\sigma)_{\mathrm{HFW}} \\ F^{\alpha}_{\mu\sigma} &= F^{\alpha}_{\mu\sigma} - P^{\alpha}_{\nu\lambda}\,(\mu\nu\lambda\sigma)_{\mathrm{HFW}} \\ F^{\alpha}_{\nu\lambda} &= F^{\alpha}_{\nu\lambda} - P^{\alpha}_{\mu\sigma}\,(\mu\nu\lambda\sigma)_{\mathrm{HFW}} \end{aligned} \tag{8.9}$$

The β-Fock matrix is constructed analogously.

8.4 Calculating $(\mu\nu\lambda\sigma)_G$ integrals

We have defined the correlation integrals $(\mu\nu\lambda\sigma)_G$ above in equation (8.3). Clearly the form of these integrals will be dependent on the choice of the correlation kernel and we will now review the various approaches which have been employed to calculate these integrals focusing mainly on the correlation kernel $G(u,v) = cj_0(\zeta uv)$ but also looking at some more general approaches. As mentioned in the previous chapter the correlation integrals are more challenging to calculate than most integrals in quantum chemistry and none of the methods I will mention are entirely satisfactory.

8.4.1 Correlation integrals by quadrature

This is the crudest and slowest method of calculating the correlation integrals but it has the advantage of being an easy way to get some indicative results. This has only been used in the calculation of post-HF correlation energies and provides a very rapid way of checking the efficacy of a new correlation kernel. By constructing a library of Wigner intracules we can take any new correlation kernel and calculate the integral (8.1) to get quick, but not highly accurate estimates, to the correlation energy. Table 8.1 shows how accurately we can calculate the volume under the Wigner intracule for a selection of atoms and molecules and all of them lie within $\sim 1\%$ of the true value. This suggests that we should obtain results of reasonable accuracy when we integrate the product of the intracule and a correlation kernel. In order to do this integral as efficiently as possible the

Figure 8.1: To show the how accurately the Wigner intracule can be integrated numerically.

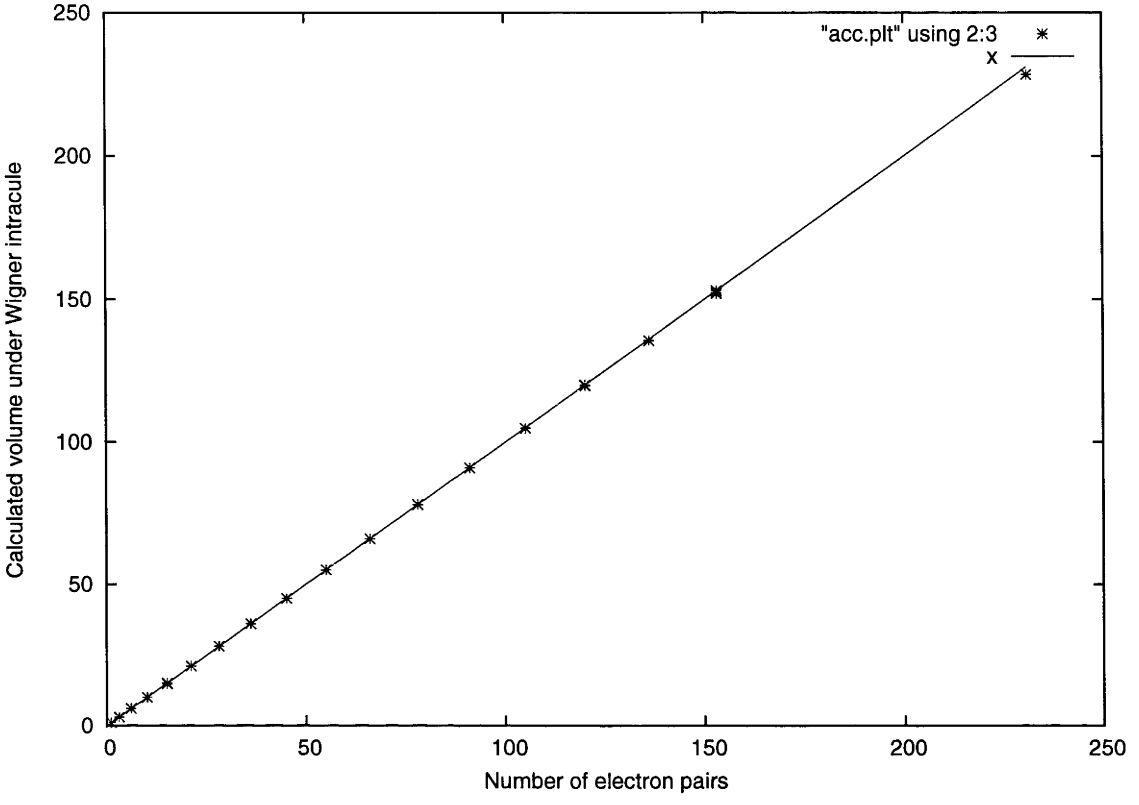

Wigner intracules are calculated across the product of a u and v radial quadrature grid. In particular we used a 50-point Euler-Maclaurin grid. Of course since the Wigner intracules were calculated using a 302-point Lebedev quadrature, this means that obtaining the final correlation energy required a 4-dimensional quadrature. Clearly this is not practical in a SCF calculation where the Wigner intracule would have to be recalculated at each step.

8.4.2 Correlation integrals for a Gaussian correlation kernel

In quantum chemistry when we are faced with a difficult integral, a common approach to evaluating it is to approximate it my a sum of easier integrals. The most familiar example of this is the approximation of a STO by a linear combination of GTOs which results in the great simplification of molecular integrals. With this in mind we hoped that most of the correlation kernels we would be interested in could be well approximated by a linear

combination of Gaussians. Starting from eqn. (4.29) and inserting $G(u,v) = \mathrm{e}^{-\zeta u^2 v^2}$ gives

$$[ssss]_G = \frac{\pi \mathrm{e}^{-R}}{2(\alpha+\delta)^{3/2}(\beta+\gamma)^{3/2}} \int v^2 \mathrm{e}^{-\lambda^2 u^2 - \mu^2 v^2 - \mathbf{P}.\mathbf{u}} j_0(|\mathbf{Q} + \eta\mathbf{u}|v) \mathrm{e}^{-\zeta u^2 v^2} \mathrm{d}v\mathrm{d}\mathbf{u} \quad (8.10)$$

The integral over v is straightforward and after some rearrangement yields

$$\begin{aligned}[ssss]_G =& \frac{\pi^{5/2}\mathrm{e}^{-R}}{4(\alpha+\delta)^{3/2}(\beta+\gamma)^{3/2}} \\ &\times \int \frac{u^2}{(u^2\zeta+\mu^2)^{3/2}} \mathrm{e}^{-\lambda^2 u^2 - \frac{Q^2+\eta^2u^2}{4(u^2\zeta+\mu^2)} - \left|\mathbf{P}+\frac{2\eta\mathbf{Q}}{2(u^2\zeta+\mu^2)}\right| u\cos\theta} \sin\theta \mathrm{d}\theta\mathrm{d}u\end{aligned} \quad (8.11)$$

Doing the integral over θ leaves us with the one dimensional integral

$$\begin{aligned}[ssss]_G =& \frac{\pi^{5/2}\mathrm{e}^{-R}}{2(\alpha+\delta)^{3/2}(\beta+\gamma)^{3/2}} \\ &\times \int \frac{u^2}{(u^2\zeta+\mu^2)^{3/2}} \mathrm{e}^{-\lambda^2 u^2 - \frac{Q^2+\eta^2u^2}{4(u^2\zeta+\mu^2)}} i_0\left(\left|\mathbf{P}+\frac{2\eta\mathbf{Q}}{2(u^2\zeta+\mu^2)}\right| u\right) \mathrm{d}u\end{aligned} \quad (8.12)$$

This integral can be evaluated quite efficiently by quadrature and due to the exponential character of the integrand we find that the MultiExp grid [193] is particularly effective. Fig. 8.2 shows the convergence of the correlation energy of ethane with increasing grid size. By just a 19-point rule the correlation energy has converged to within 0.1 mE_h. Furthermore, the form of this integral, with respect to forming integrals of higher angular momentum, is isomorphic to the Wigner integrals so with some relatively minor alterations to the Wigner integral code, correlation integrals for s- and p-orbitals can be calculated.

This formulation can be used to calculate any linear combination of Gaussians but we are particularly interested in a combination which yields a good approximation to a zeroth-order spherical Bessel function.

$$j_0(z) = \sum_{i=1}^{\infty} c_i \exp(-\alpha_i z^2) \quad (8.13)$$

To determine the coefficients c_i and exponents α_i of such an expansion we first substitute

Figure 8.2: How the correlation energy of ethane changes with increasing quadrature grid size.

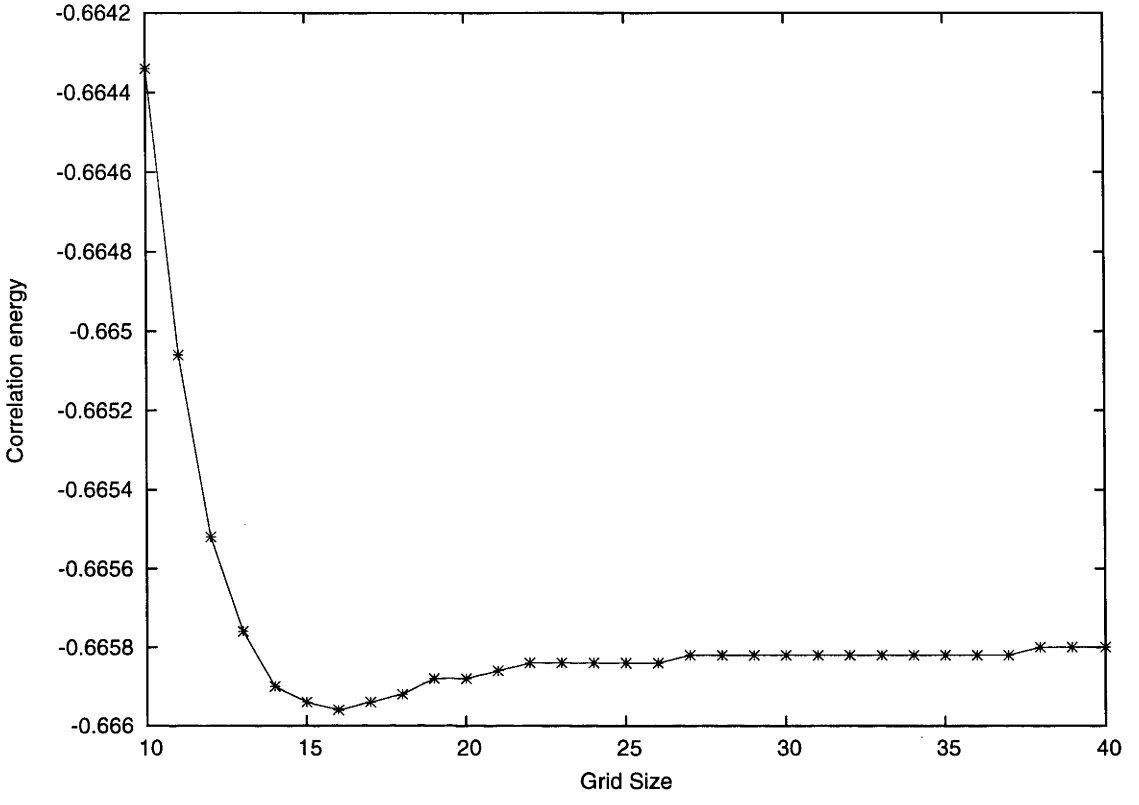

the Taylor series for both the Bessel function and the Gaussian

$$j_0(z) = \sum_{k=0}^{\infty} \frac{-z^2}{(2k+1)!} = \sum_{i=1}^{\infty} c_i \sum_{k=0}^{\infty} \frac{(-\alpha_i z)^2}{k!} \tag{8.14}$$

$$= \sum_{k=0}^{\infty} \sum_{i=1}^{\infty} c_i \frac{(-\alpha_i z)^2}{k!} \tag{8.15}$$

Equating powers of z^2 yields the moments equation

$$\sum_{i=1}^{\infty} c_i \alpha_i^k = \frac{k!}{(2k+1)!} \tag{8.16}$$

The exponents are the roots of the orthogonal polynomials on $[0,1]$ with the weight function $w(z)$ that satisfies

$$\int_0^1 z^k w(z) \mathrm{d}z = \frac{k!}{(2k+1)!} \tag{8.17}$$

To determine the exponents and coefficients we follow the method described by Szego [194] which efficiently produces high order expansions. These expansions consist of complex con-

Figure 8.3: 2-, 4-, 8- and 16-Gaussian representations of the zeroth order spherical Bessel function

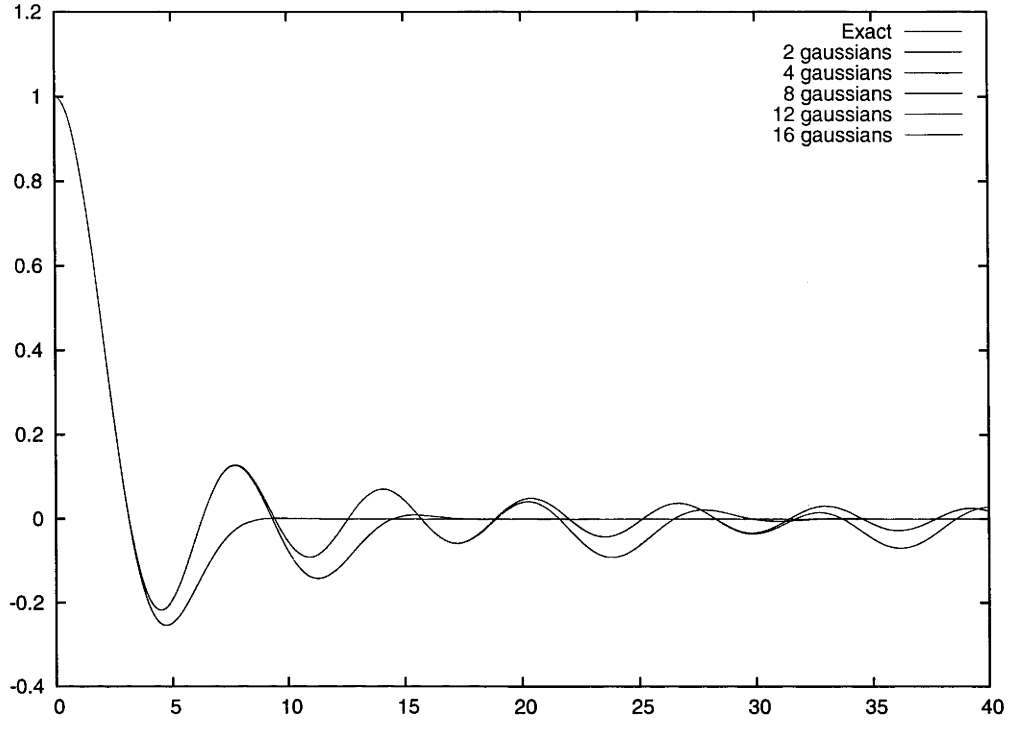

jugate pairs of exponents and coefficients. Figure 8.3 shows a selection of the expansions.

Unfortunately high order expansions require very high precision and beyond about 20 Gaussians double precision accuracy does not suffice and the expansions become noisy and inaccurate. One might expect that most of the correlation energy will result from small values of uv and hence large expansions would not be required but as was seen in section 5, action intracules decay very slowly and although all of the oscillations in $G(uv)$ may not be physically important, their presence may be important in the cancellation of one another. This is seen in fig. 8.4 which shows how the correlation energy oscillates with the number of Gaussians used in the expansion of $j_0(\zeta uv)$. If we were to take just even (or odd) numbered expansions we can see that the correlation energy seems to be converging. However the ambiguity in the correlation energy is still ~ 5 mE_h and we cannot add any more Gaussians due to the loss of precision. It would also require that several calculations be performed on each molecule to ensure we are approaching convergence as the size of expansion required will differ for molecules of different sizes.

Figure 8.4: How the correlation energy of ethane changes with increasing numbers of Gaussians used to approximate $j_0(\zeta uv)$.

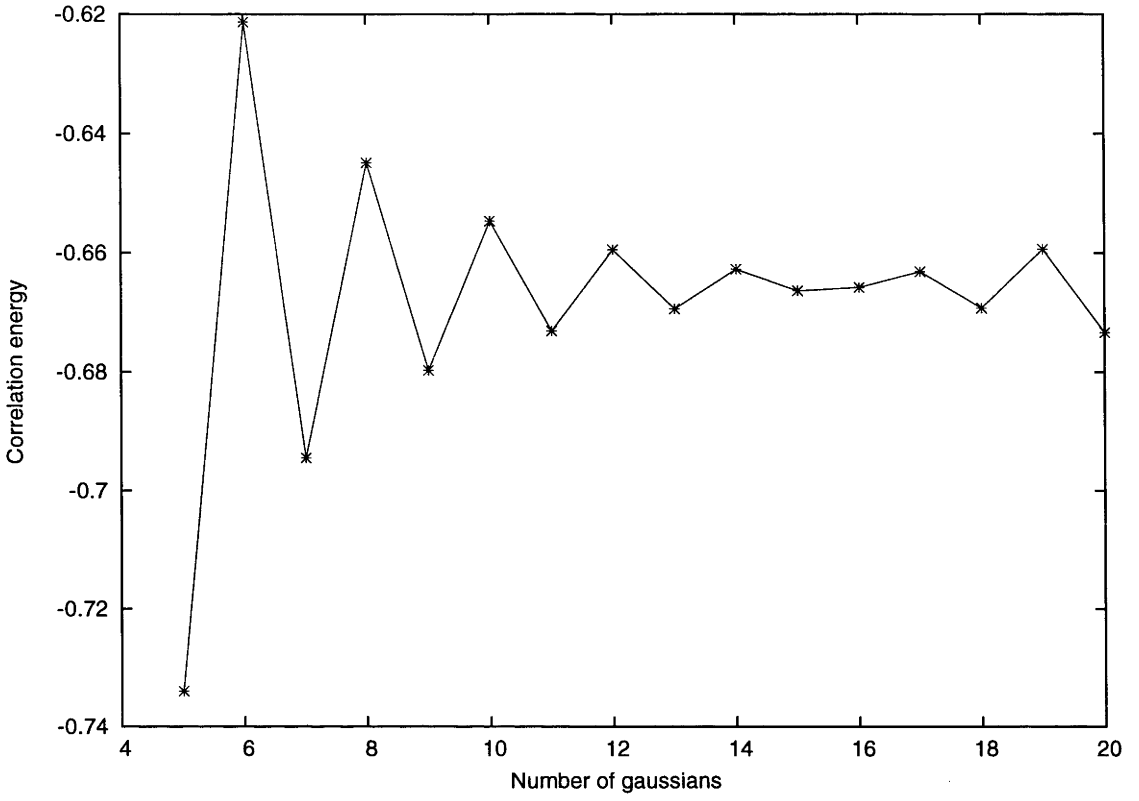

8.4.3 Correlation integrals for a general class of correlation kernels

Rather than specifying a correlation kernel, a much more powerful approach would be to develop a method to evaluate the correlation integrals for a more general class of correlation kernel. We will limit ourselves to looking at kernels which can be written as even power series of u and v

$$G(u,v) = \sum_{m=0}^{\infty}\sum_{n=0}^{\infty} a_{m,n} u^{2m} v^{2n} \tag{8.18}$$

where the $a_{m,n}$ are expansion coefficients. The resulting correlation integrals will require the evaluation of the even-order u and v moments of the Wigner integrals

$$[ssss]_G = \sum_{m=0}^{\infty}\sum_{n=0}^{\infty} a_{m,n} \iint_0^{\infty} u^{2m} v^{2n} [ssss]_W \mathrm{d}u\mathrm{d}v = \sum_{m=0}^{\infty}\sum_{n=0}^{\infty} a_{m,n} [ssss]_W^{(2m,2n)} \tag{8.19}$$

We will discuss the calculation of these moments in the next section, but first we will introduce a powerful tool for finding recurrence relations which has been invaluable in this

work and an integral which will occur in several places.

Sister Celine's Method

The problem of finding a recurrence relation for a set of polynomials can be somewhat of a black art and the problem becomes only more difficult in the case of multivariate polynomials. However there is a general class of polynomials for which there is a systematic way of finding recurrence relations. These polynomials result from hypergeometric series which truncate after a finite number of terms. Many of the standard orthogonal polynomials are examples of such hypergeometric series. Sister Celine's method [195] is used for finding recurrence relations for such hypergeometric polynomials given the series expansion. For a hypergeometric sum

$$f(n) = \sum_k F(n,k) \tag{8.20}$$

in which F is doubly hypergeometric, i.e.,

$$\frac{F(n+1,k)}{F(n,k)} \quad \text{and} \quad \frac{F(n,k+1)}{F(n,k)} \tag{8.21}$$

are both rational functions of n and k. Sister Celine's method will first find a recurrence of the form

$$\sum_{i=0}^{I}\sum_{j=0}^{J} a_{i,j}(n)F(n-j,k-i) = 0 \tag{8.22}$$

for the summand F and note that $a_{i,j}$ is free of k. It is then straightforward to deduce a recurrence relation for $f(n)$. To demonstrate how this is done we will consider a very simple example

$$f(n) = \sum_k \binom{n}{k} \tag{8.23}$$

The first step is to fix the limits I and J in the recurrence relation (8.22), say $I = J = 1$ and let us assume that $a_{0,0} = 1$, which leads to the following recurrence

$$\binom{n}{k} + a_{0,1}\binom{n}{k-1} + a_{1,0}\binom{n-1}{k} + a_{1,1}\binom{n-1}{k-1} = 0 \tag{8.24}$$

Now divide through the expression by $F(n,k) = \binom{n}{k}$, place over a common denominator and collect the numerator in powers of k

$$-(1+a_{1,0})(n+n^2)+(a_{1,0}-a_{1,1}+n(1-a_{0,1}+2a_{1,0}-a_{1,1}))k+(-a_{1,0}+a_{1,1})k^2=0 \quad (8.25)$$

Equating each of the powers of k to zero and solving the set of linear equations yields $a_{0,1}=0, a_{1,0}=a_{1,1}=-1$.

$$\binom{n}{k} = \binom{n-1}{k} + \binom{n-1}{k-1} \quad (8.26)$$

We now have a recurrence for $F(n,k)$. Since the coefficients will always be independent of k deducing a relation for $f(n)$ using eqn. (8.23) is simple

$$f(n) = f(n-1) + f(n-1) = 2f(n-1) \quad (8.27)$$

Clearly this is a trivial example which does not require the use of the algorithm but it serves to illustrate the steps involved in Sister Celine's technique. In more complex examples choosing $I = J = 1$ will lead to a set of linear equations for which there is no solution and larger values of I and/or J are required. In fact if $F(n,k)$ is a proper hypergeometric term

$$F(n,k) = P(n,k)\frac{\prod_i (a_i n + b_i k + c_i)!}{\prod_i (u_i n + v_i k + w_i)!} x^k \quad (8.28)$$

where P is a polynomial and the parameters are integers and the limits of the products are finite, then Sister Celine's method is guaranteed to find a recurrence provided the span of the assumed recurrence is large enough.

Sister Celine's method has been generalized to multivariate hypergeometric polynomials by Wilf and Zeilberger [196]. This has been extended and implemented by Wegshaider [197] in the MultiSum MATHEMATICA package and we have used it to determine recurrence relations for the trivariate polynomials which occur in the evaluation of the correlation integrals. In theory Sister Celine's method is guaranteed to find a recurrence for hypergeometric polynomials, but in practice, if the recurrence relation is too complicated then the set of linear equations becomes prohibitively large. Even if such a recurrence could be deduced, it is unlikely that it would be numerically stable and thus computationally

useful.

A useful integral

Consider the overlap integral of two monomials, centred at **A** and **B**, and a Gaussian at the origin

$$\langle a|b\rangle = \pi^{-3/2}\int |\mathbf{r}-\mathbf{A}|^{2a}|\mathbf{r}-\mathbf{B}|^{2b}\mathrm{e}^{-r^2}\mathrm{d}\mathbf{r} \tag{8.29}$$

This deceptively simple looking integral turns out to be rather complicated to evaluate. If we consider the monomials in terms of the following derivatives

$$\langle a|b\rangle = \pi^{-3/2}\int \frac{\partial^{a+b}}{\partial\alpha^a\beta^b}\left\{\mathrm{e}^{\alpha|\mathbf{r}+\mathbf{A}|^2-\beta|\mathbf{r}-\mathbf{B}|^2-r^2}\right\}_{\alpha=\beta=0}\mathrm{d}\mathbf{r} \tag{8.30}$$

Interchanging the order of integration and differentiation we are left with the derivative with respect to a three-centre overlap integral. This integral is trivial, and by writing the resultant as a three-fold Maclaurin series in A^2, B^2 and $AB^2 = |\mathbf{A}-\mathbf{B}|^2$, the required derivatives can be evaluated to yield

$$\langle a|b\rangle = \left(\frac{3}{2}\right)_{a+b}\sum_{i=0}^{\infty}\sum_{j=0}^{\infty}\sum_{k=0}^{\infty}\frac{(-a)_{i+k}(-b)_{j+k}}{(\frac{3}{2})_{i+j+k}(-a-b-\frac{1}{2})_k}\frac{(-A^2)^i}{i!}\frac{(-B^2)^j}{j!}\frac{(AB^2)^k}{k!} \tag{8.31}$$

where $(z)_n$ is the Pochhammer symbol [21]. Although written as a three-fold infinite summation the expansion truncates for $i+k>a$ and $j+k>b$ to yield trivariate polynomials, a few of which are shown below

a \ b	0	1	2
0	1	$\frac{3}{2}+B^2$	$\frac{15}{4}+5B^2+B^4$
1	$\frac{3}{2}+A^2$	$\frac{15}{4}+\frac{5A^2}{2}-AB^2+\frac{5B^2}{2}+A^2B^2$	$\frac{105}{8}+\frac{35A^2}{4}-5AB^2+\frac{35B^2}{2}$ $+7A^2B^2-2AB^2B^2+\frac{7B^4}{2}+A^2B^4$
2	$\frac{15}{4}+5A^2+A^4$	$\frac{105}{8}+\frac{35A^2}{2}+\frac{7A^4}{2}-5AB^2$ $-2A^2AB^2+\frac{35B^2}{4}+7A^2B^2+A^4B^2$	$\frac{945}{16}+\frac{315A^2}{4}+\frac{63A^4}{4}-35AB^2$ $-14A^2AB^2+2AB^4+\frac{315B^2}{4}+\ldots$

As can be seen, even for small values of a and b the expressions quickly become unwieldy and it is clearly not practical to perform these summations directly. Furthermore, since

the summand is not always of the same sign, such a direct approach would most likely be numerically unstable. However, the $\langle a|b\rangle$ are hypergeometric polynomials and thus we should be able to find a recurrence relation using Sister Celine's method which could then be used to evaluate them. An example of such a recurrence relation is

$$\begin{aligned}\langle a|b\rangle^{(\mu)} =& \frac{1}{2(a-b)}\Bigg\{a(1+2a)\left(\langle a-1|b\rangle^{(\mu)} + \frac{2A^2}{3+2\mu}\langle a-1|b\rangle^{(\mu+1)}\right) \\ & - b(1+2b)\left(\langle a|b-1\rangle^{(\mu)} + \frac{2B^2}{3+2\mu}\langle a|b-1\rangle^{(\mu+1)}\right)\Bigg\}\end{aligned} \tag{8.32}$$

where the auxiliary index μ has been introduced as follows

$$\langle a|b\rangle^{(\mu)} = \left(\frac{3}{2}\right)_{a+b}\sum_{i=0}^{\infty}\sum_{j=0}^{\infty}\sum_{k=0}^{\infty}\frac{(-a)_{i+k}(-b)_{j+k}}{(\frac{3}{2}+\mu)_{i+j+k}(-a-b-\frac{1}{2})_k}\frac{(-A^2)^i}{i!}\frac{(-B^2)^j}{j!}\frac{(AB^2)^k}{k!} \tag{8.33}$$

We note that this recurrence can only be used when $a \neq b$, but there are other recurrences which can be used to get around this. It is possible, to derive a recurrence for $\langle a|b\rangle$ without introducing an auxiliary index but the smallest recurrence relation has ten terms and is unlikely to be useful.

8.4.4 The moment integrals

Starting from the form of the Wigner integral for four s-type Gaussian functions with centres **A**, **B**, **C**, **D** and exponents α, β, γ and δ given in eqn. (4.29), the moment integrals are given by

$$[ssss]_W^{(2m,2n)} = \frac{\pi e^{-(R+\lambda^2u^2+\mu^2v^2)}}{2(\alpha+\delta)^{3/2}(\beta+\gamma)^{3/2}}\int u^{2m}v^{2n+2}e^{-\mathbf{P}.\mathbf{u}}j_0(|\mathbf{Q}+\eta\mathbf{u}|v)\mathrm{d}\mathbf{u}\mathrm{d}v \tag{8.34}$$

Considering first the integral over v we have

$$\int_0^{\infty} v^{2n+2}\exp(-\mu^2v^2)j_0(|\mathbf{Q}-\eta\mathbf{u}|v)\mathrm{d}v = \frac{n!\sqrt{\pi}}{4\mu^{2n+3}}e^{-\frac{|\mathbf{Q}-\eta\mathbf{u}|^2}{4\mu^2}}L_n^{1/2}\left(\frac{|\mathbf{Q}-\eta\mathbf{u}|^2}{4\mu^2}\right) \tag{8.35}$$

where $L_n^\lambda(z)$ are the generalized Laguerre polynomials [21]. Using this integral and also the substitution

$$\mathbf{u} = \sqrt{\frac{4\mu^2}{\eta^2 + 4\mu^2\lambda^2}}\,\mathbf{r} + \frac{2\mu^2\mathbf{P} + \eta\mathbf{Q}}{\eta^2 + 4\mu^2\lambda^2} \tag{8.36}$$

it can be shown that

$$[ssss]_W^{(2m,2n)} = SK_{m,n}(m|n) \tag{8.37}$$

where

$$S = \left(\frac{\pi}{\alpha+\beta}\right)^{3/2}\left(\frac{\pi}{\gamma+\delta}\right)^{3/2} \mathrm{e}^{-\frac{\alpha\beta}{\alpha+\beta}|A-B|^2 - \frac{\gamma\delta}{\gamma+\delta}|C-D|^2} \tag{8.38}$$

$$K_{m,n} = \left(\frac{1}{\alpha+\beta}+\frac{1}{\gamma+\delta}\right)^m\left(\frac{1}{\alpha+\delta}+\frac{1}{\beta+\gamma}\right)^{-n} \tag{8.39}$$

$$(m|n) = \frac{2^{2n}n!}{\pi^{3/2}}\int |\mathbf{r}-\mathbf{R}_1|^{2m} L_n^{1/2}\left(\theta^2|\mathbf{r}-\mathbf{R}_2|^2\right)\mathrm{e}^{-r^2}\mathrm{d}\mathbf{r} \tag{8.40}$$

and

$$\mathbf{R}_1 = -\left(\frac{1}{\alpha+\beta}+\frac{1}{\gamma+\delta}\right)^{-1/2}\left(\frac{\alpha\mathbf{A}+\beta\mathbf{B}}{\alpha+\beta} - \frac{\gamma\mathbf{C}+\delta\mathbf{D}}{\gamma+\delta}\right) \tag{8.41}$$

$$\mathbf{R}_2 = \left(\frac{1}{\alpha+\beta}+\frac{1}{\gamma+\delta}\right)^{-1/2}\frac{\alpha+\beta+\gamma+\delta}{\alpha\gamma-\beta\delta}\left(\frac{\alpha\beta}{\alpha+\beta}(\mathbf{A}-\mathbf{B}) - \frac{\gamma\delta}{\gamma+\delta}(\mathbf{C}-\mathbf{D})\right) \tag{8.42}$$

$$\theta^2 = \frac{(\alpha\gamma-\beta\delta)^2}{(\alpha+\beta)(\gamma+\delta)(\alpha+\delta)(\beta+\gamma)} \tag{8.43}$$

We must now consider the three-dimensional $(m|n)$ integral. First we expand the Laguerre polynomial

$$(m|n) = 2^{2n}\Gamma(n+\frac{3}{2})\sum_{b=0}^{n}\frac{(-n)_b}{\Gamma(b+3/2)}\frac{\theta^{2b}}{b!}\langle m|b\rangle \tag{8.44}$$

where $\Gamma(z)$ is the gamma function [21] and the $\langle m|b\rangle$ are defined in eqn. (8.29). Now inserting the expression given in eqn. (8.31) for $\langle a|b\rangle$ into eqn. (8.44) yields the following

$$\begin{aligned}(m|n) =& 2^{2n}m!(2n+1)!\sum_{b=0}^{n}\sum_{i=0}^{\infty}\sum_{j=0}^{\infty}\sum_{k=0}^{\infty}\frac{(-\theta^2)^b}{(n-b)!(b-j-k)!(m-i-k)!}\\ &\times\frac{(b+\frac{3}{2})_m}{(\frac{3}{2})_{i+j+k}(-m-b-\frac{1}{2})_k}\frac{(R_1^2)^i}{i!}\frac{(R_2^2)^j}{j!}\frac{(|\mathbf{R}_1-\mathbf{R}_2|^2)^k}{k!}\end{aligned} \tag{8.45}$$

The $(m|n)$ integrals are also hypergeometric polynomials and as such recurrence relations can be found using the method of Sister Celine (although 2 parameters must be added

to find a reasonable relation). We do not list the recurrence relation here as there are several problems with this formulation. Firstly, the series is in general slowly convergent although this will of course be dependent on the choice of correlation kernel. To sum such a series would require the ability to accurately and efficiently evaluate $(m|n)$ for large m and n. Unfortunately the recurrence relation which was deduced is not numerically stable for large m and n. Also, the sign of the $(m|n)$ are neither the same nor oscillating which means that even if we could evaluate the high order terms the numerical stability of the summation would be problematic.

The possible solution to all of these problems would be to accelerate the convergence of the series. Many of the convergence acceleration techniques, such as Aitken's δ^2-process [198] and Wynn's ϵ-method [199], are based on extrapolation and require the terms to be decreasing before they can be used. This is not the case for the $(m|n)$ integrals. There is another method called Kummer's transformation [21] in which an auxiliary series, whose sum is known and has the same asymptotic behaviour as the one being summed, is used to dramatically increase the rate of convergence. The challenge in this method is to find an appropriate and summable auxiliary series. To determine the asymptotic behaviour of the $(m|n)$s or the $\langle a|b\rangle$s we tried to use the method of stationary phase in which the integrand is approximated by a Gaussian. However determining the location of the maximum of these integrands, the point at which the Gaussian would be placed, has proved too difficult and the asymptotic behaviour of these integrals has not been determined. If this could be done, and a suitable auxiliary series devised, the required sum could be evaluated. This would indeed be an achievement as it allow the computation of correlation integrals for any correlation kernel with an even power series.

8.4.5 Correlation integrals for a zeroth-order spherical Bessel function

Although we could again begin at eqn. (4.29) and insert $G(u,v) = j_0(\zeta uv)$, it is informative to get to this point from the general formulation. Taking eqn. (8.44) and inserting eqn.

(8.29) yields the following form for the correlation integral

$$[ssss]_G = S\sum_{m,n} a_{m,n}K_{m,n}2^{2n}\Gamma(n+\frac{3}{2})\sum_{b=0}^{\infty}\frac{(-n)_b}{\Gamma(b+\frac{3}{2})}\frac{\theta^{2b}}{b!} \times\left\{\pi^{-3/2}\int|\mathbf{r}-\mathbf{R}_1|^{2m}|\mathbf{r}-\mathbf{R}_2|^{2b}\mathrm{e}^{-r^2}\mathrm{d}\mathbf{r}\right\} \tag{8.46}$$

and with some rearrangement gives

$$[ssss]_G = S\sum_{b=0}^{\infty}\frac{(-1)^b(2\theta)^{2b}}{(2b+1)!}\left\{\pi^{-3/2}\int f_b(|\mathbf{r}-\mathbf{R}_1|)|\mathbf{r}-\mathbf{R}_2|^{2b}\mathrm{e}^{-r^2}\mathrm{d}\mathbf{r}\right\} \tag{8.47}$$

and

$$f_b(x) = \sum_{m,n} a_{m,n}K_{m,n}\frac{(2n+1)!}{(n-b)!}x^{2m} \tag{8.48}$$

Limiting ourselves just to functions of uv, i.e., $n = m$, and letting $a_{m,m} = a_m$ and $K_{m,m} = K_m$ gives

$$f_b(x) = K_b x^{2b}\sum_m a_{m+b}K_m\frac{(2m+2b+1)!}{m!}x^{2m} \tag{8.49}$$

The simplest, non-trivial, choice of correlation kernel is one in which $a_m = \frac{(-1)^m\zeta^{2m}}{(2m+1)!}$ as this will result in the outer sum having all positive terms and the inner sum reducing to a Gaussian function

$$f_b(x) = (-1)^b K_b\zeta^{2b}x^{2b}\mathrm{e}^{-\zeta^2K_1x^2} \tag{8.50}$$

Such a correlation kernel is obviously the zeroth-order spherical Bessel function $j_0(\zeta x)$. Even if this choice of correlation kernel is not physically correct, it may be a good mathematical choice of basis within which to expand other kernels.

For this choice of correlation kernel the outer sum can be performed analytically, or obtained directly from the original integral, to give

$$[ssss]_G = S\pi^{-3/2}\int i_0\left(\frac{2\sqrt{K}\theta\zeta}{1+\zeta^2K}|\mathbf{r}-\mathbf{R}_1||\mathbf{r}-\mathbf{R}_2|\right)\mathrm{e}^{-r^2-\zeta^2K|\mathbf{r}-\mathbf{R}_1|^2}\mathrm{d}\mathbf{r} \tag{8.51}$$

where $K = K_1$. Shifting the Gaussian to the origin and returning to the series expansion

form of the integral

$$[ssss]_G = \frac{Se^{-\frac{\zeta^2 K R_1^2}{1+\zeta^2 K}}}{(1+\zeta^2 K)^{3/2}} \sum_{b=0}^{\infty} \langle b \rangle \tag{8.52}$$

$$\langle b \rangle = \frac{\kappa^{2b}}{(2b+1)!} \langle b|b \rangle \tag{8.53}$$

where $\kappa = \frac{2\sqrt{K}\theta\zeta}{1+\zeta^2 K}$ and $-1 \leq \kappa \leq 1$. The monomials in the $\langle b|b \rangle$ integral are centered at

$$\mathbf{U} = \frac{\mathbf{R}_1}{\sqrt{1+\zeta^2 K}} \tag{8.54}$$

$$\mathbf{V} = \frac{(1+\zeta^2 K)\mathbf{R}_2 - \zeta^2 K \mathbf{R}_1}{\sqrt{1+\zeta^2 K}} \tag{8.55}$$

$$\tag{8.56}$$

and we let

$$\mathbf{UV} = \mathbf{U} - \mathbf{V} = \sqrt{1+\zeta^2 K}\,(\mathbf{R}_1 - \mathbf{R}_2) \tag{8.57}$$

The convergence of the sum in eqn. (8.52) will depend on the values of each of the parameters but if we consider just the concentric case, where **U** and **V** are both zero, it simplifies to

$$[ssss]_G = \frac{Se^{-\frac{\zeta^2 K R_1^2}{1+\zeta^2 K}}}{(1+\zeta^2 K)^{3/2}} \sum_{b=0}^{\infty} \frac{\kappa^{2b}}{(2b+1)!} \left(\frac{3}{2}\right)_{2b} \tag{8.58}$$

in which the terms decrease only as $\sim \frac{\kappa^{2b}}{\sqrt{2b+\frac{3}{2}}}$. It is clearly favourable that κ be as small as possible for rapid convergence. To determine the values of κ which will be encountered in a typical molecule we took all of the exponents from the cc-pVTZ [13] basis sets for C, H, N and O and evaluated all values of κ. The distribution of these values is shown in fig. 8.5. Unfortunately this shows that values in the vicinity of one are by far the most prevalent, so we can expect the series to converge poorly.

We will now consider the $\langle m \rangle$ integrals in eqn. (8.53). They are given by

$$\langle m \rangle = \frac{\kappa^{2m}}{(2m+1)!} \left(\frac{3}{2}\right)_{2m} \sum_{i=0}^{\infty}\sum_{j=0}^{\infty}\sum_{k=0}^{\infty} \frac{(-m)_{i+k}(-m)_{j+k}}{(\frac{3}{2})_{i+j+k}(-2m-\frac{1}{2})_k} \frac{(-U^2)^i}{i!} \frac{(-V^2)^j}{j!} \frac{(UV^2)^k}{k!} \tag{8.59}$$

Figure 8.5: Distribution of κ values in a typical molecule

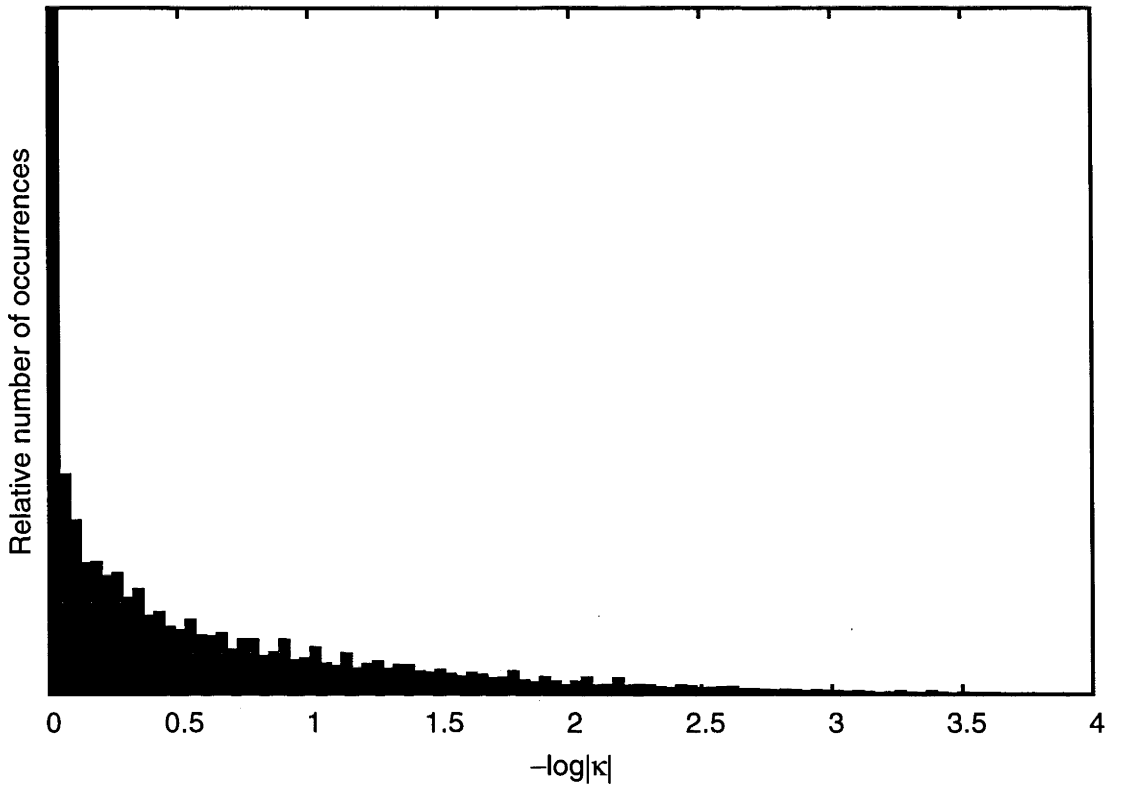

Sister Celine Fasenmyers' method provides the following 5-term relation

$$\begin{aligned}\langle m\rangle^{(\mu)} =& \frac{(16m^2-1)\kappa^2}{8m(1+2m)(3+2\mu)(5+2\mu)}\Big((3+2\mu)(5+2\mu)\langle m-1\rangle^{(\mu)} \\ &+2\left(U^2+V^2-\frac{(2+4m-8m^2)}{3+8m-16m^2}UV^2\right)(5+2\mu)\langle m-1\rangle^{(\mu+1)} \\ &+4U^2V^2\langle m-1\rangle^{(\mu+2)}-2\kappa^2UV^4\frac{1-3m+2m^2}{3-16m+16m^2}\langle m-2\rangle^{(\mu+2)}\Big)\end{aligned} \tag{8.60}$$

where we have now introduced an auxiliary index as follows

$$\langle m\rangle^{(\mu)} = \frac{\kappa^{2m}}{(2m+1)!}\left(\frac{3}{2}\right)_{2m}\sum_{i=0}^{\infty}\sum_{j=0}^{\infty}\sum_{k=0}^{\infty}\frac{(-m)_{i+k}(-m)_{j+k}}{(\frac{3}{2}+\mu)_{i+j+k}(-2m-\frac{1}{2})_k}\frac{(-U^2)^i}{i!}\frac{(-V^2)^j}{j!}\frac{(UV|^2)^k}{k!} \tag{8.61}$$

and the starting values for the recurrence are

$$\langle 0\rangle^{(\mu)} = 1 \tag{8.62}$$

The validity of this relation can be checked by using Hankel's contour integral

$$\frac{1}{\left(\frac{3}{2}+\mu\right)_{i+j+k}} = \frac{\Gamma(\frac{3}{2}+\mu)}{2\pi \mathrm{i}} \int_L \mathrm{e}^t t^{-i-j-k-\mu-\frac{3}{2}} \mathrm{d}t \tag{8.63}$$

where the path of integration L starts at $-\infty$ on the real axis, circles the origin in the counterclockwise direction and returns to the starting point. Inserting this identity into eqn. (8.61) allows the sum to be performed analytically

$$\begin{aligned} \langle m \rangle^{(\mu)} = & \frac{\kappa^{2m}}{(2m+1)!} \left(\frac{3}{2}\right)_{2m} \frac{\Gamma(\frac{3}{2}+\mu)}{2\pi \mathrm{i}} \int_L \mathrm{e}^t t^{-\mu-\frac{3}{2}} \left(1+\frac{U^2}{t}\right)^m \left(1+\frac{V^2}{t}\right)^m \\ & \times {}_2F_1\left(-m,-m,-\frac{1}{2}-2m, \frac{UV^2}{t}\left(1+\frac{U^2}{t}\right)^{-1}\left(1+\frac{V^2}{t}\right)^{-1}\right) \mathrm{d}t \end{aligned} \tag{8.64}$$

where ${}_2F_1(a,b,c,z)$ is Gauss' hypergeometric function [21]. Substitution of this expression into the recurrence relation then requires the proof of the following hypergeometric identity

$$\begin{aligned} {}_2F_1\left(-m,-m,-\frac{1}{2}-2m,z\right) = & \\ & \left(\frac{2+4m-8m^2}{-3-8m+16m^2}z+1\right) {}_2F_1\left(-m+1,-m+1,\frac{3}{2}-2m,z\right) \\ & -4z^2 \frac{(1-3m+2m^2)^2}{(4m-3)^2(5-24m+16m^2)} {}_2F_1\left(-m+2,-m+2,\frac{7}{2}-2m,z\right) \end{aligned} \tag{8.65}$$

and this is straightforward to show using the infinite series representations for the hypergeometric functions.

Practical considerations

Given the recurrence relation (8.60) we are now in a position to calculate the correlation integral for four s-type functions. Great care must be taken in the implementation of the recurrence relation as the terms may grow rapidly to large numbers which can cause overflow in double precision arithmetic. Since the series is unimodal we can simply scale the starting values to be very small such that the largest numerical range is available for the summation. As mentioned above this series is in general not rapidly convergent so we employ Aitken's δ^2-process to accelerate convergence. Aitken's δ^2-process is an extrapolative procedure which yields an improved estimate T_n to the sum of a series given

Table 8.1: The number of terms N_T required to sum to an accuracy of 10^{-10} when Aitken's δ^2-process is applied N_{Ait} times.

N_{Ait}	N_T
0	6107
3	4996
5	5915
8	3490
10	3049
13	3145

several consecutive partial sums

$$T_n = S_n - \frac{(S_n - S_{n-1})^2}{S_n - 2S_{n-1} + S_{n-2}} \tag{8.66}$$

where S_i is the ith partial sum. This process can then be applied again to the T_n and so on, and iterative application of this method has been shown to significantly accelerate the convergence of a series [199]. Shown in table 8.1 is the number of terms required to sum to a convergence of 10^{-10} for parameters $\kappa = 0.99$, $U = 10$, $V = 9.9$ and $\mathbf{U}$ and $\mathbf{V}$ are collinear. As can be seen from the table there is a dramatic increase in convergence with successive applications of the process. This does not go on indefinitely and by 13 applications we see that it is now becoming detrimental. Care must be taken when using these types of convergence acceleration methods as numerical precision may be lost if they are used too many times. We include numerical checks which terminate the iteration depth if numerical precision is at stake.

Certain integrals can be avoided if they are known *a priori* to be negligibly small. Starting from eqn. (8.51) and applying a simple transformation and using the fact that $i_0(x) \leq \exp(|x|)$ leads to

$$\begin{aligned}
&\pi^{3/2} \int i_0(\kappa|\mathbf{r}-\mathbf{U}||\mathbf{r}+\mathbf{V}|)\mathrm{e}^{-r^2}\mathrm{d}\mathbf{r} \\
&\leq \pi^{3/2} \int \exp\left(-\left(\mathbf{r}-\frac{\mathbf{U}+\mathbf{V}}{2}\right)^2 + |\kappa|\left|\mathbf{r}+\frac{\mathbf{V}-\mathbf{U}}{2}\right|\left|\mathbf{r}-\frac{\mathbf{V}-\mathbf{U}}{2}\right|\right)\mathrm{d}\mathbf{r} \qquad (8.67)\\
&\leq \pi^{3/2} \int \exp\left(-\left(\mathbf{r}-\frac{\mathbf{U}+\mathbf{V}}{2}\right)^2 + |\kappa|\left(r^2+\left|\frac{\mathbf{V}-\mathbf{U}}{2}\right|^2\right)\right)\mathrm{d}\mathbf{r} \qquad (8.68)\\
&= \left(\frac{1}{1-|\kappa|}\right)^{3/2} \exp\left(\frac{|\kappa|}{2(1-|\kappa|)}\left(U^2+V^2-\frac{|\kappa|}{2}UV^2\right)\right) \qquad (8.69)
\end{aligned}$$

However this bound is very poor in the case where the angle between **U** and **V** is small, i.e., $U^2 + V^2 \gg UV^2$, and as such has not proved very useful.

Gill has shown that in the case of the four centres being collinear the following analytical expression can be obtained using confocal elliptical coordinates

$$\int i_0(\kappa|\mathbf{r}-\mathbf{Z}||\mathbf{r}+\mathbf{Z}|)\mathrm{e}^{-|\mathbf{r}-\mathbf{T}|^2}\mathrm{d}\mathbf{r} = \frac{\pi^2 \mathrm{e}^{Z^2-T^2}}{2\kappa\sqrt{(1-\kappa^2)Z^2-T^2}} \times \left(\mathrm{erfc}\sqrt{\frac{(1-\kappa^2)Z^2-T^2}{1+\kappa}} - \mathrm{erfc}\sqrt{\frac{(1-\kappa^2)Z^2-T^2}{1-\kappa}}\right) \tag{8.70}$$

where

$$\mathbf{Z} = \frac{\mathbf{V}-\mathbf{U}}{2} \qquad \mathbf{T} = \frac{\mathbf{U}+\mathbf{V}}{2} \tag{8.71}$$

and $\mathrm{erfc}(z)$ is the complementary error function. This now provides an upper and lower bound on the integral as the integral decreases monotonically as **U** and **V** go from being antiparallel to parallel. Care must be taken when evaluating the above expression as the arguments of the error function may be very large and be either real or imaginary. In the case where the error function has an imaginary argument it can be evaluated using the Faddeeva function $w(z) = \mathrm{e}^{-z^2}\mathrm{erfc}(\mathrm{i}z)$. At small values of the argument a series expansion is used, at moderate values rational approximations are used and for large values of the argument a short asymptotic expansion [200] is used. In the case of a real argument it is most prudent to evaluate $\mathrm{e}^{x^2}\mathrm{erfc}(x)$ as the error function decays very rapidly. For small arguments a series expansion is used, for moderate values the expression is evaluated explicitly and for large arguments an asymptotic formula is used. When taking the difference between the two error functions can be prone to loss of numerical precision and results from this formulation must be treated with caution.

In practice only the upper bound is used as the lower bound does not allow the negation of any integrals. This upper bound will be exact when **U** and **V** are antiparallel and will be strongest when UV is close to its maximum. However, at the opposite extreme, when **U** and **V** are parallel and both large it will be very weak as $U - V$ and $U + V$ may differ by several orders of magnitude. It is however stronger than the previous bound. Neither

Figure 8.6: Distribution of η values in a typical molecule

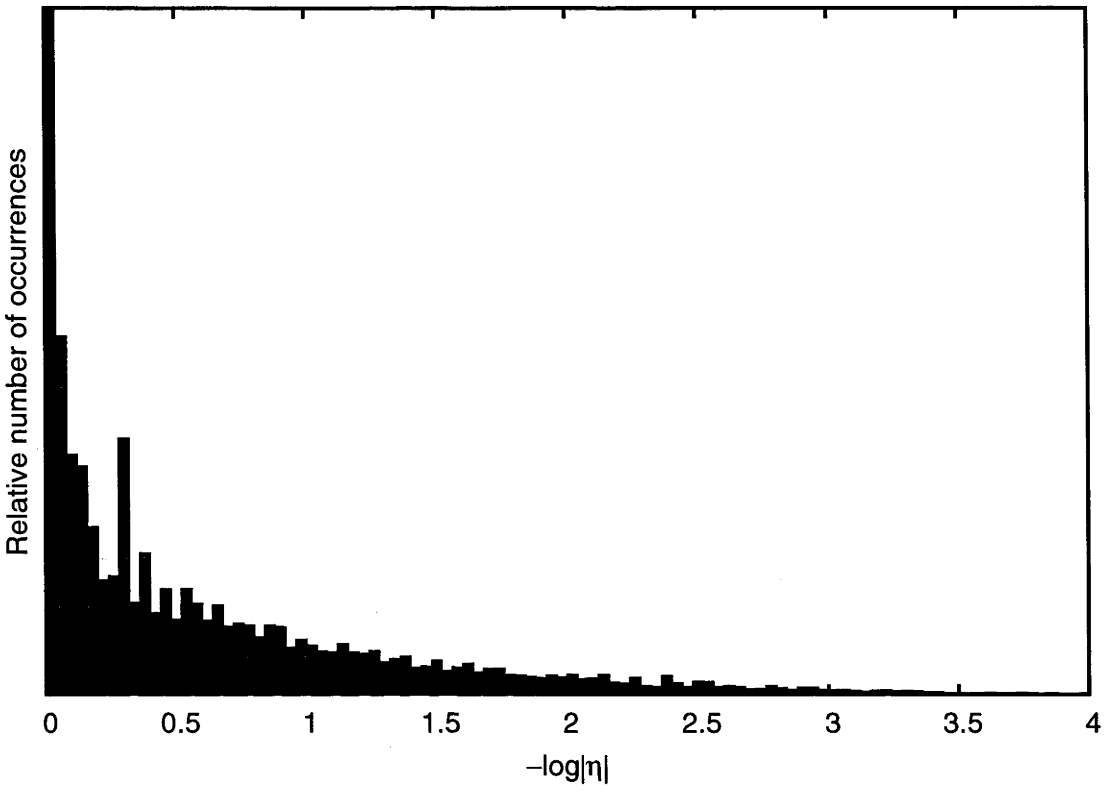

are totally satisfactory and the development of a robust and computationally cheap bound on the correlation integrals will be an important step in increasing the efficiency of HFW calculations.

We note at this point that the formulation presented is not valid when $\eta = 0$. In this case the integral can be evaluated in closed form to yield

$$[ssss]_G = \frac{\pi^3 \exp\left(-R + \frac{\mu^2 P^2 - \lambda^2 Q^2}{\zeta^2 + 4\lambda^2\mu^2}\right)}{(\alpha+\delta)^{3/2}(\beta+\gamma)^{3/2}(\zeta^2+4\lambda^2\mu^2)^{3/2}} i_0\left(\frac{\zeta PQ}{\zeta^2+4\lambda^2\mu^2}\right) \tag{8.72}$$

This special case is invoked for values of η less than 10^{-12} but typically η is either exactly zero or sufficiently far enough away from it to ensure that there is no ambiguity as to which algorithm to use. Figure 8.6 shows the distribution of η values obtained from all combinations of exponents of the cc-pVTZ basis sets for C, H, N, and O. Values equal or close to unity are very frequent and this dies off quickly, and values less than 10^{-4} are relatively infrequent.

8.4.6 Integrals of higher angular momentum

Ideally integrals for higher angular momentum basis functions would be generated using recursively but we have not been able to find a recurrence relation to do this for the correlation integrals. We therefore have to follow the method of Boys and differentiate with respect to the nuclear coordinates [11]. In the case where $\eta \neq 0$ the following is used

$$\begin{aligned}\frac{\partial}{\partial A_i}[ssss]_G = \frac{\partial T}{\partial A_i} I[X,Y,Z] + \frac{\partial U^2}{\partial A_i} I[X+1,Y,Z] \\ + \frac{\partial V^2}{\partial A_i} I[X,Y+1,Z] + \frac{\partial UV^2}{\partial A_i} I[X,Y,Z+1]\end{aligned} \tag{8.73}$$

where the following fundamental integrals are defined

$$\begin{aligned} I[X,Y,Z] &= \frac{\partial^{X+Y+Z}}{\partial (U^2)^X (V^2)^Y (UV^2)^Z}[ssss]_G \\ &= \frac{S\mathrm{e}^{-\frac{\zeta^2 K R_1^2}{1+\zeta^2 K}}}{(1+\zeta^2 K)^{3/2}} \sum_{m=0}^{\infty} \frac{\kappa^{2m}}{(2m+1)!} \left(\frac{3}{2}\right)_{2m} \\ &\times \sum_{i=0}^{\infty}\sum_{j=0}^{\infty}\sum_{k=0}^{\infty} \frac{(-m)_{i+k+X+Z}(-m)_{j+k+Y+Z}}{(\frac{3}{2}+\mu)_{i+j+k+X+Y+Z}(-2m-\frac{1}{2})_{k+Z}} \frac{(-U^2)^i}{i!} \frac{(-V^2)^j}{j!} \frac{(UV^2)^k}{k!} \end{aligned} \tag{8.74}$$

and these are generated recursively using an analogous relation as that in eqn. (8.60)

$$\begin{aligned} \langle m \rangle^{(\mu)}_{X,Y,Z} &= \frac{m(4(2m-Z)^2-1)\kappa^2}{8(1+2m)(m-X-Z)(m-Y-Z)(3+2\mu)(5+2\mu)} \\ &\times \Bigg\{ (3+2\mu)(5+2\mu)\langle m-1 \rangle^{(\mu)}_{X,Y,Z} \\ &+ 2\left(U^2+V^2+2UV^2\frac{1-4m^2+4XY+(2m+X+Y)(1+2Z)}{(4m-2Z-3)(4m-2Z+1)}\right)(5+2\mu)\langle m-1 \rangle^{(\mu+1)}_{X,Y,Z} \\ &+ 4U^2V^2\langle m-1 \rangle^{(\mu+2)}_{X,Y,Z} - 2\kappa^2 UV^4 \frac{(m-1)(2m+2X-1)(2m+2Y-1)}{(2m-1)(4m-2Z-3)(4m-2Z-1)}\langle m-2 \rangle^{(\mu+2)}_{X,Y,Z} \Bigg\} \end{aligned} \tag{8.75}$$

where the starting values for the recurrence are

$$\langle a \rangle^{(\mu)}_{X,Y,Z} = \begin{cases} (-1)^Z \left(\frac{\kappa^2}{4}\right)^{Y+Z} \frac{\Gamma(1+Y+Z)\Gamma(\frac{3}{2}+\mu)}{\Gamma(\frac{3}{2}+Y+Z)(\frac{3}{2}+2Y+Z)_\mu} L_{Y-X}^{\frac{1}{2}+X+Y+Z+\mu}(-U^2) & X<Y \\ (-1)^Z \left(\frac{\kappa^2}{4}\right)^{X+Z} \frac{\Gamma(1+X+Z)\Gamma(\frac{3}{2}+\mu)}{\Gamma(\frac{3}{2}+X+Z)(\frac{3}{2}+2X+Z)_\mu} L_{X-Y}^{\frac{1}{2}+X+Y+Z+\mu}(-V^2) & Y<X \end{cases} \tag{8.76}$$

where $\langle a \rangle$ is the first non-zero and $a = \max(X,Y) + Z$ and $L_n^\lambda(z)$ are the generalized Laguerre polynomials. The Laguerre polynomials are evaluated as required, increasing λ using the following recurrence relation

$$L_n^\lambda = \frac{1}{z}\Big((n+\lambda)L_n^{\lambda-1}(z) - (n+1)L_{n+1}^{\lambda-1}(z)\Big) \tag{8.77}$$

and n using the standard 3-term recurrence relation

$$L_{n+1}^\lambda(z) = \frac{1}{n+1}\Big\{(2n - z + \lambda + 1)L_n^\lambda(z) - (n+\lambda)L_{n-1}^\lambda(z)\Big\} \tag{8.78}$$

and we use the starting values $L_0^\lambda(z) = 1$ and $L_0^\lambda(z) = 1 - z + \lambda$.

Some of the derivatives are related to each other by the following recurrence

$$I(X,Y,Z) = -I(X-1,Y,Z) - I(X-1,Y+1,Z) - I(X,Y+1,Z-1) \tag{8.79}$$

$$I(X,Y,Z) = -I(X,Y-1,Z) - I(X+1,Y-1,Z) - I(X+1,Y,Z-1) \tag{8.80}$$

These can be used for integrals, for which X, Y and Z are all non-zero.

The generation of integrals of higher angular momentum is a laborious process, so to expedite this and to try to avoid human error, the code to calculate these integrals was produced using a custom written Perl program which recursively uses eqn. (8.73) to generate derivatives. This was used to generate code for s-, p- and d-type functions.

In the case where $\eta = 0$, to attempt to simplify the task of differentiation, the following infinite series representation is used so geometric parameters appear only in even powers.

$$\langle X,Y\rangle = \frac{\partial^{X+Y}}{\partial(P^2)^X\partial(Q^2)^Y}[ssss]_G \tag{8.81}$$

$$= \frac{\pi^3 \exp\left(-R + \frac{\mu^2P^2 - \lambda^2Q^2}{\zeta^2+4\lambda^2\mu^2}\right)}{(\alpha+\delta)^{3/2}(\beta+\gamma)^{3/2}(\zeta^2+4\lambda^2\mu^2)^{3/2}} \times \sum_{m=0}^{\infty}\frac{1}{(2m+1)!}\left(\frac{\zeta}{\zeta^2+4\lambda^2\mu^2}\right)^{2m}\frac{(P^2)^{m-X}}{(m+1)_{-X}}\frac{(Q^2)^{m-Y}}{(m+1)_{-Y}} \tag{8.82}$$

These derivatives may then be easily generated using the following recurrence relations

and starting values.

$$\langle X,Y\rangle = \frac{1-X+Y}{P^2}\langle X-1,Y\rangle + \frac{Q^2}{P^2}\langle X-1,Y+1\rangle \tag{8.83}$$

$$\langle X,Y\rangle = \frac{1+X-Y}{Q^2}\langle X,Y-1\rangle + \frac{P^2}{Q^2}\langle X+1,Y-1\rangle \tag{8.84}$$

with starting values

$$\langle X,0\rangle = \left(\frac{\zeta Q}{2(\zeta^2+4\lambda^2\mu^2)}\right)^{2X} i_X\left(\frac{\zeta PQ}{\zeta^2+4\lambda^2\mu^2}\right) \tag{8.85}$$

$$\langle 0,Y\rangle = \left(\frac{\zeta P}{2(\zeta^2+4\lambda^2\mu^2)}\right)^{2Y} i_Y\left(\frac{\zeta PQ}{\zeta^2+4\lambda^2\mu^2}\right) \tag{8.86}$$

Again, these integrals have been implemented for s-, p- and d-functions using a Perl program to generate the code. The Bessel functions are calculated as described in ref. [116].

8.5 Summary

In this chapter we have laid out a complete description of how a HFW calculation is performed. HFW theory allows electron correlation to be included in a self-consistent fashion while retaining the favourable scaling of a HF calculation. The required correlation integrals have only four-fold permutational symmetry and there are approximately twice as many as normal HF integrals. The integrals involved in HFW theory are also more difficult to evaluate than those normally encountered in quantum chemistry. We have laid out several approaches to calculating these.

The first method was to use quadrature. Although this provides a conceptually simple route to results, it does not provide a practical solution to the problem as the time taken and the accuracy attained using a four-dimensional quadrature is not satisfactory.

The second method was to expand the correlation kernel as a linear combination of Gaussian functions. Although this requires the use of a one-dimensional quadrature, convergence is achieved with relatively small grids. However, accurately expressing a zeroth-order spherical Bessel function as a linear combination of Gaussians requires numerical preci-

sion beyond that of normal double precision calculations and this method is also deemed unsatisfactory.

The final two methods involve expressing the correlation kernel as an infinite series and calculating the terms recursively. The method of Sister Celine Fasenmyer has been used to derive recurrence relations for the integrals. The first of these approaches, which specifies only a very general class of correlation kernels, suffers from numerical instability and we have not been able to overcome these problems. The second approach, is specifically for $G(u,v) = j_0(\zeta uv)$ and this has been successful in generating the required correlation integrals. Although this approach seems be able to provide accurate results, the series converges slowly and the integrals are relatively slow to calculate.

Chapter 9

Results and Analysis

9.1 Introduction

In the last chapter the theory behind Hartree-Fock-Wigner calculations was introduced. Now we need to examine how this new theory performs and how it can be improved. We note from the outset that some of these calculations may still contain some numerical errors. As we saw in the last chapter, the evaluation of the correlation integrals is very challenging and poses serious numerical problems. We have endeavoured to overcome these but we still lack a satisfactory method of checking all of the millions of integrals which occur in a given calculation and although we have checked many we have reason to believe that some numerical problems remain. However, we believe that in the case of a post-HF calculation these errors do not become significant and a qualitative analysis of the results is still useful and will help us in the development of HFW theory.

Firstly we will present the performance of correlation kernels for the benchmark data set introduced in chapter 6. We will examine the effect of basis set on the calculated correlation energy and also look at two differently parameterized correlation kernels. Using these results to help us devise a scheme we move onto all of the reactions in the G2 set [156] to examine how well HFW theory can reproduce experimental results. Finally, we will look at the self-consistent formulation of HFW theory and see how it performs for atomic

cases and look briefly at some problems encountered in the molecular case.

9.2 Benchmark data set

Table 9.1: The exact and HFW correlation energies for the dataset from chapter 6 for different basis sets. The first four HFW columns use the correlation kernel parameterized using just He and Ne. The final column uses a kernel parameterized using all of the atoms from the first and second rows. Large–*df* denotes that the 6-311++G(3*df*,3*dp*) basis set was used but no contributions from *d* or *f* functions were used in the calculation of the HFW correlation energy. The mean absolute deviation (MAD) is given for the atoms and then for all species. All energies are in m$E_h$and MADs in %.

Molecule	$-E_c^{ex}$	$-E_c^{HFW}$				
		6-311G	3-21G	6-311G*	Large–*df*	6-311G(G_{17})
He	42	42	42	42	42	42
Li	45	47	47	47	45	47
Be	94	89	89	89	89	89
B	121	120	120	120	120	119
C	151	156	155	155	155	153
N	185	195	195	195	195	191
O	249	256	257	256	256	250
F	318	322	323	322	321	313
Ne	391	391	393	391	390	380
Na	396	401	399	401	401	389
Mg	438	448	446	448	448	435
Al	465	480	478	480	479	466
Si	500	516	515	516	516	501
P	540	557	555	557	557	539
S	597	619	618	619	619	600
Cl	658	686	685	686	686	664
Ar	723	757	756	757	757	733
MAD		2.8	2.8	2.8	2.6	1.5
H_2	41	41	41	41	42	42
LiH	83	90	90	90	88	90
BeH	93	109	109	109	107	108
CH	194	204	204	204	201	200
$CH_2(^1A_1)$	239	254	255	255	238	234
$CH_2(^3B_1)$	208	240	239	240	251	250
CH_3	254	301	300	301	298	294
CH_4	299	362	360	361	356	352
NH	236	250	250	250	248	244
NH_2	287	310	310	310	306	302
NH_3	340	373	373	373	368	363
OH	309	316	316	316	313	307
H_2O	371	379	379	379	374	369
HF	389	384	386	385	380	373

Table 9.1: (*continued*)

Molecule	$-E_c^{ex}$	$-E_c^{HFW}$				
		6-311G	3-21G	6-311G*	Large–*df*	6-311G(G_{17})
$SiH_2(^1A_1)$	567	606	605	606	595	589
$SiH_2(^3B_1)$	540	590	589	589	581	572
SiH_3	575	641	640	638	625	623
SiH_4	606	689	689	685	666	670
PH_2	611	614	612	614	605	596
PH_3	652	716	716	716	702	694
H_2S	683	734	733	734	727	711
HCl	707	746	746	747	743	722
Li_2	124	134	134	134	133	134
LiF	441	436	435	436	431	425
HCCH	480	505	504	504	510	494
H_2CCH_2	518	589	590	586	584	573
H_3CCH_3	561	678	678	675	660	659
CN	483	436	440	444	429	421
HCN	515	509	514	514	498	495
CO	535	511	518	511	493	499
HCO	553	545	544	575	528	526
H_2CO	586	593	590	592	574	577
H_3COH	629	682	681	689	670	662
N_2	549	517	518	518	508	504
H_2NNH_2	641	691	692	689	669	671
NO	596	552	553	549	537	539
O_2	636	598	599	607	586	579
HOOH	711	695	698	700	681	673
F_2	757	697	700	673	696	677
CO_2	876	849	855	840	822	824
Na_2	819	836	855	817	847	816
Si_2	1077	1003	1021	868	1091	972
P_2	1205	1182	1357	1190	1111	1219
S_2	1275	1343	1339	1283	1315	1182
Cl_2	1380	1550	1502	1550	1589	1475
NaCl	1101	1153	965	1183	1135	1120
SiO	879	882	757	786	802	823
CS	867	864	888	855	823	869
SO	957	930	930	1003	917	795
ClO	1002	1036	1024	1003	935	1053
ClF	1063	1061	1051	1048	1059	988
Si_2H_6	1183	1356	1408	1286	1325	1307
CH_3Cl	968	1052	1046	1053	1009	1000
CH_3SH	946	1060	1017	1365	1090	1017
HOCl	1045	1069	1054	1049	1081	1059
SO_2	1334	1437	1273	1533	1457	1128
MAD		6.0	6.2	6.7	6.0	5.6

Table 9.1 shows the exact and calculated correlation energies for the 73 atoms and molecules from the benchmark data set introduced in chapter 6. The first four columns use the same correlation kernel parameterized to reproduce the correlation energies of the helium and neon atoms using the 6-311G basis set. It is given by

$$G_2(u,v) = 0.0992 j_0(0.893uv) \tag{9.1}$$

The final column uses a correlation kernel which is parameterized to produce the smallest least-squares relative error in the correlation energies of 17 atoms in the first and second rows He-Ar (this correlation kernel was introduced in chapter 7)

$$G_{17}(u,v) = 0.102 j_0(0.907uv) \tag{9.2}$$

We note that even though the parameters in the two kernels are quite similar, ~ 0.1 and ~ 0.9 in both, they yield significantly different results indicating quite a high sensitivity of the correlation energy to the kernel. This is not a very desirable quality as it increases the specificity of a kernel whereas we would prefer a more broadly applicable one.

Looking first at the atoms using the G_2 kernel we see remarkable insensitivity to basis set in the calculated correlation energies. Obviously we do not expect to see any difference between the 6-311G and 6-311G* bases as for atoms the d-functions do not contribute but one might expect that the 3-21G basis set would show marked differences. The addition of the diffuse functions in the Large$-df$ case seems to reduce the MAD slightly but not significantly so. The largest error in all cases is $\sim$ 34 mE_h for Ar suggesting that our parameterisation has not covered enough of phase-space to properly account for it. The G_{17} kernel, unsurprisingly, performs better for the atoms reducing the MAD by over 1%. The largest error in this case is 11 mE_h for Ne.

The molecular results for the G_2 kernel show more sensitivity to basis set and we see that the smallest error is for the 6-311G basis. Interestingly, the smaller basis set gives better results than the addition of d-functions which gives us the possibility of estimating correlation energies quite cheaply. However, any physical reasoning for this basis set effect would be dubious but it does serve to illustrate that the Wigner intracule and hence the

Figure 9.1: The G_{17} HFW correlation energy plotted against the exact correlation energy. All energies are in $\mathrm{m}E_\mathrm{h}$.

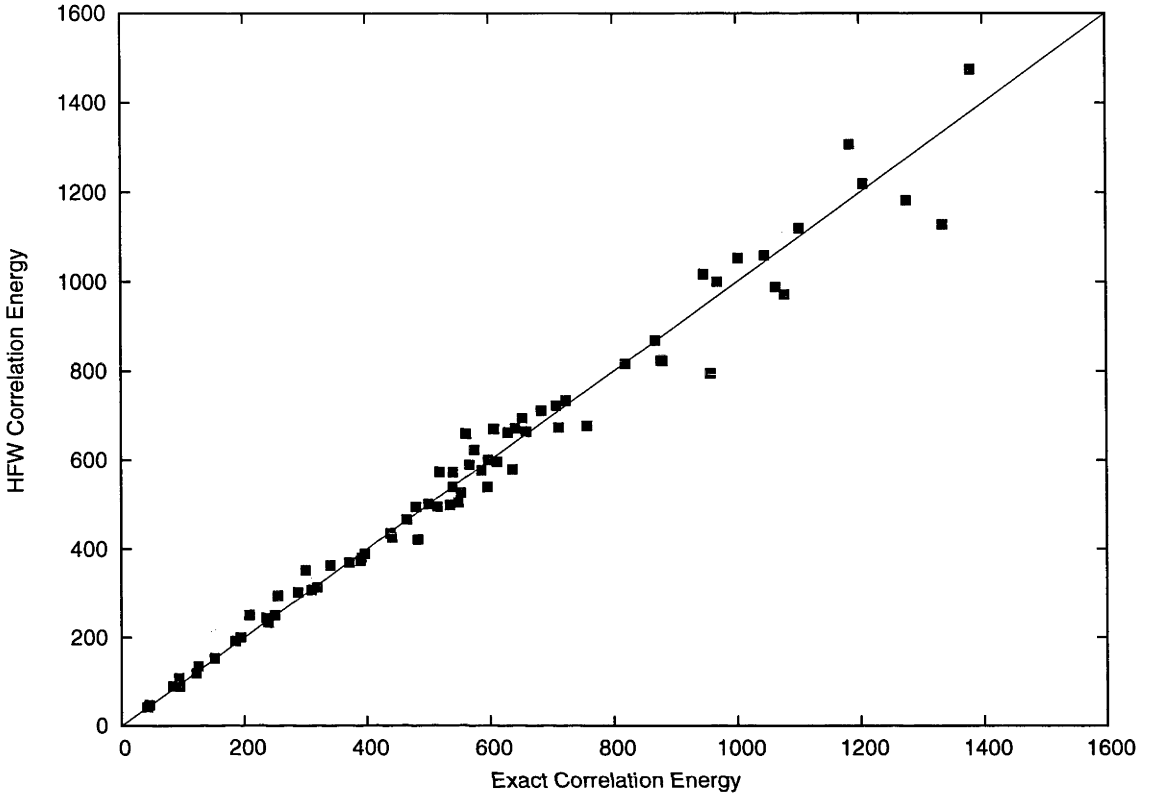

correlation energy is quite insensitive to basis set. The G_{17} kernel gives slightly better molecular results which is not surprising as none of the molecules in the data set contain Ne or He whereas they contain nearly all of the atoms included in the G_{17} parameterisation.

We have also included the Large$-df$ calculation as if the HFW correlation energy is quite insensitive to basis set, then we should be able to use only a small part of the basis set to get a good estimate of the correlation energy while using the whole basis set to get a highly accurate HF energy. Since the HF energy converges exponentially with the highest angular momentum of basis function used, a very large basis set, such as those used in wavefunction based correlation treatments, is not required. The results in table 9.1 show that the correlation energy is relatively unaffected by this pruning of basis functions and in fact the MAD is unchanged by this modification.

It is instructive to look at the results shown graphically in fig. 9.1. Ideally all of the points would lie along the line and for smaller molecules we see quite a narrow spread around

it. The higher accuracy for small molecules probably stems from the atomic bias in the correlation kernel, i.e., large u regions of the Wigner intracule have not been explored in the atomic parameterisation. On closer examination of the figure we can see clusters of points which have approximately the same HFW correlation energies but different exact energies. Some of these clusters are isoelectronic series of molecules. For example, the 10-electron series is CH_4, NH_3, H_2O, HF and Ne which have HFW correlation energies of 352, 363, 369, 373 and 380 m$E_h$respectively compared to the true values of 299, 340, 371, 389 and 391. Although the HFW numbers are showing the correct trend they are failing to differentiate correctly between the more diffuse methane and the more localized neon — all of these systems are being treated too much like neon.

One might ask whether the action intracules are sufficiently different to capture this effect. To answer this we can look at the action intracules for the five species shown in fig. 9.2. This figure also shows plots of the differences between the action intracule for each species and the action intracule for neon. Although the action intracules look nearly indistinguishable the difference plots are much more informative. We can see that there are systematic differences in the intracules going from Ne to CH_4 which should be able to be correlated to the corresponding differences in the correlation energies. To investigate if a Bessel function could capture these differences we tried to optimize the parameters to reproduce the correlation energy of Ne and CH_4 but we were not able to significantly improve on the results from the atomic fit. Even though we have two parameters and two data, the non-linear nature of the problem prevents us from obtaining the desired solution. It appears that a single Bessel function is not flexible enough to do this. We have also tried to fit a second Bessel function to the errors associated with these molecules, but again this form of correlation kernel cannot correct the errors. Other functional forms for the correlation kernel have been tried but as of yet none can adequately capture these facets of electronic structure.

Figure 9.2: The action intracules $A(s)$ and the difference between them and the intracule for Ne, i.e., $A(s) - A(s)_{\mathrm{Ne}}$ for CH_4, NH_3, H_20, HF and Ne. The final plot overlays all of the previous ones. The exact correlation energies are listed beside the intracules.

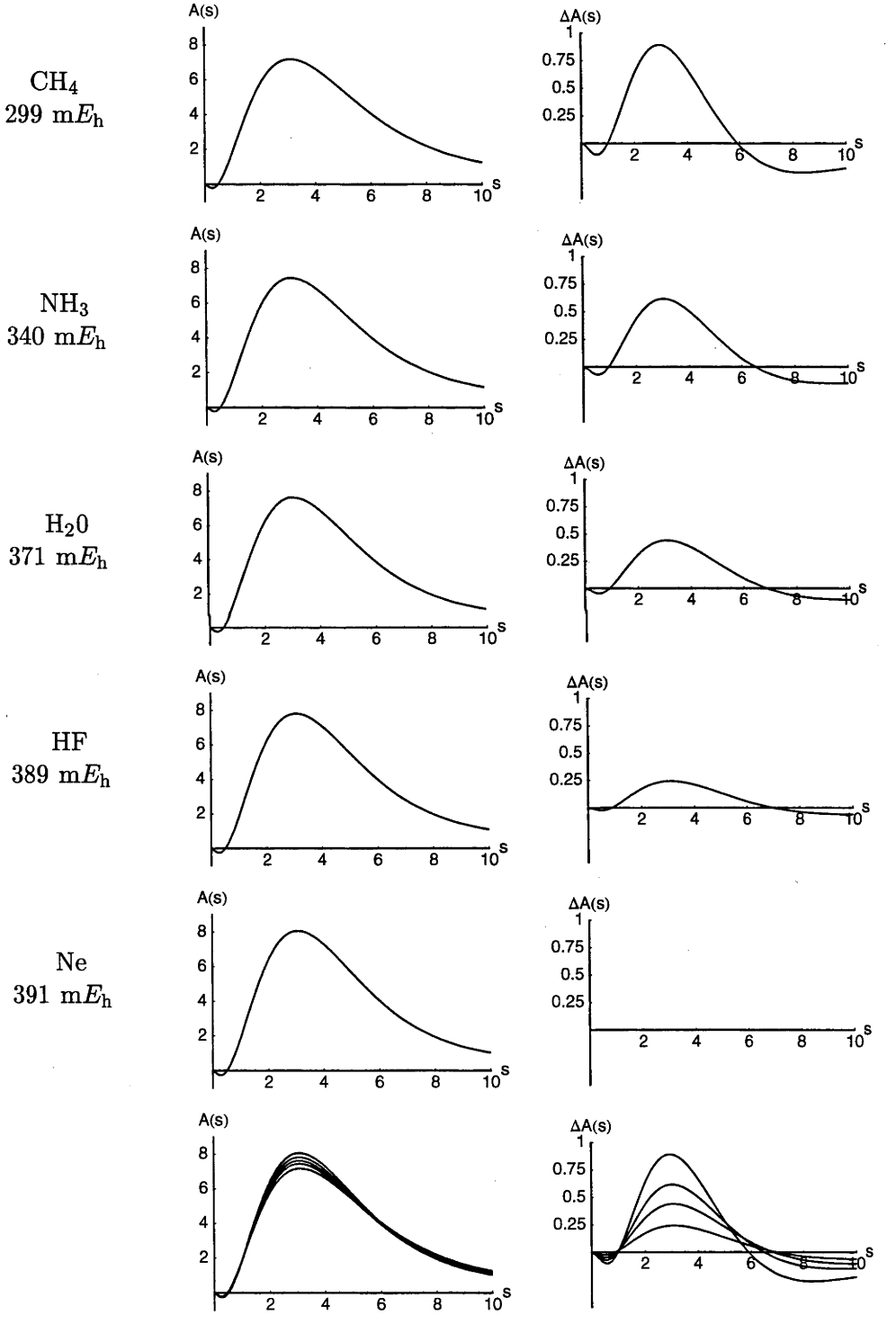

9.3 The G2 reactions

For the G2 reactions we do not use the reference geometries as used in the benchmark data set, but instead all energies are calculated at the standard G2 geometries which are calculated using MP2/6-31G*. All energies have been corrected for zero-point energy (ZPE) using scaled MP2 ZPEs [165]. Since we will not be looking at absolute correlation energies but instead at relative energies, it is important that the HF portion of the energy is accurate so we shall use the Large$-df$ basis set as described above. The analysis on the benchmark data also showed that fitting to all of the atoms rather than to just two noble gases yields better atomic and molecular results so we have used the following kernel which is optimized to reproduce the correlation energies of the 17 atoms from He to Ar using the Large$-df$ basis set. It is given by

$$G_{17L}(u,v) = 0.103 j_0(0.909uv) \tag{9.3}$$

Unsurprisingly this does not differ significantly from the G_{17} kernel. The atomisation energies for the G2 set are given in table 9.2. The MAD for the atomisation energies is 36.9 kcal/mol compared to 35.4 for LYP and 84.3 for HF. We are getting comparable results to LYP and are improving dramatically on HF. The MAD is still very large and this is due to the disparity between our atomic and molecular results — we obtain accurate atomic results but not commensurately accurate molecular results. In the case of atomisation energies this difference will cause significant errors. The cases in which the performance is worst is for molecules containing second row elements.

The ionisation potentials for the G2 set are given in table 9.3. The MAD for these is 1.5eV compared to 1.2eV for LYP and 1.8eV for HF. Again we are improving on the HF results but in this case we are still quite inferior to the LYP results. Looking more closely at the results we see that we are doing very badly for the second-row diatomics whereas in most other cases (with the exception of the first 3 atoms listed which LYP performs comparably for) HFW quite accurately predicts the ionisation potentials.

The electron affinities for the G2 set are given in table 9.4. The MAD for these is 1.1eV

Table 9.2: The G2 atomisation energies (kcal/mol) calculated using HFW.

Reaction	HFW	Exp	Reaction	HFW	Exp
$LiH \longrightarrow Li + H$	101.84	56.00	$HCN \longrightarrow H + C + N$	274.39	301.80
$BeH \longrightarrow Be + H$	57.79	46.90	$CO \longrightarrow C + O$	219.54	256.20
$CH \longrightarrow C + H$	81.16	79.90	$HCO \longrightarrow H + C + O$	238.10	270.30
$CH_2(^3B_1) \longrightarrow C + 2H$	194.00	179.60	$H_2CO \longrightarrow 2H + C + O$	337.21	357.20
$CH_2(^1A_1) \longrightarrow C + 2H$	174.47	170.60	$H_3COH \longrightarrow 4H + C + O$	497.82	480.80
$CH_3 \longrightarrow C + 3H$	310.89	289.20	$N_2 \longrightarrow 2N$	183.86	225.10
$CH_4 \longrightarrow C + 4H$	420.61	392.50	$H_2NNH_2 \longrightarrow 2N + 4H$	402.99	405.40
$NH \longrightarrow N + H$	79.24	79.00	$NO \longrightarrow N + O$	112.53	150.10
$NH_2 \longrightarrow N + 2H$	173.11	170.00	$O_2 \longrightarrow 2O$	71.61	118.00
$NH_3 \longrightarrow N + 3H$	283.24	276.70	$F_2 \longrightarrow 2F$	-18.22	36.90
$OH \longrightarrow O + H$	98.07	101.30	$CO_2 \longrightarrow C + 2O$	345.30	381.90
$OH_2 \longrightarrow O + 2H$	214.04	219.30	$Na_2 \longrightarrow 2Na$	15.73	16.60
$FH \longrightarrow F + H$	127.07	135.20	$Si_2 \longrightarrow 2Si$	77.43	74.00
$SiH_2(^1A_1) \longrightarrow Si + 2H$	151.53	144.40	$P_2 \longrightarrow 2P$	231.49	116.10
$SiH_2(^3B_1) \longrightarrow Si + 2H$	137.49	123.40	$S_2 \longrightarrow 2S$	194.27	100.70
$SiH_3 \longrightarrow Si + 3H$	232.69	214.00	$Cl_2 \longrightarrow 2Cl$	175.96	57.20
$SiH_4 \longrightarrow Si + 4H$	327.81	302.80	$NaCl \longrightarrow Na + Cl$	98.19	97.50
$PH_2 \longrightarrow P + 2H$	159.31	144.70	$SiO \longrightarrow Si + O$	130.44	190.50
$PH_3 \longrightarrow P + 3H$	246.38	227.40	$SC \longrightarrow S + C$	124.61	169.50
$SH_2 \longrightarrow S + 2H$	184.77	173.20	$SO \longrightarrow S + O$	162.82	123.50
$ClH \longrightarrow Cl + H$	108.06	102.20	$ClO \longrightarrow Cl + O$	17.14	63.30
$Li_2 \longrightarrow 2Li$	115.25	24.00	$ClF \longrightarrow Cl + F$	35.47	60.30
$LiF \longrightarrow Li + F$	171.28	137.60	$Si_2H_6 \longrightarrow 2Si + 6H$	582.95	500.10
$HCCH \longrightarrow 2C + 2H$	388.78	388.90	$CH_3Cl \longrightarrow C + 3H + Cl$	395.51	371.00
$H_2CCH_2 \longrightarrow 2C + 4H$	560.98	531.90	$CH_3SH \longrightarrow C + 4H + S$	477.75	445.10
$H_3CCH_3 \longrightarrow 2C + 6H$	714.55	666.30	$HOCl \longrightarrow O + H + Cl$	119.82	156.30
$CN \longrightarrow C + N$	137.59	176.60	$SO_2 \longrightarrow S + 2O$	-150.19	254.00

Table 9.3: The G2 ionisation potentials (eV) calculated using HFW.

Reaction		Exp
$Li \longrightarrow Li^+$	3.57	5.39
$Be \longrightarrow Be^+$	13.14	9.32
$B \longrightarrow B^+$	22.56	8.30
$C \longrightarrow C^+$	11.71	11.26
$N \longrightarrow N^+$	14.91	14.54
$O \longrightarrow O^+$	13.63	13.61
$F \longrightarrow F^+$	17.36	17.42
$CH_4 \longrightarrow CH_4^+$	13.09	12.62
$NH_3 \longrightarrow NH_3^+$	10.21	10.18
$OH \longrightarrow OH^+$	12.99	13.01
$OH_2 \longrightarrow OH_2^+$	12.60	12.62
$FH \longrightarrow FH^+$	16.02	16.04
$Na \longrightarrow Na^+$	5.08	5.14
$Mg \longrightarrow Mg^+$	7.68	7.65
$Al \longrightarrow Al^+$	6.33	5.98
$Si \longrightarrow Si^+$	8.49	8.15
$P \longrightarrow P^+$	10.88	10.49
$S \longrightarrow S^+$	10.82	10.36
$Cl \longrightarrow Cl^+$	13.48	12.97
$SiH_4 \longrightarrow SiH_4^+$	11.52	11.00
$PH \longrightarrow PH^+$	10.76	10.15
$PH_2 \longrightarrow PH_2^+$	10.58	9.82
$PH_3 \longrightarrow PH_3^+$	10.21	9.87
$SH \longrightarrow SH^+$	10.83	10.37
$SH \longrightarrow SH^+$	10.83	10.37
$ClH \longrightarrow ClH^+$	13.28	12.75
$H_2CCH_2 \longrightarrow H_2CCH_2^+$	10.66	11.40
$CO \longrightarrow CO^+$	14.57	14.01
$O_2 \longrightarrow O_2^+$	14.53	16.70
$P_2 \longrightarrow P_2^+$	16.76	12.07
$S_2 \longrightarrow S_2^+$	14.72	10.53
$Cl_2 \longrightarrow Cl_2^+$	18.93	9.36
$ClF \longrightarrow ClF^+$	13.49	12.66
$SC \longrightarrow SC^+$	12.10	11.33

Table 9.4: The G2 electron affinities (eV) calculated using HFW.

Reaction	HFW	Exp
$C \longrightarrow C^-$	1.43	1.26
$CH \longrightarrow CH^-$	1.53	1.24
$NH \longrightarrow NH^-$	0.01	0.38
$NH_2 \longrightarrow NH_2^-$	0.49	0.74
$O \longrightarrow O^-$	0.93	1.46
$OH \longrightarrow OH^-$	1.31	1.83
$F \longrightarrow F^-$	2.79	3.40
$O_2 \longrightarrow O_2^-$	-4.49	0.44
$NO \longrightarrow NO^-$	0.27	0.02
$CN \longrightarrow CN^-$	4.40	3.82
$Si \longrightarrow Si^-$	1.79	1.39
$P \longrightarrow P^-$	1.15	0.75
$Cl \longrightarrow Cl^-$	4.14	3.62
$SiH \longrightarrow SiH^-$	1.68	1.28
$SiH_3 \longrightarrow SiH_3^-$	1.81	1.44
$PH \longrightarrow PH^-$	1.41	1.00
$PH_2 \longrightarrow PH_2^-$	1.70	1.26
$PO \longrightarrow PO^-$	2.46	1.09
$S_2 \longrightarrow S_2^-$	6.53	1.66
$Cl_2 \longrightarrow Cl_2^-$	-2.78	2.39

Table 9.5: The G2 proton affinities (eV) calculated using HFW.

Reaction	HFW	Exp
$NH_3 \longrightarrow NH_4^+$	204.88	202.50
$OH_2 \longrightarrow OH_3^+$	164.45	165.10
$SiH_4 \longrightarrow SiH_5^+$	144.53	154.00
$PH_3 \longrightarrow PH_4^+$	183.82	187.10
$SH_2 \longrightarrow SH_3^+$	160.73	168.80
$ClH \longrightarrow ClH_2^+$	125.89	133.60

compared to 0.7eV for LYP and 1.4eV for HF. Like in the case of the ionisation potentials, we improve on HF but not as much as LYP does. Again the most spectacular errors are for the second-row diatomics (and O_2 for which LYP actually does worse).

Finally, the proton affinities for the G2 set are given in table 9.5. The MAD for these is 5.3eV as compared to 2.5eV for LYP and 2.1eV for HF. In this case HF outperforms both HFW and LYP. HFW has performed particularly badly for these reactions and again we see that the second row molecules yield the most dramatic errors.

Table 9.6: The non-SCF and SCF HFW correlation energies for the first- and second-row atoms. All energies in $\mathrm{m}E_\mathrm{h}$.

Molecule	non-SCF	SCF
He	42.8	42.8
Li	45.7	45.9
Be	90.4	90.5
B	120.1	120.3
C	154.0	154.3
N	191.9	192.3
O	251.3	251.6
F	314.7	315.0
Ne	381.6	381.9
Na	391.4	392.0
Mg	438.4	438.8
Al	469.2	469.7
Si	504.1	504.5
P	543.0	543.4
Cl	668.8	669.2
Ar	737.7	737.9

9.4 Self-consistent Hartree-Fock-Wigner calculations

As mentioned in the introduction there are currently some numerical problems associated with the SCF version of HFW theory. Before discussing this let us look at the atomic results to see first what the effect of performing a HFW calculation self-consistently. Table 9.6 shows the HFW correlation energies obtained by performing a HFW calculation non-self-consistently and self-consistently using the G_{17L} correlation kernel. One would not expect a significant difference between these two calculations as the inclusion of the HFW correlation energy should not overly perturb the HF solution and this expectation is borne out in the atomic results which show, at most, shifts of only several tenths of millihartrees.

In the molecular case for some molecules we observe the expected convergence of the HFW calculation as shown in fig. 9.3 for FH. The kink in the plot at the thirteenth SCF cycle is where the HF calculation had converged and the first HFW cycle was performed. Following this the energy converges smoothly with the final energy only differing from the first HFW cycle by ~ 4 $\mathrm{m}E_\mathrm{h}$. However, this is the exception rather than the rule and fig. 9.4 shows the convergence of CN. The HF calculation has converged after 25 SCF cycles and following this we get several HFW cycles with little change but quickly the

Figure 9.3: The convergence of the HFW SCF procedure for HF.

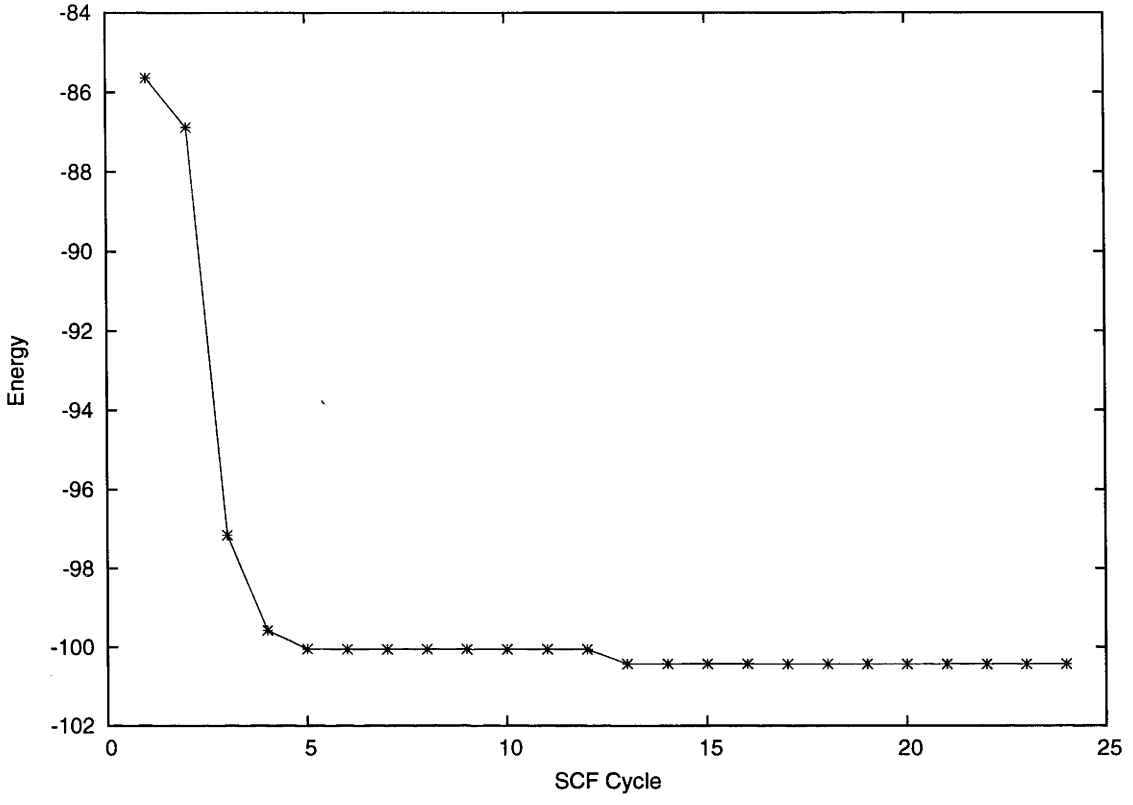

changes in energy become erratic and we see HFW correlation energies much larger than the non-self-consistent correlation energy. These energies seem to be unbounded and at the far right of the plot we see the energy plummeting. This type of behaviour and much worse has been observed in many of the molecules investigated.

The reason for this numerical breakdown is not yet clear. It has been encountered using both the Gaussian expansion form of the correlation integrals and the infinite series formulation. The most likely reason is that there are integrals which are not being calculated accurately but which are of negligible importance when contracted with the HF density matrix but when the calculation is performed self-consistently the errors present in them become hugely magnified. Unfortunately, whereas for many integrals encountered in quantum chemistry there are usually robust, albeit inefficient, methods to evaluate the integrals which can be used to check for errors in any more efficient route, we do not possess a mechanism by which to check our integrals. As many as possible have been checked using MATHEMATICA or special cases of the integrals for which there are exact solutions,

Figure 9.4: The convergence of the HFW SCF procedure for CN.

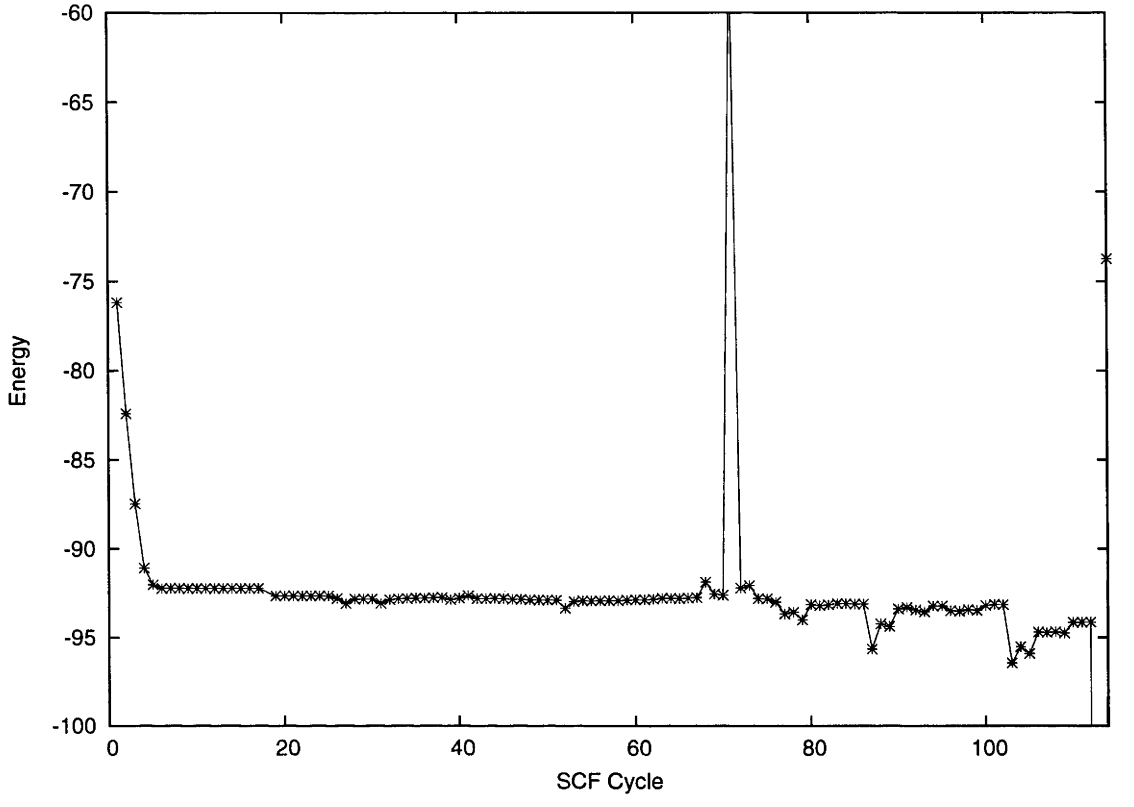

and we have not found significant differences, but these can only check a tiny fraction of the many of millions of integrals encountered in a single calculation. A completely robust formulation for the correlation integrals must be found which yields numerically satisfactory results and this work has been on-going as this thesis has been written.

There can be other reasons for erratic SCF behaviour such as being too aggressive in the cut-off schemes or possibly using the wrong algorithm to perform the SCF but these too have been investigated. All cut-offs have been switched off and all SCF algorithms have been tested but this problem still persists. We hope that this problem can be ironed out quickly and that we can report on self-consistent HFW calculations in the near future.

Chapter 10

Future directions and concluding remarks

10.1 Technical challenges

Probably the greatest obstacle faced during the course of this thesis has been of a technical nature. The nature of the Wigner intracule and any of the derived quantities, such as the action intracule or correlation energy, results in more mathematically challenging integrals than are normally encountered in quantum chemistry. This added complexity is the trade-off we make when we introduce the "extra" phase-space information. In the case of the Wigner and action intracules we have been able to calculate them to moderate accuracy using a couple of techniques but in this work we have focused primarily on the use of quadrature. Although quadrature has provided a practically straightforward result to calculating these intracules, the accuracy and efficiency of such an approach is not optimal. The intracules are, however, used mostly as a visual tool in understanding the electrons positions in phase space and their importance in electron correlation and as such high accuracy is not of paramount importance. Although it would be satisfying if the phase-space intracules could be generated efficiently and accurately in a similar way to the position and momentum intracules, their utility is ultimately limited and expending a great deal of effort on this would not be prudent.

The correlation integrals, on the other hand, represent a much more important area of research. During this work, the largest portion of time has been devoted to the accurate evaluation of the correlation integrals and many different approaches have been investigated and several of the more successful ones presented in this thesis. Yet we still do not have a completely robust, and certainly not efficient, method for calculating these integrals. We have made much progress in this area and laid some of the foundations but there is still much to be done. It may be that there are different methods by which to evaluate the correlation integrals and Crittenden and Gill have begun investigating one such approach based around the the modified addition theorem which expresses the correlation integral as a more rapidly converging infinite series. Ideally there would be a single approach to producing the correlation integrals but it seems more likely that as arsenal of methods may be required, choosing the most appropriate one for each set of integral parameters encountered. Developing a method which can evaluate the required correlation integrals without any ambiguity will be a key step in the development of HFW theory as this will lay to rest any uncertainty over the SCF problems encountered during this work.

Of course, any quantum chemical method is of limited utility if the computational cost is prohibitive. It is difficult, though, without highly accurate results to introduce cost-cutting measures, such as cut-off schemes, as the effect of such measures on accuracy will be hard to gauge. Increasing the efficiency of HFW calculations will be key to their success. The development of strong integral bounds to avoid the calculation of as many integrals as possible would be a straightforward place to begin and later moving on to the sorting of the integrals (simply looping over the list of Coulomb integrals twice is not optimal) and introducing incremental Fock construction and density cut-offs should also increase the utility of the method.

10.2 Chemical challenges

The main thrust of this work has been theoretical — an attempt to introduce a new method and to begin to show how one might go about practically executing it. It is clear

that there is much work still to be done in this area but we must not lose sight of the wood for the trees, as ultimately we are working towards providing a theoretical model chemistry — a tool which can usefully be employed by chemists. It is important that during the next phase of this work, more relevant chemical problems be addressed such as geometry optimisations, frequency calculations, transition states and the myriad of other properties that chemists are interested in, as it is the performance of HFW theory in these areas that will make or break it.

10.3 Conceptual challenges

It is clear that there are numerous technical challenges to be faced in HFW theory but equally as important are the conceptual challenges that lie in this new theory. This work has been a preliminary investigation into this new area — although we have been feeling around in the dark, we have learnt much about what is important and where our efforts should be focused. We have discovered one correlation kernel which has been shown to work well, but we still need to improve the accuracy of this kernel if HFW theory is to become a viable quantum chemical method. Though we have tried to investigate other kernels, none have worked so well as $G(u,v) = cj_0(\zeta uv)$. However, in these investigations we have mainly, though not exclusively, limited ourselves to kernels in uv and an important next step is to look beyond these kernels in action space and onto more general kernels in (u,v). Unfortunately the possibilities for such a kernel are infinite so we need some theoretical guidance.

10.3.1 Dispersion

One of the major failings of DFT is its inability to treat dispersion — the long range interaction of two electrons. In HFW theory, on the other hand, two-electron information is explicitly included and it may be possible to include the correct behaviour of the long-range correlation energy in our choice of correlation kernel. Let us first examine the behaviour of the correlation energy derived from $G(u,v) = cj_0(\zeta uv)$. If we consider two hydrogen

atoms, each represented by a single GTO with exponent α, separated by a distance, R, such that their overlap is negligible, then the UHF wavefunction and associated intracules are given by

$$\Psi(\mathbf{r}_1,\mathbf{r}_2) = \left(\frac{2\alpha}{\pi}\right)^{3/2} \mathrm{e}^{-\alpha r_1^2-\alpha|\mathbf{r}_1-\mathbf{R}|^2} \tag{10.1}$$

$$W(u,v) = \frac{2u^2v^2}{\pi}\exp\left(-\alpha R^2-\alpha u^2-\frac{v^2}{4\alpha}\right) i_0(2\alpha Ru) \tag{10.2}$$

$$A(s) = \frac{2s^2}{\pi}\mathrm{e}^{-\alpha R^2}\sum_{m=0}^{\infty}\frac{(2\alpha R^2 s)^m}{(2m+1)}K_m(s) \tag{10.3}$$

The associated correlation energy is thus

$$E_{\mathrm{Corr}} = (1+\zeta)^{-3/2}\exp\left(-\frac{\alpha\zeta^2R^2}{1+\zeta^2}\right) \tag{10.4}$$

showing a Gaussian dependence on the distance R. The correct dependence, as shown by London [181], is R^{-6} which is a much slower decay than from our method. Gill has shown that in order for a correlation kernel to exhibit the correct dependence, it must have s^{-6} decay. He has also shown how, by specifying the long-range behaviour of the correlation kernel, the form of the kernel can be deduced using Laplace transforms. This has led to another correlation kernel, $G(u,v) = M(3,\frac{3}{2},-\gamma^2u^2v^2)$, where $M(a,b,z)$ is a confluent hypergeometric function. This has been shown to give comparable results to $G(u,v) = cj_0(\zeta uv)$ but even though it gives the correct long-range description of the correlation energy, the intermediate distances are erroneous and even of the wrong sign. However, there are an infinite choice of other kernels with the correct decay behaviour and this constraint can only help in the search for new and better correlation kernels.

10.3.2 Hooke's Law Atom

In section 5.2.2 we derived all of the intracules for hookium — a hypothetical atom in which the electrons are bound to the nucleus by a harmonic force but still repel each other Coulombically. This system has the attractive quality of being exactly soluble for certain values of the force constant, although the HF solution must still be found numerically. If this system is treated using perturbation theory, in a similar way to Hylleraas' expansion

of the exact energy of He in powers of Z^{-1} or Linderberg's similar expansion for the HF energy, expressions for the exact and HF energies of the Hooke's Law atom can be found. Gill has done this for the lowest singlet and triplet states of the Hooke's Law atom [201]. As the force constant $Z \to \infty$ the exact correlation energy of these two species can be found and furthermore the wavefunctions are simply the wavefunctions for a pair of uncoupled harmonic oscillators. For these simple systems the Wigner and action intracules are straightforward (for example see eqns. (3.8) and (3.11) for the singlet state) and for most reasonable correlation kernels the correlation energy could easily be evaluated either analytically or numerically. When this is done for $G(u,v) = cj_0(\zeta uv)$ and the parameters are chosen to reproduce exactly the correlation energies of the two states, it yields remarkably similar parameters ($c = -0.119, \zeta = 0.889$) to those which result from fitting to the correlation energies of the atoms ($c = 0.102, \zeta = 0.907$). These exact systems could be used as constraints which any new correlation functional must satisfy although, requiring that these hypothetical systems be treated exactly, like the uniform electron gas in DFT, does not necessarily yield better results.

10.3.3 Intracule functional theory

Empirical results can be used to show that a theory has merit but ultimately it needs a firm theoretical grounding. DFT has this in the form of the Hohenberg-Kohn theorems [37] but currently we lack such theorems. We have explored various avenues to try to prove that the Wigner intracule does indeed contain enough information from which to extract the exact correlation energy and even though we have thought ourselves close to a proof, it has so far eluded us. Such a proof would no doubt silent critics and encourage others to begin research in this field and help to make more rapid advances so that HFW theory might become a viable tool for computational chemists. It is, however, difficult to search for such a proof and we must wait until inspiration strikes us.

10.4 Conclusions

It is clear that many-electron information is important in the understanding of the phenomenon of electron correlation but understanding the many dimensions of the wavefunction is not humanly possible. Intracules provide a way to investigate correlation in only two dimensions while retaining information about two electrons and can be used to gain insight into the process. This was first done by Coulson and Nielson in position space and then by Banyard and Reed in momentum space. We have built on this work by introducing a phase-space intracule which provides all of the information in the other intracules and also seems to provide extra insight. In this work we have presented these intracules and shown how to calculate them and looked at some simple examples of them. In an analogous way to Coulson and Neilson we have examined the effect of correlation on the intracules of some simple molecules.

Although there exist a plethora of methods to calculate the correlation energy, evaluating the exact absolute correlation energy is still computationally intractable as this would require a full CI calculation with a very large basis set. However, a set of exact correlation energies would be useful in the calibration and assessment of any new methods, so we have compiled a list of near-exact energies for some small molecules using accurate experimental and theoretical data. This data has been invaluable throughout this work and should provide a useful resource to developers of other methods.

Intracules provide insight into electron correlation but we feel that they could also be used quantitatively to estimate the electron correlation. Electron correlation is directly related to the distance between two electrons — this term appears in the electronic Hamiltonian. It must also be related to how much time the electrons spend in each others vicinity so we believe that the relative momentum of the electrons is important. We have proposed that the Wigner intracule can be used by contraction with a correlation kernel to estimate the correlation energy. Furthermore, this idea can be folded into the HF SCF procedure providing a self-consistent route to a correlated energy. This is conceptually useful but also computationally useful when looking at molecular properties. We have presented several different methods to calculate the correlation integrals in HFW theory. This turns out

to be rather challenging and of the methods investigated so far, none have proved ideal. The infinite series formulation should be able to provide highly accurate results, albeit at a high computational expense, and this should provide a useful reference point for future research. Some preliminary results have been presented which show that HFW theory performs comparably to the well established LYP functional in DFT though the HFW correlation kernel has half as many parameters and a much simpler form.

In the introduction we said the goal of this project was to develop a new theoretical model chemistry — has this been achieved? This may have been a little too ambitious a target, as taking an idea from the drawing board all the way through to a working product is a long process and all of the popular methods in quantum chemistry have been developed for decades. Although we may not yet be rivalling the established methods like DFT and coupled-cluster theory we have taken the first steps. In this work we have done much exploration into this new field and laid some of the theoretical and technical foundation required for further research. I am hopeful that I will stay involved, in some small way, in the development of HFW theory and am optimistic that it will go on to be a useful and popular theoretical model chemistry.

Bibliography

[1] M. Planck, Ann. Phys. **4**, 553 (1901).

[2] L. de Broglie, Ph.D. thesis, Paris (1924).

[3] C. J. Davisson and L. H. Germer, Proc. Nat. Acad. Sc. **14**, 317 (1928).

[4] W. Heisenberg, *The Physical Principles of the Quantum Theory* (Dover, New York, 1930).

[5] E. Schrödinger, Ann. Phys. **79**, 361 (1926).

[6] A. Szabo and N. S. Ostlund, *Modern Quantum Chemistry* (McGraw-Hill, 1989).

[7] D. R. Hartree, Proc. Camb. Phil. Soc. **24**, 89 (1928).

[8] V. Fock, Z. Phys. **61**, 126 (1930).

[9] C. Froese-Fischer, *The Hartree-Fock method for atoms: a numerical approach* (Wiley, New York, 1977).

[10] J. C. Slater, Phys. Rev. **36**, 57 (1930).

[11] S. F. Boys, Proc. Roy. Soc. A (London) **200**, 542 (1950).

[12] W. J. Hehre, R. F. Stewart, and J. A. Pople, J. Chem. Phys. **51**, 2657 (1969).

[13] T. H. Dunning, Jr., J. Chem. Phys. **90**, 1007 (1989).

[14] R. Ditchfield, W. J. Hehre, and J. A. Pople, J. Chem. Phys. **54**, 724 (1971).

[15] J. S. Binkley, J. A. Pople, and W. J. Hehre, J. Am. Chem. Soc. **102**, 939 (1980).

[16] R. Krishnan, J. S. Binkley, R. Seeger, and J. A. Pople, J. Chem. Phys. **72**, 650 (1980).

[17] S. Obara and A. Saika, J. Chem. Phys. **84**, 3963 (1986).

[18] S. Obara and A. Saika, J. Chem. Phys. **89**, 1540 (1988).

[19] M. Head-Gordon and J. A. Pople, J. Chem. Phys. **89**, 5777 (1988).

[20] P. M. W. Gill, Adv. Quantum Chem. **25**, 141 (1994).

[21] M. Abramowitz and I. A. Stegun (eds.), *Handbook of Mathematical Functions* (Dover, New York, 1965).

[22] C. A. White, B. G. Johnson, P. M. W. Gill, and M. Head-Gordon, Chem. Phys. Lett. **253**, 268 (1996).

[23] O. Vahtras and J. Almlöf, Chem. Phys. Lett. **213**, 514 (1993).

[24] C. Ochsenfeld, C. A. White, and M. Head-Gordon, J. Chem. Phys. **109**, 1663 (1998).

[25] P. O. Löwdin, Adv. Chem. Phys. **2**, 207 (1959).

[26] P. E. M. Siegbahn, *Methods in Computational Molecular Physics* (D. Reidel, Dordrecht, 1983).

[27] R. J. Bartlett and G. B. Purvis, Int. J. Quant. Chem., Quantum Chem. Symp. **14**, 561 (1978).

[28] J. A. Pople, J. S. Binkley, and R. Seeger, Int. J. Quant. Chem. Symp. **10**, 1 (1976).

[29] C. D. Sherrill and H. F. Schaefer, Adv. Quantum Chem. **34**, 143 (1999).

[30] C. Schwartz, Phys. Rev. **126**, 1015 (1962).

[31] P. Saxe, H. F. Schaefer, and N. C. Handy, Chem. Phys. Lett. **79**, 202 (1981).

[32] C. Møller and M. S. Plesset, Phys. Rev. **46**, 618 (1934).

[33] J. Olsen, O. Christiansen, H. Koch, and P. Jørgensen, J. Chem. Phys. **113**, 8908 (1996).

[34] J. Olsen, P. Jørgensen, T. Helgaker, and O. Christiansen, J. Chem. Phys. **112**, 9736 (2000).

[35] J. Paldus and X. Z. Li, Adv. Chem. Phys. **110**, 1 (1999).

[36] R. Parr and W. Yang, *Density-functional theory of atoms and molecules* (Oxford University Press, Inc., New York, 1989).

[37] P. Hohenberg and W. Kohn, Phys. Rev. B **136**, 864 (1964).

[38] W. Kohn and L. J. Sham, Phys. Rev. **A140**, 1133 (1965).

[39] S. J. Vosko, L. Wilk, and M. Nusair, Can. J. Phys. **58**, 1200 (1980).

[40] D. M. Ceperly and B. J. Alder, Phys. Rev. Lett. **45**, 566 (1980).

[41] P. M. W. Gill, Aust. J. Chem. **54**, 661 (2001).

[42] W. Klopper, *Encyclopedia of Computational Chemistry*, vol. 4 (John Wiley & Sons., 1998).

[43] E. A. Hylleraas, Z. Phys. **54**, 347 (1929).

[44] R. N. Barnett and W. A. Lester, *Computational chemistry: Reviews of current trends*, vol. 2 (World Scientific, 1997).

[45] D. A. Mazziotti, Phys. Rev. A **57**, 4219 (1998).

[46] H. Nakatsuji, Phys. Rev. Lett. **93**, 030403 (2003).

[47] C. A. Coulson and A. H. Neilson, Proc. Phys. Soc. **78**, 831 (1961).

[48] A. J. Coleman, Int. J. Quantum Chem. Symp. **1**, 457 (1967).

[49] A. J. Thakkar and V. H. Smith Jr, Chem. Phys. Lett. **42**, 476 (1976).

[50] A. J. Thakkar and V. H. Smith Jr, J. Chem. Phys. **67**, 1191 (1977).

[51] A. J. Thakkar, A. N. Tripathi, and V. H. Smith Jr, Int. J. Quant. Chem. **26**, 157 (1984).

[52] R. J. Boyd, C. Sarasola, and J. M. Ugalde, J. Phys. B. **21**, 2555 (1988).

[53] J. H. Wang, A. N. Tripathi, and V. H. Smith Jr, J. Chem. Phys. **97**, 9188 (1992).

[54] J. H. Wang, A. N. Tripathi, and V. H. Smith Jr, J. Phys. B. **26**, 205 (1993).

[55] J. H. Wang and V. H. Smith Jr, J. Chem. Phys. **99**, 9745 (1993).

[56] J. H. Wang and V. H. Smith Jr, Int. J. Quant. Chem. **49**, 147 (1994).

[57] J. H. Wang and V. H. Smith Jr, Theor. Chim. Acta **88**, 35 (1994).

[58] X. Fradera, M. Duran, and J. Mestres, J. Chem. Phys. **107**, 3576 (1997).

[59] J. Cioslowski and G. H. Liu, J. Chem. Phys. **110**, 1882 (1999).

[60] X. Fradera, M. Duran, and J. Mestres, J. Chem. Phys. **113**, 2530 (2000).

[61] P. Ziesche, J. Mol. Struct. THEOCHEM **527**, 35 (2000).

[62] L. Dominguez, M. Aguado, C. Sarasola, and J. M. Ugalde, J. Phys. B. **25**, 1137 (1992).

[63] X. Fradera, C. Sarasola, J. M. Ugalde, and R. J. Boyd, Chem. Phys. Lett. **304**, 393 (1999).

[64] P. M. W. Gill, A. M. Lee, N. Nair, and R. D. Adamson, J. Mol. Struct.(Theochem) **506**, 303 (2000).

[65] E. Valderrama and J. M. Ugalde, Int. J. Quant. Chem. **86**, 40 (2002).

[66] C. Sarasola, J. M. Ugalde, and R. J. Boyd, J. Phys. B **23**, 1095 (1990).

[67] J. M. Ugalde, C. Sarasola, L. Dominguez, and R. J. Boyd, J. Math. Chem. **6**, 51 (1991).

[68] M. Aguado, C. Sarasola, L. Dominguez, and J. M. Ugalde, J. Mol. Struct. THEOCHEM **85**, 311 (1992).

[69] J. H. Wang and V. H. Smith Jr, Chem. Phys. Lett. **220**, 331 (1994).

[70] J. Cioslowski and G. H. Liu, J. Chem. Phys. **105**, 4151 (1996).

[71] A. M. Lee and P. M. W. Gill, Chem. Phys. Lett. **313**, 271 (1999).

[72] T. Koga and H. Matsuyama, J. Chem. Phys. **107**, 8510 (1997).

[73] T. Koga and H. Matsuyama, Theor. Chem. Acc. **99**, 320 (1998).

[74] T. Koga and H. Matsuyama, J. Mol. Struct. THEOCHEM **462**, 261 (1999).

[75] T. Koga and H. Matsuyama, Theor. Chem. Acc. **102**, 39 (1999).

[76] T. Koga and H. Matsuyama, J. Chem. Phys. **111**, 9191 (1999).

[77] T. Koga, J. Chem. Phys. **112**, 6966 (2000).

[78] T. Koga, Y. Nii, and H. Matsuyama, J. Phys. B **33**, 2775 (2000).

[79] T. Koga, J. Mol. Struct. THEOCHEM **527**, 1 (2000).

[80] T. Koga, Chem. Phys. Lett. **325**, 440 (2000).

[81] T. Koga, Chem. Phys. Lett. **350**, 135 (2001).

[82] T. Koga, J. Chem. Phys. **116**, 6614 (2002).

[83] T. Koga, Theor. Chem. Acc. **107**, 246 (2002).

[84] K. E. Banyard and C. E. Reed, J. Phys. B **11**, 2957 (1978).

[85] C. E. Reed and K. E. Banyard, J. Phys. B **13**, 1519 (1980).

[86] R. J. Mobbs, J. Chem. Phys. **78**, 6106 (1983).

[87] P. K. Youngman and K. E. Banyard, J. Phys. B **20**, 3133 (1987).

[88] K. E. Banyard and P. K. Youngman, J. Phys. B **20**, 5585 (1987).

[89] K. E. Banyard, K. H. Al-Bayati, and P. K. Youngman, J. Phys. B **21**, 3177 (1988).

[90] K. E. Banyard and R. J. Mobbs, J. Chem. Phys. **88**, 3788 (1988).

[91] K. E. Banyard and J. Sanders, J. Chem. Phys. **99**, 5281 (1993).

[92] D. R. T. Keeble and K. E. Banyard, J. Phys. B **30**, 13 (1997).

[93] J. M. Ugalde, J. Phys. B **20**, 2153 (1987).

[94] V. G. Levin, V. G. Neudatchin, A. V. Pavlitchenkov, and Y. F. Smirnov, J. Phys. B **17**, 1525 (1984).

[95] H. Matsuyama, T. Koga, E. Romera, and J. S. Dehesa, Phys. Rev. A **57**, 1759 (1998).

[96] T. Koga and H. Matsuyama, J. Phys. B. **31**, 3765 (1998).

[97] T. Koga and H. Matsuyama, J. Chem. Phys. **111**, 643 (1999).

[98] H. Matsuyama, T. Koga, and Y. Kato, J. Phys. B **32**, 3371 (1999).

[99] T. Koga, H. Matsuyama, J. M. Molina, and J. S. Dehesa, Eur. Phys. Journ. D. **7**, 17 (1999).

[100] T. Koga and H. Matsuyama, J. Chem. Phys. **113**, 10114 (2000).

[101] T. Koga, J. Phys. B **34**, 1383 (2001).

[102] T. Koga, Chem. Phys. Lett. **340**, 547 (2001).

[103] T. Koga, Y. Kato, and H. Matsuyama, Theor. Chem. Acc. **106**, 237 (2001).

[104] T. Koga, Theor. Chem. Acc. **107**, 246 (2002).

[105] N. A. Besley, A. M. Lee, and P. M. W. Gill, Mol. Phys. **100**, 1763 (2002).

[106] E. Wigner, Phys. Rev. **40**, 749 (1932).

[107] M. Springborg and J. P. Dahl, Phys. Rev. A **36**, 1050 (1987).

[108] H. Groenewold, Physica **12**, 405 (1946).

[109] J. P. Dahl and M. Springborg, Mol. Phys. **47**, 1001 (1982).

[110] N. A. Besley, D. P. O'Neill, and P. M. W. Gill, J. Chem. Phys. **118**, 2033 (2003).

[111] J. Kong, C. A. White, A. I. Krylov, C. D. Sherrill, R. D. Adamson, T. R. Furlani, M. S. Lee, A. M. Lee, S. R. Gwaltney, T. R. Adams, C. Ochsenfeld, A. T. B. Gilbert, G. S. Kedziora, V. A. Rassolov, D. R. Maurice, N. Nair, Y. Shao, N. A. Besley, P. E. Maslen, J. P. Dombroski, H. Daschel, W. Zhang, P. P. Korambath,

J. Baker, E. F. C. Byrd, T. van Voorhis, M. Oumi, S. Hirata, C.-P. Hsu, N. Ishikawa, J. Florian, A. Warshel, B. G. Johnson, P. M. W. Gill, M. Head-Gordon, and J. A. Pople, J. Comput. Chem. **21**, 1532 (2000).

[112] V. I. Lebedev, Zh. Vychisl. Mat. Mat. Fiz. **16** (1976).

[113] V. I. Lebedev, Sibirsk. Mat. Zh. **18**, 132 (1977).

[114] V. I. Lebedev and D. N. Laikov, Dokl. Math. **366**, 741 (1999).

[115] A. Jablonski, J. Comput. Phys. **111**, 256 (1994).

[116] S. Zhang and J. Jin, *Computation of special functions* (John Wiley & Sons, Inc., 1996).

[117] W. J. Hehre, R. Ditchfield, and J. A. Pople, J. Chem. Phys. **56**, 2257 (1972).

[118] T. Clark, J. Chandrasekhar, and P. V. R. Schleyer, J. Comput. Chem. **4**, 294 (1983).

[119] *Mathematica* (Wolfram Research, Inc., Champaign, Illinois, 2003), version 5.0 edn.

[120] D. P. O'Neill and P. M. W. Gill, Phys. Rev. A **68**, 022505 (2003).

[121] N. R. Kestner and O. Sinanoglu, Phys. Rev. **128**, 2687 (1962).

[122] S. Kais, D. R. Herschbach, and R. D. Levine, J. Chem. Phys. **91**, 7791 (1989).

[123] U. Merkt, J. Huser, and M. Wagner, Phys. Rev. B **43**, 7320 (1991).

[124] R. J. White and W. Byers Brown, J. Chem. Phys. **53**, 3869 (1970).

[125] J. M. Benson and W. Byers Brown, J. Chem. Phys. **53**, 3880 (1970).

[126] M. Taut, Phys. Rev. A **48**, 3561 (1993).

[127] M. Taut, J. Phys. A **27**, 1045 (1994).

[128] C. Filippi, C. J. Umrigar, and M. Taut, J. Chem. Phys. **100**, 1290 (1994).

[129] H. F. King, Theor. Chim. Acta **94**, 345 (1996).

[130] Y. Huang, S. A. Barts, and J. B. Halpern, J. Phys. Chem. **96**, 425 (1992).

[131] M. Taut, A. Ernst, and H. Eschrig, J. Phys. B **31**, 2689 (1998).

[132] Z. Qian and V. Sahni, Phys. Rev. A **57**, 2527 (1998).

[133] N. H. March, T. Gál, and Á. Nagy, Chem. Phys. Letters **292**, 384 (1998).

[134] P. Ziesche, V. H. Smith Jr, M. Hô, S. P. Rudin, P. Gersdorf, and M. Taut, J. Chem. Phys. **110**, 6135 (1999).

[135] K. Ivanov, K. Burke, and M. Levy, J. Chem. Phys. **110**, 10262 (1999).

[136] P. Hessler, J. Park, and K. Burke, Phys. Rev. Lett. **82**, 378 (1999).

[137] N. H. March, C. Amovilli, and D. J. Klein, Chem. Phys. Letters **325**, 645 (2000).

[138] J. Cioslowski and K. Pernal, J. Chem. Phys. **113**, 8434 (2000).

[139] A. Artemyev, E. V. Ludena, and V. Karasiev, J. Mol. Struct.(Theochem) **580**, 47 (2002).

[140] E. Romera, J. Phys. B **35**, L309 (2002).

[141] C. Amovilli and N. H. March, Phys. Rev. A **67**, 022509 (2003).

[142] P. M. W. Gill, D. P. O'Neill, and N. A. Besley, Theor. Chem. Acc. **109** (2003).

[143] `http://www.netlib.org/quadpack/`.

[144] C. W. Murray, N. C. Handy, and G. W. Laming, Mol. Phys. **78**, 997 (1993).

[145] N. C. Handy, private communication.

[146] The exponents used were 0.0375, 0.0750, 0.23185, 0.30241, 0.37297, 0.6000, 1.2000, 2.4000.

[147] K. A. Peterson, W. D. E., and D. T. H., J. Chem. Phys. **100**, 7410 (1994).

[148] F. Arias de Saavedra, E. Buendía, and F. J. Gálvez, Z. Phys. D **38**, 25 (1996).

[149] A. Sarsa, F. J. Gálvez, and E. Buendía, J. Chem. Phys. **110**, 5721 (1999).

[150] F. J. Gálvez, E. Buendía, and A. Sarsa, Chem. Phys. Lett. **370**, 327 (2003).

[151] T. Koga, Chem. Phys. Lett. **350**, 135 (2001).

[152] D. P. O'Neill and P. M. W. Gill, Mol. Phys. **103**, 763 (2005).

[153] P. J. Stephens, F. J. Devlin, C. F. Chablowski, and M. J. Frisch, J. Phys. Chem. **98**, 11623 (1994).

[154] J. A. Pople, M. Head-Gordon, D. J. Fox, K. Raghavachari, and L. A. Curtiss, J. Chem. Phys. **90**, 5622 (1989).

[155] L. A. Curtiss, C. Jones, G. W. Trucks, K. Raghavachari, and J. A. Pople, J. Chem. Phys. **93**, 2537 (1990).

[156] L. A. Curtiss, K. Raghavachari, G. W. Trucks, and J. A. Pople, J. Chem. Phys. **94**, 7221 (1991).

[157] L. A. Curtiss, K. Raghavachari, P. C. Redfern, V. Rassolov, and J. A. Pople, J. Chem. Phys. **109**, 7764 (1998).

[158] P. J. Reynolds, D. M. Ceperley, B. J. Alder, and W. A. Lester, J. Chem. Phys. **77**, 5593 (1982).

[159] P. J. Reynolds, M. Dupuis, and W. A. Lester, J. Chem. Phys. **82**, 1983 (1985).

[160] D. Feller, C. M. Boyle, and E. R. Davidson, J. Chem. Phys. **86**, 3424 (1986).

[161] C. Filippi and C. J. Umrigar, J. Chem. Phys. **105**, 213 (1996).

[162] A. Lüchow, J. B. Anderson, and D. Feller, J. Chem. Phys. **106**, 7706 (1997).

[163] S.-I. Lu, J. Chem. Phys. **21**, 9528 (2003).

[164] K. P. Huber and G. Herzberg, *Molecular Spectra and Molecular Structure: Constants of Diatomic Molecules*, vol. 4 (Van Nostrand Reinhold, New York, 1979).

[165] A. P. Scott and L. Radom, J. Phys. Chem. **100**, 16502 (1996).

[166] L. A. Curtiss, K. Raghavachari, and J. A. Pople, J. Chem. Phys. **103**, 4192 (1995).

[167] D. Feller and K. A. Peterson, J. Chem. Phys. **110**, 8384 (1999).

[168] J. M. L. Martin, A. Sundermann, P. L. Fast, and D. G. Truhlar, J. Chem. Phys. **113**, 1348 (2000).

[169] S. J. Chakravorty, S. R. Gwaltney, E. R. Davidson, F. A. Parpia, and C. Froese-Fischer, Phys. Rev. A **47**, 3649 (1993).

[170] K. Kuchitsu (ed.), *Structure of free polyatomic molecules : basic data* (Springer, Berlin, 1998).

[171] J. A. Pople, M. Head-Gordon, and K. Raghavachari, J. Chem. Phys. **87**, 5968 (1987).

[172] L. A. Curtiss, P. C. Redfern, K. Raghavachari, V. Rassolov, and J. A. Pople, J. Chem. Phys. **110**, 4703 (1999).

[173] http://comp.chem.umn.edu/database.

[174] D. E. Woon and T. H. Dunning, Jr., J. Chem. Phys. **100**, 2975 (1994).

[175] A. Halkier, T. Helgaker, P. Jørgensen, W. Klopper, and J. Olsen, Chem. Phys. Lett. **302**, 437 (1999).

[176] D. P. O'Neill, N. A. Besley, and P. M. W. Gill, *Submitted.*

[177] C. C. J. Roothaan, Rev. Mod. Phys. **23**, 69 (1951).

[178] G. G. Hall, Proc. Roy. Soc. A **208**, 328 (1951).

[179] E. Schwegler and M. Challacombe, J. Chem. Phys. **111**, 6223 (1999).

[180] This is analogous to approximating a function with a discontinuous derivative, such as $|x|$, by a sum of smooth functions.

[181] F. London, Trans. Faraday Soc. **33**, 8 (1937).

[182] E. A. Hylleraas and J. Midtdal, Phys. Rev. **103**, 829 (1956).

[183] J. Linderberg, Phys. Rev. **121**, 816 (1961).

[184] V. A. Rassolov, J. Chem. Phys. **110**, 3672 (1999).

[185] Calculated from the HF/6-311G wavefunction. See, W. J. Hehre, L. Radom, P. v. R. Schleyer, J. A. Pople, Ab initio molecular orbital theory (Wiley, New York, 1986).

[186] P. M. W. Gill, D. P. O'Neill, and N. A. Besley, Theor. Chem. Acc. **109**, 241 (2003).

[187] M. Hillery, R. F. O'Connell, M. O. Scully, and E. P. Wigner, Phys. Rep. **106**, 121 (1984).

[188] N. A. Besley and P. M. W. Gill, J. Chem. Phys. **120**, 7290 (2004).

[189] P. M. W. Gill, N. A. Besley, and D. P. O'Neill, Int. J. Quantum Chem. **100**, 166 (2004).

[190] P. M. W. Gill and D. P. O'Neill, J. Chem. Phys. **122**, 094110 (2005).

[191] D. P. O'Neill and P. M. W. Gill, in preparation.

[192] C. Lee, C. Yang, and R. G. Parr, Phys. Rev. B **37**, 785 (1988).

[193] P. M. W. Gill and S. H. Chien, J. Comput. Chem. **24**, 732 (2003).

[194] G. Szegö, *Orthogonal Polynomials* (American Mathematical Society, New York, 1959).

[195] M. C. Fasenmyer, *Some generalized hypergeometric polynomials*, Ph.D. thesis, University of Michigan (1945).

[196] H. S. Wilf and D. Zeilberger, Invent. Math. **108**, 575 (1992).

[197] K. Wegschaider, *Computer generated proofs of binomial multi-sum identities*, Ph.D. thesis, J. Kepler University (1997).

[198] W. H. Press, B. P. Flannery, S. A. Teukolsky, and W. T. Vetterling, *Numerical Recipes in Fortran* (Cambridge University Press, Cambridge, 1992).

[199] C. Brezinski, J. Comput. Appl. Math. **122**, 1 (2000).

[200] `http://mathworld.wolfram.com`.

[201] P. M. W. Gill and D. P. O'Neill, J. Chem. Phys. **122**, 094110 (2005).